**INSTITUTE**

FOR

**COSMIC RAY RESEARCH**

UNIVERSITY OF TOKYO

# ANNUAL REPORT
# (APRIL 2009 – MARCH 2010)

**Editorial Board**

YOSHIKOSHI, Takanori

OHASHI, Masatake

TAKENAGA, Yumiko

ITOH, Hideo

ⓒ**Institute for Cosmic Ray Research, University of Tokyo**

5-1-5, Kashiwanoha, Kashiwa, Chiba 277-8582, Japan

Telephone: (81) 4-7136-3102
Facsimile: (81) 4-7136-3115
WWW URL: http://www.icrr.u-tokyo.ac.jp/

# TABLE OF CONTENTS

# PREFACE

This report summarizes the scientific activities of the Institute for Cosmic Ray Research (ICRR) of the University of Tokyo in the Japanese FY 2009.

ICRR is an inter-university research institute for studies of cosmic rays. The headquarters of ICRR is located in Kashiwa, Chiba prefecture, Japan. In order to promote various cosmic-ray-related studies efficiently, ICRR has three research divisions; Neutrino and Astroparticle division, High Energy Cosmic Ray division, and Astrophysics and Gravity division. ICRR has 3 observatories in Japan; Kamioka Observatory (Kamioka underground, Gifu prefecture), Norikura Observatory (2770 meters asl, Mt. Norikura, Gifu prefecture), and Akeno Observatory (Yamanashi prefecture), together with 1 research center; Research Center for Cosmic Neutrinos (Kashiwa, Chiba prefecture). In addition, there are 3 major experimental facilities outside of Japan. They are located in Utah in USA, Yangbajing in Tibet, China, and Woomera in Australia.

More than 300 researchers from various Japanese institutions are involved in the research programs of ICRR. It should be noted that most of the scientific outputs from this institute are the results of the collaborative efforts by many institutions. In order to produce outstanding results, it is very important to carry out an experiment by an international collaboration composed of top-level researchers all over the world. Hence, most of the experimental collaborations that ICRR is involved are international ones. For example, the number of collaborators in the Super-Kamiokande experiment is about 130; among them 60 are from abroad (USA, Korea, China, Poland and Spain).

Many exciting scientific activities of ICRR are described in this report. One of the highlights is the start of the T2K long-baseline neutrino oscillation experiment, which will study neutrino oscillations in detail including a search for the third mixing angle $\theta_{13}$. We hope that this report is useful for the understanding of the current research activities of ICRR. Finally, we appreciate very much the strong support of our colleagues in this research field, the University of Tokyo and the Japanese Ministry of Education, Culture, Sports, Science and Technology. They are indispensable for the continuing, and exciting scientific outcome of ICRR.

Takaaki Kajita,
Director,
Institute for Cosmic Ray Research,
The University of Tokyo

The ICRR building at Kashiwa, Chiba, Japan.

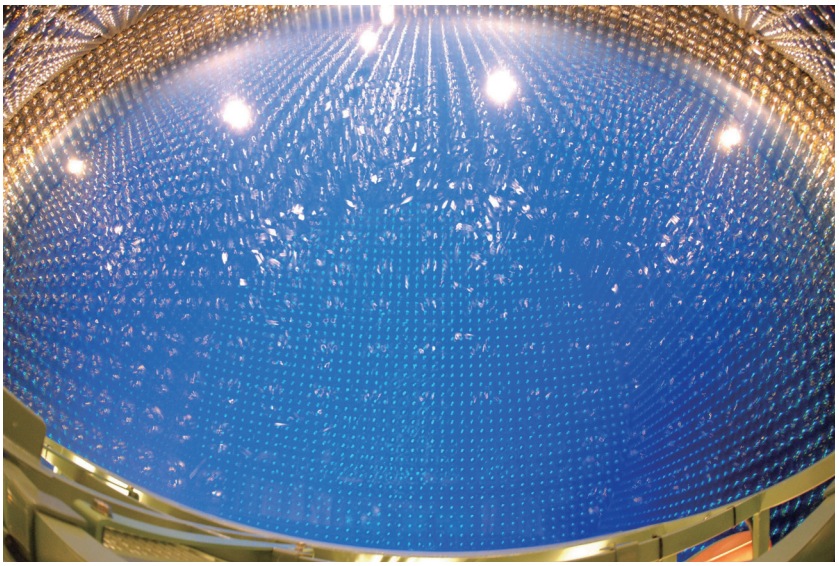

The inner detector of Super-Kamiokande-III during the full reconstruction. The purified water is under filling.

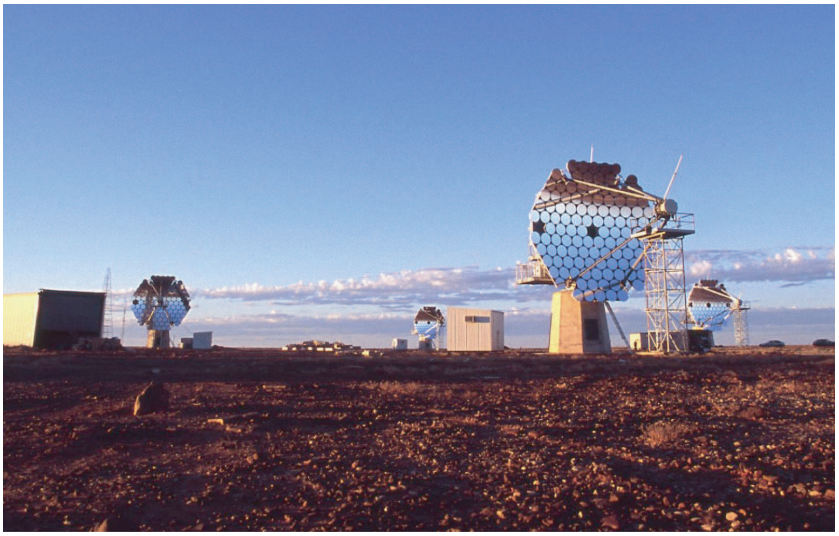

The system of four imaging atmospheric Cherenkov telescopes of 10m diameter of CANGAROO project for detection of very high energy gamma-rays The whole system is in operation since March 2004 in Woomera, South Australia.

Tibet-III air shower array (37000 $m^2$) at Yangbajing, Tibet (4300 m in altitude).

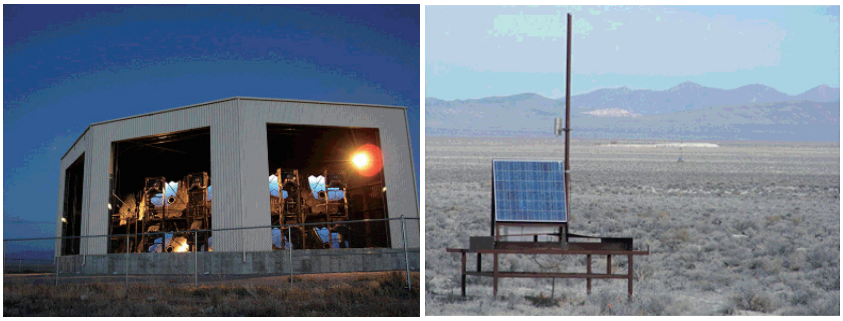

Air fluorescence telescopes (left) and a scintillator surface detector (right) of the Telescope Array experiment in Utah, USA to explore the origin of extremely high energy cosmic rays.

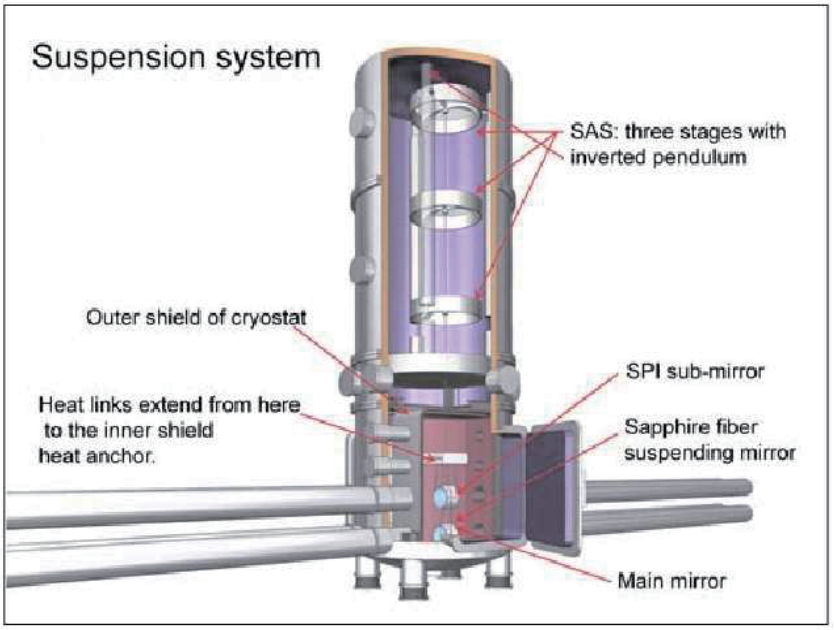


Cryogenic mirror suspension system for Large Scale Cryogenic Gravitational Wave Telescope.

Wide-view telescope of 2.5 m diameter (left telescope) in Arizona, USA for the Sloan Digital Sky Survey project.


A public lecture held by Research Center for Cosmic Neutrinos.

## Organization

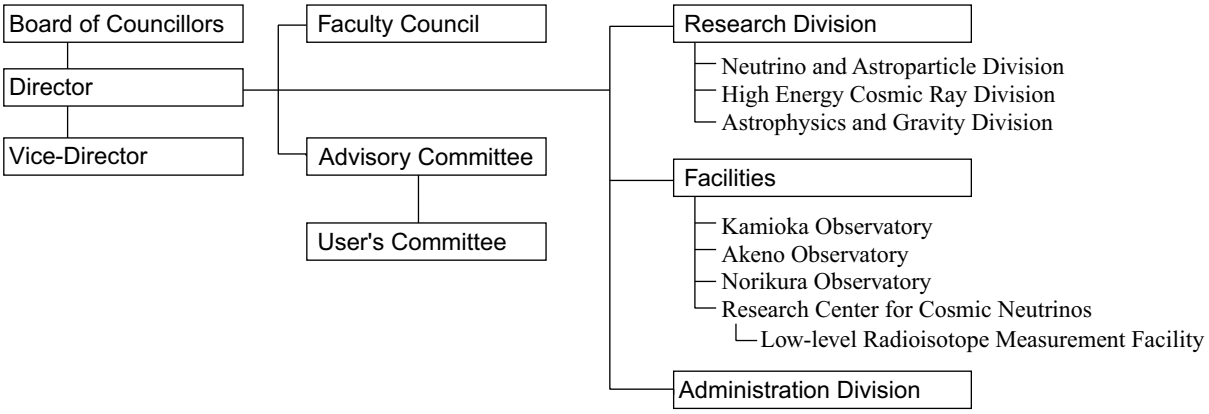


## Number of Staff Members (As of April 1, 2009)

| | Scientific Staff | Technical Staff | Research Fellows | Administrators and Secretaries | |
|---|---|---|---|---|---|
| Neutrino and Astroparticle Div. | 21 | 4 | 4 | 15 | 44 |
| High Energy Cosmic Ray Div. | 11 | 14 | 5 | 4 | 34 |
| Astrophysics and Gravity Div. | 9 | 0 | 2 | 3 | 14 |
| Administration | 1 | 0 | 0 | 13 | 14 |
| Total | 42 | 18 | 11 | 35 | 106 |

## FY 2004–2009 Budget

| | 2004 | 2005 | 2006 | 2007 | 2008 | 2009 |
|---|---|---|---|---|---|---|
| Personnel expenses | 539 000 | 465 000 | 566 000 | 624 000 | 632 000 | 590 000 |
| Non-personnel expenses | 1 902 000 | 1 822 000 | 812 000 | 1 253 000 | 1 121 000 | 1 292 000 |
| Total | 2 441 000 | 2 287 000 | 1 378 000 | 1 877 000 | 1 753 000 | 1 882 000 |

(in 1 000 yen)

# RESEARCH DIVISIONS

## Neutrino and Astroparticle Division

- **Overview**
- **Super-Kamiokande Experiment**
- **Hyper-Kamiokande**
- **T2K Experiment**
- **XMASS Experiment**

## High Energy Cosmic Ray Division

- **Overview**
- **CANGAROO-III Project**
- **TA: Telescope Array Experiment**
- **Tibet AS$\gamma$ Project**
- **Ashra Project**
- **High Energy Astrophysics Group**

## Astrophysics and Gravity Division

- **Overview**
- **Gravitational Wave Group**
  - LCGT Project
  - CLIO Project
- **Sloan Digital Sky Survey**
- **Primary Cosmic Ray Group**
- **Theory Group**
  - Particle Phenomenology
  - Astrophysics and Cosmology

# NEUTRINO AND ASTROPARTICLE DIVISION

## Overview

This division aims to study particle physics that is not accessible within accelerator facilities, with prime interests in physics of neutrinos and proton decay, and astroparticle physics with the use of underground experimental facilities.

Our most important facility is the Super-Kamiokande (SK) detector. It is a 50 kton water Cherenkov detector using 11,129 50 cm-diameter photomultipliers (PMTs) for its inner detector and 1,885 20 cm-diameter PMTs for its outer detector. The data taking of SK started in April 1996. The most important physics results are the discovery of neutrino oscillation in atmospheric neutrinos in 1998 and thereby demonstrating that neutrinos have a finite mass, and the accurate measurement of the solar neutrino flux from the decay of $^8$B which served to confirm the long-conjectured neutrino oscillation hypothesis in solar neutrinos beyond doubt. The search for nucleon decay at SK gives the current best limit which strongly constrains the grand unification scenario of particle interactions. SK has been monitoring for neutrinos from supernova bursts. If a supernova burst occurs at a distance from the center of our galaxy, SK will be able to detect about 8,000 neutrino events. A high intensity neutrino beam experiment using the J-PARC accelerator (T2K) was started in 2009. The T2K experiment uses the SK detector as the far detector. High precision measurement of oscillation parameters and the third oscillation pattern (the effect of the mixing angle $\theta_{13}$) will be investigated by T2K. Moreover, feasibility study has been performed for the next generation nucleon decay and neutrino detector Hyper-Kamiokande.

Another activity of the Neutrino and Astroparticle division is a multi-purpose experiment using liquid xenon aiming at the detection of cold dark matter, neutrino absolute mass using neutrinoless double beta decay, and low energy solar neutrinos. A 800 kg liquid xenon detector which is dedicated for the dark matter search was being constructed in 2009.

Recent progress of research activities in the Neutrino and Astroparticle division is presented here.

## Super-Kamiokande experiment

### Supernova neutrinos

Kamiokande and IMB observed neutrino burst from supernova 1987a. Those observations confirmed that the energy release by neutrinos is about several $\times 10^{53}$erg. However, the observed numbers of events were only 11 by Kamiokande and 8 by IMB, respectively. Super-Kamiokande is able to detect several thousand neutrino events if it happens near the center of our galaxy. Such observation would enable us to investigate detailed mechanism of the supernova explosion. Galactic supernovae has been searched almost in real time at SK. The online data acquisition system running in the mine sends data to the offline computer system in the surface building of Kamioka observatory. As soon as a block of data (usually a block corresponds to several minutes) is transferred to the offline system, a program called SNWATCH searches for time clustered events. Current criteria of SNWATCH are (1) more than or equal to 7 events within 0.5sec, (2) more than or equal to 8 events within 2sec, and (3) more than or equal to 13 events within 10sec. When at least one of the criteria is met, SNWATCH reconstructs vertex position and energy of those events together with neighboring cosmic ray muons. Most of the case, those clusters are due to spallation products whose vertex positions are aligned along their parent cosmic ray muon. If SNWATCH finds an event cluster whose vertex spread is larger than a given criterion, an alarm signal is sent to experts by an e-mail. Then, the experts check whether it is a real supernova signal or not by looking at various plots which are uploaded to a secured site accessible from Internet (including i-mode keitai). Such alarms happen almost once per month. They are usually due to accidental coincidence of two cosmic ray induced clusters. Until now, no real supernova neutrino burst signal has not been observed at Super-Kamiokande yet.

We also search for neutrinos from old supernovae, which are called Supernova Relic Neutrino (SRN). The SRN is the diffuse supernova neutrino background from all the supernovae in the past. It is expected that the SRN would become dominant in 18–40MeV energy region, which is the gap between the energy ranges of solar neutrinos and atmospheric neutrinos. We have applied the special data selections to enhance the SRN candidates. The research in 2009 was to improve the analysis by refining the selection criteria and combining SK-I, SK-II, and SK-III data. The results of the improved analysis are expected in 2010.

### R&D study for gadolinium project

The purpose of this research is to develop a method to detect SRNs. The flux of SRNs is estimated to be about several tens of neutrinos per second and per square centimeters. It sounds like a strong flux, but it is much smaller than the flux of Boron-8 solar neutrinos at the orbit of the Earth they have a flux of about 6 million neutrinos in the same units. Because neutrinos have very small cross section for interactions on matter, a large volume detector like Super-Kamiokande (SK) is necessary to detect SRNs. In SK, we expect somewhere between 0.8 and 5 SRN signals per year, where the wide range of this event rate is due to prediction model uncertainties. However, in order to find SRN events among natural backgrounds induced by cosmic rays and solar neutrinos, a new method to identify the real signal is necessary. Supernovae produce all types of neutrinos. Electron-anti-neutrinos have the largest cross section on matter among them, and their interaction on free protons produce positrons and neutrons. So, if we can detect not only positrons but also neutrons, we can select pure SRN signals. For this purpose, we need to put 0.2% gadolinium compound into the SK water tank. Gadolinium has a large

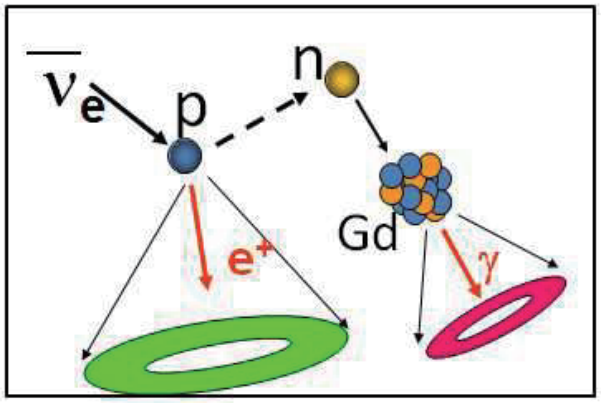


Fig. 1. The coincidence method for the detection of SRN anti-neutrino signals. In the previous method, only the positron signal was analyzed. By adding about 0.2% of gadolinium compound to SK, gamma rays from neutron capture will give a coincidence signal to tag the anti-neutrino.

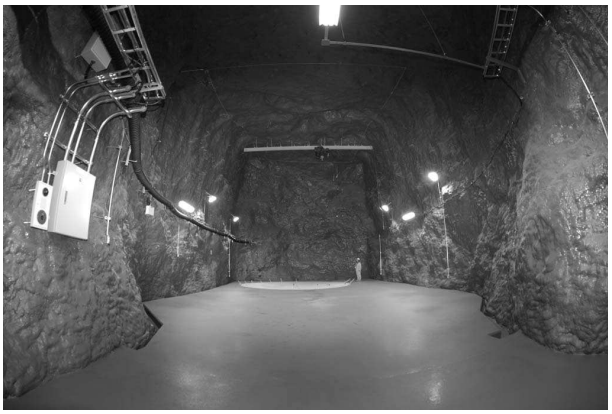

Fig. 2. A new cavern was excavated for the R&D study of the gadolinium project in 2009. The size of the cavern is 10 m wide, 15 m long, 8∼10 m high. A 200-ton water tank and a water purification system will be installed in 2010.

| Source | Total flux |
|---|---|
| Energy scale | $\pm 1.4$ |
| Energy resolution | $\pm 0.2$ |
| Theoretical uncertainty of $^8B$ spectrum | $\pm 0.2(^{+1.1}_{-1.0})$ |
| Trigger efficiency | $\pm 0.5$ |
| Angular resolution | $\pm 0.67(\pm 1.2)$ |
| Vertex shift | $\pm 0.54(\pm 1.3)$ |
| Event quality cuts | $\pm 0.65(^{+2.1}_{-1.6})$ |
| Spalltion | $\pm 0.2$ |
| External event cut | $\pm 0.25$ |
| Small cluster hits cut | $\pm 0.5$ |
| Background shape | $\pm 0.1$ |
| Signal extraction method | $\pm 0.7$ |
| Livetime | $\pm 0.1$ |
| Cross section | $\pm 0.5$ |
| Total | $\pm 2.1(^{+3.5}_{-3.2})$ |

Table 1. Systematic uncertainty summary for the total flux in %. SK-I values are also shown in parentheses for the largely improved systematic sources in the current SK-III analysis.

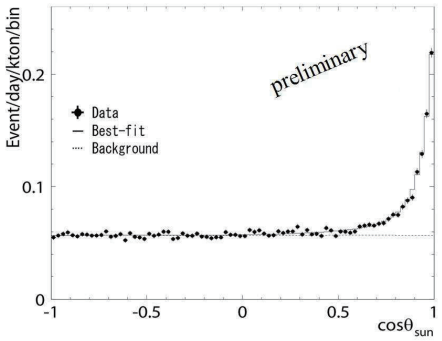


Fig. 3. Solar angle distribution of the SK-III final sample. The livetime is 298 days for the energy range from 5 to 6.5 MeV and 548 days for the energy range from 6.5 to 20 MeV. Data points are fitted using the $^8$B spectrum calculated by Winter *et al.*. The best fit curve is indicated by the solid curve.

neutron capture cross section and emits high energy gamma rays which can be detected by the photomultipliers in the SK tank. Those positron and gamma ray signals have close reconstructed vertex positions and also time coincidence of about 20 $\mu$sec as shown in Fig.1. This coincidence method will reduce background with 4-5 orders of magnitudes and it would enable the detection of SRN.

SK is a multiple purpose detector, which is used for precise study of neutrino oscillations using solar, atmospheric, and man-made neutrinos. We therefore need to demonstrate that gadolinium will not cause any problems for other physics at SK before introducing it into the SK tank. In this R&D study, we are making a 200 ton test tank to mimic the SK detector and prove the principle. In 2009, a new cavern for the R&D study was excavated as shown in Fig.2. A 200 ton water tank will be constructed from April 2010. Then, a system to dissolve and purify gadolinium and a water circulation system which purifies the 0.2% gadolinium doped water without removing gadolinium will be constructed in summer/fall of 2010.

## Solar neutrinos

SK detects solar neutrinos through elastic neutrino-electron scattering, $\nu + e \rightarrow \nu + e$, where the energy, direction and time of the recoil electron are measured. Due to its large fiducial mass of 22.5 kiloton, SK gives the most precise measurement of the solar neutrinos' flux with accurate information of the energy spectrum and time variations. To achieve this high precision, precise calibrations are performed for the energy scale, energy resolution, angular resolution and the vertex position resolution using a LINAC and $^{16}$N radioisotope generated by a DT neutron generator.

This year, the SK-III data have been analyzed with a livetime of 298 days for the total electron energy range between 5 MeV and 6.5 MeV, and 548 days for the range between 6.5 MeV and 20 MeV. The SK-III data have a lower background level in the low energy region than the SK-I data because the amount of the Rn contamination within the fiducial volume has been reduced by changing the water flow inside the tank and keeping the water with relatively rich radioactivity from

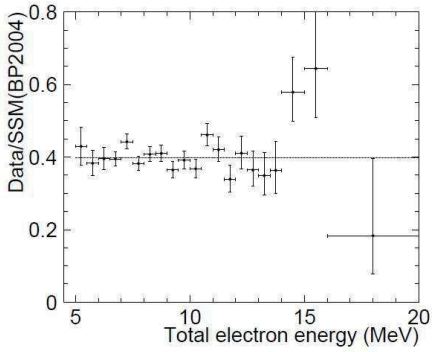


Fig. 4. Energy spectrum of solar neutrino flux in SK-III data from 5 MeV to 20 MeV. Each point shows the ratio of the data and the expected flux calculated from the SSM. The line indicates the averaged value of the SK-III data.

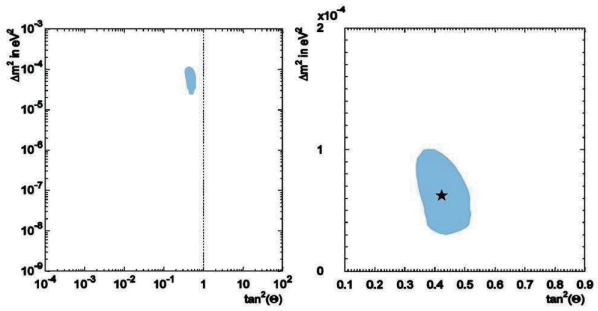


Fig. 5. Allowed region(95% C.L.) for neutrino oscillation parameters, $\Delta m^2$ and $\tan^2\theta$ from solar analysis. The left figure shows the results from the SK-I, II and III combined analysis with the $^8$B flux constrained by SNO NC measurement. The right figure presents the result of global analysis including SK and other solar experiments(SNO, Borexino, Homestake, GALLEX-GNO and SAGE).

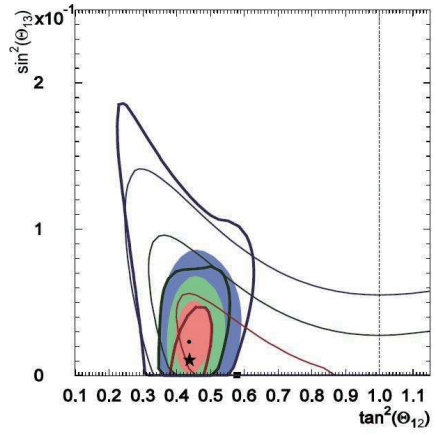


Fig. 6. Allowed region for $\sin^2\theta_{13}$ and $\tan^2\theta_{12}$ from the three flavor analysis. The thick lines and the star mark show the allowed regions and the best fit point of the global solar analysis. The thin lines and the square mark show the allowed regions and the best fit point of our KamLAND analysis. The filled areas and the filled circle mark show the allowed regions and the best fit point of the combined analysis. For all regions, the innermost area (red), the middle area (green) and the outermost area (blue) show 68.3, 95, 99.7 % C.L. respectively.

entering into the fiducial volume. Also because pure water was supplied through a RO (reverse osmosis) system which seems to have removed radium content in water. Detector simulation and event reconstruction tools have been improved in this analysis, which give lower systematic uncertainties (See Table 1). Among the improvements in the detector simulation, the position dependence of the water transparency in the tank was newly implemented and the reflectivity of the sheet, optically separating the inner detector from the outer detector, was carefully measured and updated. An example of refinement in the reconstruction tools is the improvement in the direction fitter, which yields a 10 % better angular resolution. With all those improvements, the systematic uncertainties for total flux of the SK-III data becomes $\pm 2.1\%$, which is reduced from $^{+3.5}_{-3.2}\%$ of the SK-I data [1].

Fig. 3 shows a preliminary result of the solar angle distribution for the SK-III final sample. After subtracting background and fitting with the $^8$B energy spectrum by Winter *et al.* [2], we obtained the $^8$B flux value of $2.32 \pm 0.04(stat.) \pm 0.05(sys.) \times 10^6 cm^{-2}s^{-1}$, which is consistent with the previous SK-I and II results. The energy spectrum of the solar neutrino flux for the SK-III data is shown in Fig. 4. The energy range used for the analysis is from 5 to 20 MeV. As shown in the figure, the ratio of the data and the expected flux from the Standard Solar Model (SSM) [3] scatters almost flat at 0.4, and the energy spectrum distortion which is expected from the LMA solution is not observed yet.

Oscillation analysis has also been done including the SK-III solar neutrino data. The two flavor analysis for the determination of the solar oscillation parameters, $\theta_{12}$ and $\Delta m^2_{12}$ was done with the combined SK-I, II and III data. In the analysis, the total $^8$B flux is constrained by the SNO NC measurement[4][5]. The result is shown in Fig.5. As shown in the left figure, the LOW solution is excluded and the LMA solution is only allowed to explain the solar neutrino oscillation. Note that this result was obtained using SK results only (not global analysis) with the $^8$B flux constraint.

We have also done the same analysis using the data from SK and other solar experiments, i.e. SNO[4][5][6][7], Borexino[8], and radiochemical experiments (Homestake[9], SAGE[10] and GALLEX-GNO[11]). The allowed region from the global analysis is shown in Fig.5(right). The best-fit parameters are $\tan^2\theta_{12} = 0.44 \pm 0.03$ and $\Delta m^2_{21} = (7.6 \pm 0.2) \times 10^{-5}\mathrm{eV}^2$.

In addition to the two flavor analysis, three flavor analysis was also done. We used three oscillation parameters, $\Delta m^2_{12}$, $\theta_{12}$ and $\theta_{13}$ as free parameters and set a fixed value of $2.4 \times 10^{-3}\mathrm{eV}^2$ for $\Delta m^2_{23}$. Fig.6 shows the allowed region for $\sin^2\theta_{13}$ and $\tan^2\theta_{12}$ from the three flavor analysis of SK and other solar experiments together with the KamLAND three flavor analysis[12]. The allowed region for the combined analysis from the solar global and KamLAND analyses is also indicated. The limit of $\sin^2\theta_{13}$ is 0.060 at 95% C.L. for the solar global analysis. After combination with the KamLAND result, the best fit value of $\sin^2\theta_{13}$ is found to be $0.025^{+0.018}_{-0.016}$ and upper bound is obtained as $\sin^2\theta_{13} < 0.059$ at 95% C.L. These results will be published soon.

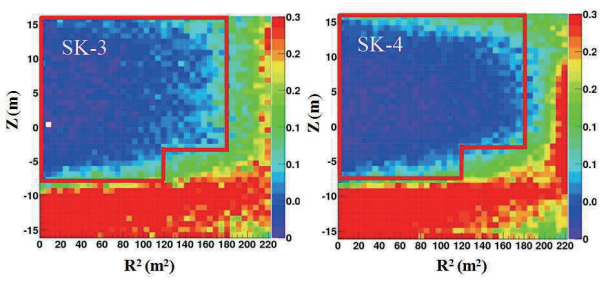


Fig. 7. Vertex distribution of event rate for final data sample for solar neutrino with energy between 4.5-5.0 MeV. The left figure shows SK-III data and the right figure shows SK-IV data. The unit of the event rate is events day$^{-1}$ (14.0m$^3$)$^{-1}$. The red frame shows the fiducial volume used in the SK-III analysis for this energy range.

Since SK-IV was started with new electronics and online system in October 2008, we continue taking the solar neutrino data without large unscheduled downtime. By the end of May 2010, data of about 420 days livetime were collected. In SK-IV period, we have introduced a precise temperature control system for the inlet water to avoid water convection which causes Rn rich water to enter the fiducial volume. In Fig.7, the event rate in the 4.5-5.0 MeV energy region is shown for the SK-III(left) and SK-IV(right) final samples. It indicates that the SK-IV data have a similar distribution of the background events to the SK-III data and also achieve a low background rate inside the fiducial volume. The SK-IV data analysis is now ongoing.

## Atmospheric neutrinos

Cosmic ray interactions in the atmosphere produce neutrinos. The prediction of the absolute flux has an uncertainty of at least $\pm 20\,\%$. However, the flavor ratio of the atmospheric neutrino flux, $(\nu_\mu + \bar{\nu}_\mu)/(\nu_e + \bar{\nu}_e)$, has been calculated to an accuracy of better than $5\,\%$. Another important feature of atmospheric neutrinos is that the fluxes of upward and downward going neutrinos are expected to be nearly equal for $E_\nu >$(a few GeV) where the effect of the geomagnetic field on primary cosmic rays is negligible. The livetime and observed number of atmospheric neutrino events during the four SK run periods are summarized in Table 2. Fully contained (FC) events deposit all of their Cherenkov light in the inner detector, while partially contained (PC) events have exiting tracks which deposit some Cherenkov light in the outer detector. The neutrino interaction vertex is required to be reconstructed within a 22.5 kiloton fiducial volume, defined to be $> 2$ m from the PMT wall.

The FC events are classified into "sub-GeV" ($E_{vis} <$ 1330 MeV) and "multi-GeV" ($E_{vis} >$ 1330 MeV). These events are further separated into sub-samples based on the number of observed Cherenkov rings. Single- and multi-ring are then divided into electron-like (e-like) or muon-like ($\mu$-like) samples depending on pattern identification of the most energetic Cherenkov ring. The sub-GeV samples are additionally divided based on their number of decay-electrons and their likelihood of being a $\pi^0$.

The PC events are separated into "OD stopping" and "OD through-going" categories based on the amount of light deposit by the exiting particle in the OD.

Energetic atmospheric $\nu_\mu$'s passing through the Earth interact with rock surrounding the detector and produce muons via charged current interactions. These neutrino events are observed as upward going muons. Upward going muons are classified into two types. One is "upward through-going muons" which have passed through the detector, and the other is "upward stopping muons" which come into and stop inside the detector. The upward through-going muons are subdivided into "showering" and "non-showering" based on whether their Cherenkov pattern is consistent with light emitted from an electro-magnetic shower produced by a very high energy muon.

The livetime and number of observed events for the first three SK periods are summarized in Table 3.

Table 2. Atmospheric neutrino livetimes and the number of observed FC and PC events for each SK run period. (*)Numbers for SK-IV are preliminary since data taking is still ongoing.

| | Livetime(days) | FC | PC |
|---|---|---|---|
| SK-I | 1,489 | 12,232 | 896 |
| SK-II | 799 | 6,584 | 429 |
| SK-III | 518 | 4,356 | 343 |
| SK-IV* | 449 | 3,638 | 289 |

Table 3. Atmospheric neutrino induced upward-going muon livetime and the number of observed events for the first three SK run periods.

| | Livetime(days) | through-going | stopping |
|---|---|---|---|
| SK-I | 1,646 | 1,856 | 458 |
| SK-II | 828 | 889 | 228 |
| SK-III | 636 | 735 | 210 |

The zenith angle and lepton momentum distributions for each of the above samples compared with the atmospheric neutrino Monte Carlo predictions are shown in Fig. 8. The prediction is based on the recent precise measurements of primary cosmic rays by BESS, AMS and a three dimensional calculation of the neutrino flux by Honda *et al.* The $\mu$-like data from SK exhibit a strong up-down asymmetry in their zenith angle ($\Theta$) distribution while no significant asymmetry was observed in the $e$-like data. The data were compared with the Monte Carlo expectation without neutrino oscillations and the best-fit expectation for $\nu_\mu \leftrightarrow \nu_\tau$ oscillations. The oscillated Monte Carlo reproduces the zenith angle distributions of the data well.

We carried out a neutrino oscillation analysis using the entire SK-I, II and III atmospheric neutrino data set. Red contours in Figure 9 show the allowed neutrino oscillation parameter regions for $\nu_\mu \leftrightarrow \nu_\tau$ oscillations. The best fit oscillation parameters are $\sin^2 2\theta = 1.0$ and $\Delta m^2 = 2.2 \times 10^{-3}\mathrm{eV}^2$. The allowed oscillation parameter range is $\sin^2 2\theta > 0.96$ and $\Delta m^2 = (1.8 - 2.6) \times 10^{-3}\mathrm{eV}^2$ at $90\,\%$ C.L.

The atmospheric neutrino data are well described by neutrino oscillations. The survival probability of a $\nu_\mu$ is given by a sinusoidal function of $L/E$, where $L$ is the distance traveled by the neutrino and $E$ is the neutrino energy. We also

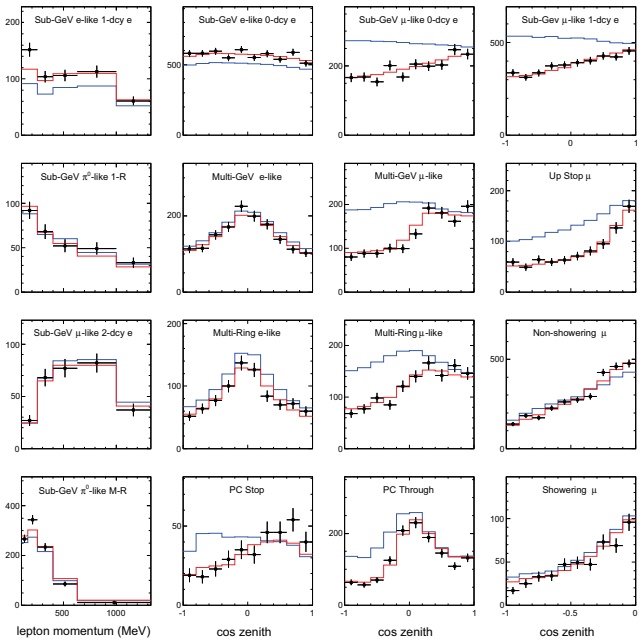


Fig. 8. The zenith angle and lepton momentum distributions for each data sample. $\cos\Theta = 1$ indicates downward-going particles. The blue histograms show the MC prediction without neutrino oscillation and the red histograms show the MC prediction for $\nu_\mu \leftrightarrow \nu_\tau$ oscillations with $\sin^2 2\theta = 1.0$ and $\Delta m^2 = 2.1 \times 10^{-3}\mathrm{eV}^2$.

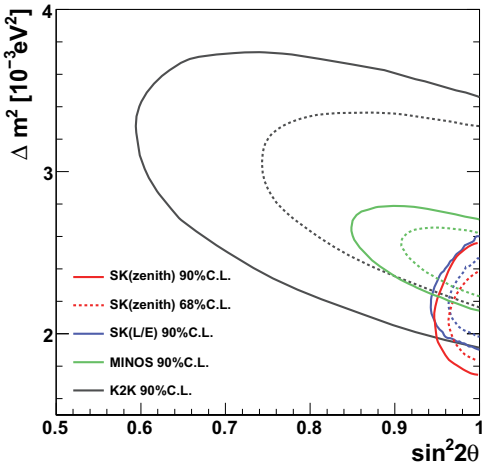


Fig. 9. Allowed region of $\nu_\mu \rightarrow \nu_\tau$ neutrino oscillation parameters obtained by SK using contained atmospheric neutrino events and upward-going muon events. Solid and dashed contours correspond to 90 and 68% C.L. respectively. Red contours are obtained by the zenith angle analysis and blue contours are obtained by the L/E analysis (see text). Allowed regions by long-baseline neutrino oscillation experiment K2K and MINOS are shown in black and green contours, respectively.

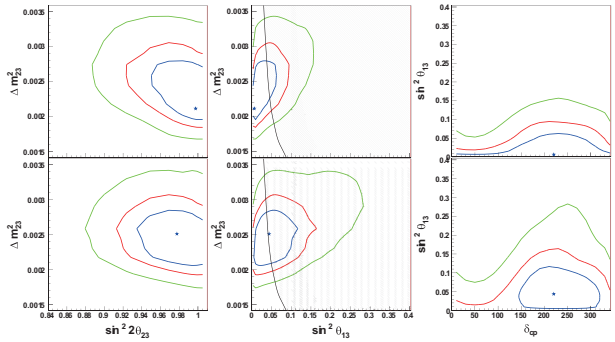

Fig. 10. The allowed regions for ($\Delta m^2$, $\sin^2 2\theta_{23}$); left, ($\Delta m^2$, $\sin^2\theta_{13}$); middle, and ($\sin^2\theta_{13}$, $\delta_{cp}$); right for the normal (upper figure) and inverted (lower figure) hierarchy. The blue, red, and green contours correspond to 68, 90 and 99% C.L. allowed regions obtained by this analysis, respectively. The shaded regions corresponds to the area excluded at 90% C.L. by the CHOOZ experiment.

performed an oscillation analysis binning the data in the combined variable $L/E$. Low energy or horizontal-going events are rejected in this analysis since they have either large scattering angles or large $dL/d\Theta_{\mathrm{zenith}}$. This creates a sample with good resolution in the $L/E$ variable that is used to search for the maximum in the oscillation probability sinusoid.

The obtained allowed oscillation parameter regions are shown by the green contours in Figure 9. This result is consistent with that of the oscillation analysis using the zenith angle binning. The observed $L/E$ distribution gives the first direct evidence that the neutrino survival probability obeys the sinusoidal function predicted by neutrino flavor oscillations.

Two flavor neutrino oscillations which assume that $\theta_{13}$=0 and $\Delta m^2_{12} \ll \Delta m^2_{23}$ successfully describe the SK atmospheric neutrino data and with maximum mixing ($\theta_{23}$=$\pi/4$). However, nonzero $\theta_{13}$ may be observable in the event rate of Multi-GeV electron neutrino events, and to a lesser extent in the oscillations of Multi-GeV muon neutrinos. Additionally, the effects of the solar oscillation parameters and non-maximal mixing can be observable as a sub-leading oscillation effect on the event rate of the Sub-GeV electron-like samples. If the CP violating term $\delta_{cp}$ is also considered, there are additional subdominant oscillation effects predicted across many of the SK atmospheric neutrino samples.

We have performed an extended oscillation analysis including all the mixing parameters and the CP violating term. The matter effect in the Earth is also considered in this calculation and both the normal and inverted mass hierarchies are tested.

Figure 10 shows the allowed regions for ($\Delta m^2$, $\sin^2 2\theta_{23}$), ($\Delta m^2$, $\sin^2\theta_{13}$), and ($\sin^2\theta_{13}$, $\delta_{cp}$) for the normal and inverted mass hierarchies. A comparison of $\chi^2$ between normal and inverted hierarchy case is shown in Figure 11.

The best fit parameter sets are ($\Delta m^2_{23}$, $\sin^2\theta_{23}$, $\sin^2\theta_{13}$, $\delta_{CP}$)= ($2.11{\cdot}10^{-3}eV^2$, 0.525, 0.006, 220°) for the normal hierarchy and ($2.51{\cdot}10^{-3}eV^2$, 0.575, 0.046, 220°) for the inverted hierarchy case. All fits are consistent with the two flavor oscillation results and CHOOZ experiment's upper limit on $\theta_{13}$. No preference for either mass hierarchy exists in the data. [13].

We also performed a test for CPT violations using the atmospheric neutrino data using separate two-neutrino disappearance models for neutrinos and anti neutrinos:

$$P(\nu_\mu \rightarrow \nu_\mu) = 1 - \sin^2 2\theta \sin(\tfrac{\Delta m^2 L}{E}),$$
$$P(\bar{\nu}_\mu \rightarrow \bar{\nu}_\mu) = 1 - \sin^2 2\bar{\theta} \sin(\tfrac{\Delta \bar{m}^2 L}{E}).$$

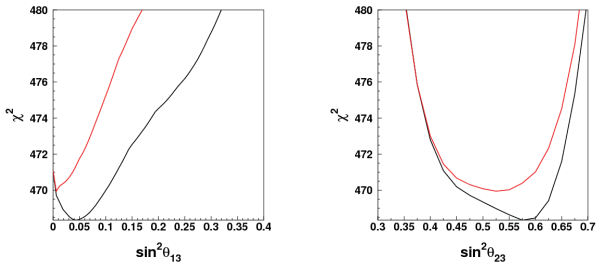


Fig. 11. $\chi^2$ distribution as a function of (left:)$\sin^2\theta_{13}$ and (right:)$\sin^2\theta_{23}$. The normal hierarchy and inverted hierarchy cases are plotted with red and black lines, respectively.

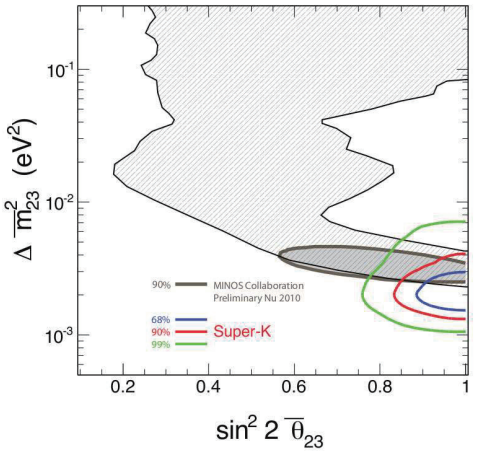


Fig. 12. Allowed regions for the anti-neutrino mixing parameters. The blue, red and green contours correspond to the 68%, 90%, and 99% C.L. allowed regions respectively. Shaded region shows the allowed regions by MINOS experiment[14],[15].

The best fit parameters are ( $\Delta m^2$, $\Delta\overline{m}^2$, $\sin^2 2\theta$, $\sin^2 2\overline{\theta}$ ) = ( $2.2\times10^{-3}$ eV$^2$, $2.0\times10^{-3}$ eV$^2$, 1.0, 1.0 ) and the allowed region for antineutrino mixing parameters is shown in Figure 12. The atmospheric mixing parameters for antineutrino oscillations are consistent with those for neutrinos and therefore no evidence for CPT violation is found.

We have observed 449days of atmospheric neutrinos data with SK-IV. The quality of the observed data are consistent with the previous SK-I, II, III results. Due to the electronics upgrade, several performance are expected to be improved, such as the performance of Michel electrons tagging, the energy resolution in multi-GeV electron sample, etc. The further analysis including SK-IV data are going on.

## Search for nucleon decay

Proton decays and bound neutron decays (nucleon decays in general) is the most dramatic prediction of Grand Unified Theories in which three fundamental forces of elementary particles are unified into a single force. Super-Kamiokande (SK) is the world's largest detector to search for nucleon decays and it has accumulated data of 91.7 kt·yrs (SK-I), 49.2 kt·yrs (SK-II), and 31.9 kt·yrs (SK-III) resulting in 173 kt·yrs data in total. Various nucleon decay modes have been looked for in the period from SK-I to SK-III data but we have found no significant signal excess so far.

A proton decay into one positron and one neutral pion ($p\to e^+\pi^0$) is one of the most popular decay modes. This decay mode is mediated by super-heavy gauge bosons and discovery of the signal would give us the information of the mass of the gauge mesons. To discriminate the signal from the atmospheric neutrino background, we reconstruct the number of particles (Cherenkov rings) and reconstruct the total visible energy corresponding to parent proton mass and total momentum corresponding to the proton's Fermi momentum. The signal efficiency of SK-I, SK-II, and SK-III are 44.9%, 43.7% and 45.2% respectively. It is remarkable that SK-II has almost same efficiency as SK-I and SK-III even though the photocoverage area of SK-II is about one half (19%) of the others. The background induced by the atmospheric neutrino interactions is estimated to be 0.37 for the period from SK-I to SK-III (173 kt·yrs). The BG rate was confirmed by an artificial neutrino beam by using 1-kton water Cherenkov detector [16]. Because there are no candidate events in data from SK-I to SK-III, we obtained a lower limit on the partial lifetime of the proton; $\tau/B_{p\to e^+\pi^0} > 1.0\times10^{34}$ years at 90% confidence level [17].

In addition, we looked for SUSY favored decay modes which include K mesons in the final state, $p\to\overline{\nu}K^+$, $n\to\overline{\nu}K^0$, $p\to\mu^+K^0$, and $p\to e^+K^0$. In $p\to\overline{\nu}K^+$ search, we have analyzed data until SK-III. In this mode, we tag the signal by decay products from $K^+$. The momentum of $K^+$ is below the Cherenkov threshold, and is stopped in the water and decay into $\mu^+\nu$ or $\pi^+\pi^0$. On the other hand, the residual nucleus after proton decay emits $\gamma$ ray ( 40% probability) and it is also useful to tag the proton decay signal.

Figure 13 shows one analysis method in which we search for muon with the monochromatic momentum 236 MeV/c. It shows the comparison between data and fitting results of the muon momentum distribution for single-ring $\mu$-like events. We have analyzed the data from SK-I to SK-III, and there are no significant signal excess in all methods. Therefore we conclude that there is no evidence of nucleon decays and we calculated partial lifetime limits taking into account systematic uncertainties. Obtained limits are $3.3\times10^{33}$ years at 90% confidence level for $p\to\overline{\nu}K^+$.

Moreover, we have performed extensive search for events; $n\to\nu\pi^0$, $pp\to K^+K^+$ but there are no candidates in the data and we got lifetime limits $1.1\times10^{33}$ years and $1.4\times10^{32}$ years, respectively.

## Bibliography

[1] Super-Kamiokande Collaboration, "Solar neutrino measurements in Super-Kamiokande-I", *Phys. Rev.* D 73 (2006) 112001.

[2] W. T. Winter *et al.*, "The $^8$B neutrino spectrum", *Phys. Rev.* C 73 (2006) 025503.

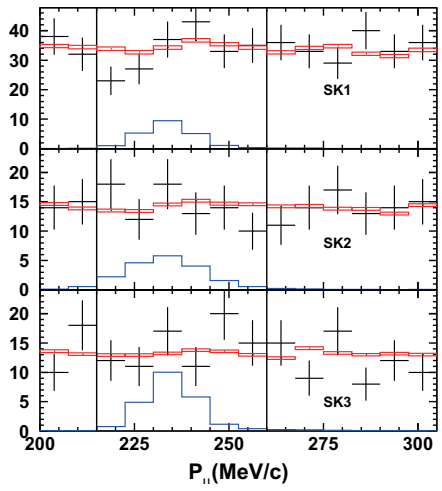


Fig. 13. The comparison between data and fitting results of the muon momentum distribution for single-ring $\mu$-like events. The filled circles show data with statistical errors. The solid line shows $p \to \bar{\nu}K^+$ MC. The dashed line shows the best fitted atmospheric neutrino MC with free normalization.


[3] J.N.Bahcall and M.H.Pinsonneault, "What Do We (Not) Know Theoretically about Solar Neutrino Fluxes?", *Phys. Rev. Lett.* 92 (2004) 121301.

[4] B. Aharmim *et al.*, "Independent Measurement of the Total Active $^8$B Solar Neutrino Flux Using an Array of $^3$He Proportional Counters at the Sudbury Neutrino Observatory", *Phys. Rev. Lett.* 101 (2008) 011301.

[5] B. Aharmim *et al.*, "Low Energy Threshold Analysis of the Phase I and Phase II Data Sets of the Sudbury Neutrino Observatory" *Phys. Rev.* C 81 (2010) 055504.

[6] B. Aharmim *et al.*, "Determination of the $\nu_e$ and Total $^8$B Solar Neutrino Fluxes with the Sudbury Neutrino Observatory Phase I Data Set", *Phys. Rev.* C 75 (2007) 045502.

[7] S.N.Ahmed *et al.*, "Electron Energy Spectra, Fluxes, and Day-Night Asymmetries of $^8$B Solar Neutrinos from the 391-Day Salt Phase SNO Data Set", *Phys. Rev.* C 72 (2005) 055502.

[8] C.Arpesella *et al.*, "Direct Measurement of the $^7$Be Solar Neutrino Flux with 192 Days of Borexino Data", *Phys. Rev. Lett.* 101 (2008) 091302.

[9] B.T.Cleveland *et al.*, "Measurement of the Solar Electron Neutrino Flux with the Homestake Chlorine Detector Bruce T. Cleveland", *Astrophys. J.* 496 (1998) 505.

[10] J.N.Abdurashitov *et al.*, "Measurement of the solar neutrino capture rate with gallium metal", *Phys. Rev.* C 60 (1999) 055801.

[11] M.Altmann *et al.*, "GNO solar neutrino observations: results for GNO I", *Phys. Lett.* B 490 (2000) 16.

[12] S. Abe *et al.*, "Precise Measurement of Neutrino Oscillation Parameters with KamLAND", *Phys. Rev. Lett.* 100 (2008) 221803.

[13] R. Wendell, C. Ishihara *et al.* [Super-Kamiokande Collaboration], "Atmospheric neutrino oscillation analysis with subleading effects in Super-Kamiokande I, II, and III", Phys. Rev. D 81 (2010) 092004.

[14] I. Danko *et al.* [MINOS Collaboration], "First Observation of Accelerator Muon Antineutrinos in MINOS", To be published in the proceedings of the DPF-2009 conference, Detroit, MI, July 27-31, 2009 [arXiv:0910.3439v1 [hep-ex]]

[15] P. Vahle, for the MINOS collaboration, "New Results from MINOS", Presented at Neutrino 2010, June 14, 2010 Athens, Greece

[16] S. Mine *et al.* [K2K Collaboration], "Experimental study of the atmospheric neutrino backgrounds for proton decay to positron and neutral pion searches in water Cherenkov detectors," Phys. Rev. D **77**, 032003 (2008) [arXiv:0801.0182 [hep-ex]].

[17] H. Nishino *et al.* [Super-Kamiokande Collaboration], "Search for Proton Decay via $p \to e^+\pi^0$ and $p \to \mu^+\pi^0$ in a Large Water Cherenkov Detector," Phys. Rev. Lett. **102**, 141801 (2009) [arXiv:0903.0676 [hep-ex]].


## Hyper-Kamiokande

Feasibility study has been performed for the next generation nucleon decay and neutrino detector Hyper-Kamiokande that aims to explore unification of elementary particles and fundamental properties of neutrinos. The water Cherenkov detector with the dimension of 1 million tones has capability of exploring nucleon lifetimes about 10 times as long as the limits set by the Super-Kamiokande. For example, the sensitivity for the decay mode $p \to e^+\pi^0$ is expected to be beyond $1 \times 10^{35}$ years. The detector also aims to study on neutrino properties such as Dirac CP phase, mass hierarchy, octant of

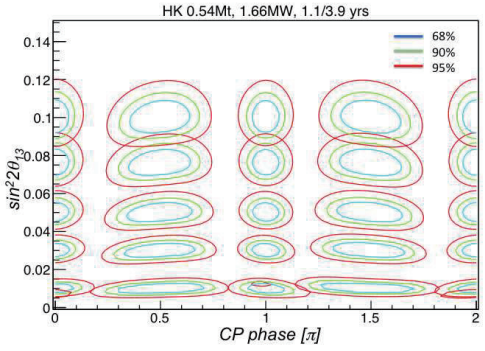


Fig. 1. The expected sensitivity for $\theta_{13}$ and $\delta$ by using upgraded JPARC $\nu$ beam and the Hyper-Kamiokande.

$\theta_{23}$, and so on by using a high power accelerator based neutrino beam and atmospheric neutrinos. Figure 1 shows the expected sensitivity for the mixing angle $\theta_{13}$ and CP phase $\delta$ by using upgraded JPARC neutrino beam with the power of 1.66 MW and the Hyper-Kamiokande detector with the fiducial volume of 0.54 Megaton.

Conceptual design, scheduling, and costing of the detector are going on based on various studies.

## T2K Experiment

[Spokesperson : T. Kobayashi]

High Energy Accelerator Research Organization (KEK), Japan

In collaboration with the members of :
ICRR, University of Tokyo, Japan; KEK, Japan; Kobe University, Japan; Kyoto University, Japan; Miyagi University of Education, Japan; Osaka City University, Japan; University of Tokyo, Japan; TRIUMF, Canada; University of Alberta, Canada; University of British Columbia, Canada; University of Regina, Canada; University of Toronto, Canada; University of Victoria, Canada; York University, Canada; CEA/DAPNIA Saclay, France; IPN Lyon (IN2P3), France; LLR Ecole polytechnique (IN2P3), France; LPNHE-Paris, France; RWTH Aachen University, Germany; INFN Sezione di Bari, Italy; INFN Sezione di Napoli, Italy; INFN Sezione di Padova, Italy; INFN Sezione di Roma, Italy; Chonnam National University, Korea; Dongshin University, Korea; Sejong University, Korea; Seoul National University, Korea; Sungkyunkwan University, Korea; Andrzej Soltan Institute for Nuclear Studies (IPJ), Poland; Henryk Niewodniczanski Institute of Nuclear Physics (IFJ PAN), Poland; Technical University, Poland; University of Silesia, Poland; University of Warsaw, Poland; Wroclaw University, Poland; Institute for Nuclear Research, Russia; IFAE, Universitat Autonoma de Barcelona, Spain; IFIC, University of Valencia, Spain; ETHZ, Switzerland; University of Bern, Switzerland; University of Geneva, Switzerland; Imperial College London, UK; Lancaster University, UK; Queen Mary, University of London, UK; STFC/Rutherford Appleton Laboratory/Daresbury Laboratory, UK; University of Liverpool, UK; University of Oxford, UK; University of Sheffield, UK; University of Warwick, UK; Boston University, USA; Brookhaven National Laboratory, USA; Colorado State University, USA; Duke University, USA; Louisiana State University, USA; Stony Brook University, USA; University of California, Irvine, USA; University of Colorado, USA; University of Pittsburgh, USA; University of Rochester, USA; University of Washington, USA;

The K2K experiment established a technique of the accelerator-based long baseline neutrino oscillation experiment and successfully confirmed neutrino oscillation. Meanwhile, several experiments have measured 2 out of 3 neutrino mixing angles and 2 mass differences using accelerator, atmospheric, solar and reactor neutrinos. However, one mixing angle, $\theta_{13}$, has not been measured and has only been found to be small. The experimental sensitivity of the $\theta_{13}$ measurement is still limited by statistics and thus, there is a chance to measure the value with a much more intense neutrino beam. Furthermore, if $\theta_{13}$ is large enough, it may be possible to search for CP violation in the lepton sector and to measure the CP phase, $\delta$, which is one of the last parameters of the neutrino oscillation. Therefore, several next generation experiments, which utilize high intensity neutrino beams, have been planned for the further investigation of the neutrino oscillations. The Tokai to Kamioka long baseline neutrino oscillation experiment (T2K) is one of the new generation experiments [1]. The intense neutrino beam is produced by using a new high intensity proton synchrotron accelerator at the J-PARC site in Tokai village. As a far detector to study neutrino oscillation phenomena, the T2K experiment utilizes Super-Kamiokande(SK), which is located at 295 km from the beam production target.

In the design of the neutrino beam-line for T2K, the concept of off-axis beam [2] is introduced. With this method, it is possible to efficiently produce a low energy neutrino beam with narrow energy spread from the high energy proton beam. Also, it is possible to tune the peak energy by changing the direction of the beam direction. Based on this concept, the direction of the neutrino beam is intentionally shifted from the direction of the SK detector by a few degrees and also the direction of the beam is tunable. The initial peak position of the neutrino beam energy is adjusted to $\sim 650$ MeV by setting the off-axis angle to $\sim 2.5^\circ$ to maximize the neutrino oscillation effects at the SK detector. The generated neutrino beam is primarily $\nu_\mu$ with a small contamination of $\nu_e$, which is estimated to be $\sim 0.4\%$ at the flux peak. The design intensity of the T2K neutrino beam is almost two orders of magnitude higher compared to the K2K neutrino beam.

As described, one of the motivations of this experiment is to measure the neutrino oscillation parameter $\theta_{13}$, which is only known to be small $(\sin^2 2\theta_{13} \lesssim 0.1)$ by the previous experiments. It is of great interest to know the value of a nonzero $\theta_{13}$ or how close to zero $\theta_{13}$ is. The T2K experiment will try to measure $\theta_{13}$ using the electron neutrino appearance channel and there is a possibility to be the first experiment to observe the neutrino oscillation signature with the appearance channel. Figure 1 shows T2K's expected sensitivity to $\theta_{13}$ as a function of $\Delta m^2_{23}$. The shaded region is the excluded region by the CHOOZ experiment. As shown in this figure, the T2K experiment has more than one order of magnitude better sensitivity compared to the current best limit.

Another major purpose of this experiment is precise measurement of $\theta_{23}$ and $\Delta m^2_{23}$. Owing to the high statistics, the precisions of these parameters are expected to be almost one order of magnitude better than before. So far, $\theta_{23}$ mixing is known to be very large and almost maximal from the Super-Kamiokande, K2K and the MINOS experiments. If $\sin^2 2\theta_{23} = 1$, it may suggest an underlying new symmetry.

To achieve these physics goals, intensive works for improving the detector sensitivity and stability have been done in Super-Kamiokande.

In summer 2008, the DAQ system was upgraded and newly developed ADC/TDC modules called QBEE were installed. Essential components on the QBEE for the analog signal processing and digitization are the custom QTC

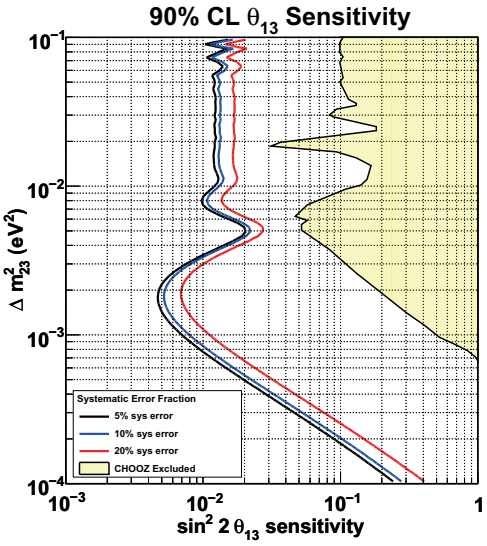


Fig. 1. Expected sensitivity to $\theta_{13}$ by T2K (750 kW beam, 5 years of running) as a function of $\Delta m^2_{23}$ compared with current best limit by the CHOOZ reactor experiment.

(Charge-to-Time Converter) ASIC and the multi-hit TDC. The QBEE realizes high-speed signal processing by combining the pipelined components like the QTC, TDC and FPGA. In the new system, all the hit signals of all the PMTs are recorded on online DAQ machines and then events are extracted by software trigger. The T2K neutrino beam induced events are stored based on the beam extraction timing from the accelerator using the GPS systems both at the SK site and the J-PARC site. With this scheme, it is possible to record all the PMT hit information around the beam arrival timing as the T2K events. In order to make this system work, the beam timing is required to be transferred within a few seconds. The dedicated network line from the J-PARC accelerator to the Kamioka site has been prepared to transfer the necessary timing information as soon as the protons are extracted. This system has been tested using the dummy timing information for several months. As a result, the typical latency to transfer the beam timing was measured to be less than several tens of ms, which is much shorter than the 3 second allowance, and the trigger system was confirmed to work as designed.

In addition, the determination of the absolute event time using the GPS system at the SK has been checked in detail. By measuring each delay in the related hardwares, the accuracy of the event time determination has been improved from $\sim 1\mu$sec to $\sim$200nsec, which is small enough to identify the beam spill structure (i.e. 581nsec bunch spacing) in the data observed at SK. The classification program of the T2K events at SK is very simple one, which classify each event into the fully-contained (FC) sample, the outer-detector (OD) event sample, and the low-energy (LE) sample. The algorithm to count the spills used for oscillation analyses, which is necessary to derive the expected number of neutrino events, has also been developed and confirmed to work well by using the data accumulated by the dummy beam timing information.

The response of the far detector, SK, must be well understood in order to maximize the sensitivities to oscillation parameters such as $\theta_{13}$, $\theta_{23}$, and $\Delta m^2_{23}$. In the electron appearance search, single $\pi^0$ production backgrounds can fake single-ring electron signals when one of the two $\gamma$ rings from a $\pi^0$ decay is not identified. Even if a small portion of $\nu_\mu$ induced events are mis-identified as electrons, it will be a serious background. Therefore, the ring identification and the particle identification capabilities of the detector have been studied very carefully. The special reconstruction program to reject $\pi^0$ BG events efficiently has been developed successfully. In order to remove any bias on the $\nu_e$ appearance analyses, the selection criteria of the $\nu_e$ signal sample were determined according to the MC studies before looking at the T2K events observed at SK. It is also important to reduce the uncertainty in the absolute energy scale measurement in order to achieve a $\Delta m^2_{23}$ measurement with a few % accuracy. The better understanding of detector responses by various calibrations and improvements of related softwares enabled us to reduce the uncertainty on energy scale stability (2%→0.5%) and the uncertainty on the absolute energy scale (2%→1%). Calibrations of the fundamental properties such as the charge and timing responses of each PMT, the light attenuation and scattering in water, and the light reflection by the detector materials have been carried out constantly.

Also, the R&D work of the possible near detector to measure the left right symmetry of the neutrino beam is going on in order to investigate the feasibility of the future extension.

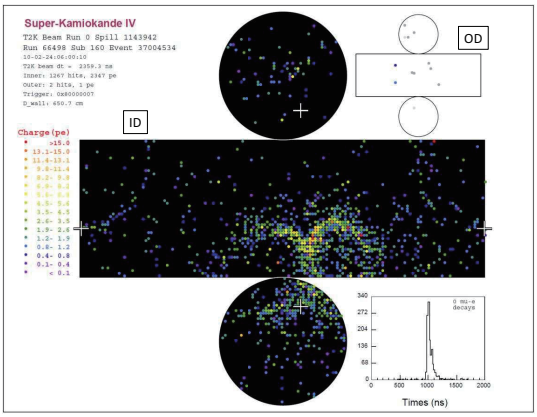


Fig. 2. Event display of the first T2K event in Super-Kamiokande. The larger unrolled cylinder shows Inner Detector (ID), and the smaller one shows Outer Detector (OD). The dots indicate hit PMTs in the detectors.

The construction of the beamline facility for the T2K experiment has been completed by the spring of 2009. After careful checks and commissioning of each component, the data accumulation for neutrino oscillation studies has started in January 2010. About $2 \times 10^{19}$ protons have been delivered to the neutrino production target by the end of March 2010. The neutrino beam is produced stably with intensity of $\sim$50kW. We plan to increase the beam intensity over 100kW autumn 2010. In part of the T2K data obtained at SK from January 2010, 22 fully-contained (FC) events were found. Figure 2 shows the event display of the first T2K event observed in SK. Figure 3 shows an event timing distribution of

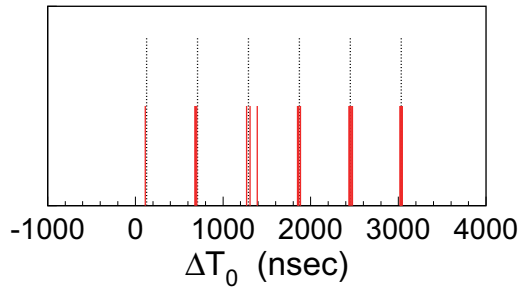


Fig. 3. Event timing distribution of FC events observed at SK (solid lines). The timing is corrected for the neutrino TOF and hardware delay so as to set the timing of the spill head at zero. The vertical dotted lines represent the fitted 581nsec-interval bunch timing.

these FC events. The beam structure (6 bunches) is clearly visible. Expected non-beam BG fraction in the FC event sample is negligibly small ($< 10^{-3}$). T2K data taking at SK has been very stable and the dead time fraction so far is less than 1%.

The first T2K result on neutrino oscillation measurement will be obtained in FY2010.

## Bibliography

[1] Y. Itow *et al.*, "The JHF-Kamioka neutrino project", (2001), hep-ex/0106019.

[2] BNL-E889 proposal, (1995).

## XMASS experiment

XMASS is a multi-purpose (detection of dark matter, neutrino-less double beta decay, and $^{7}$Be/pp solar neutrinos) experiment using liquid xenon. Primary goal is the detection of the dark matter. For this purpose, the construction was approved in 2007. We have been constructing the detector aiming to start the experiment in 2010 summer. In the future, XMASS also aims the detection of the neutrino-less double beta decay and $^{7}$Be/pp solar neutrinos.

Astronomical observations suggest that there is dark matter (non-luminous particles with mass) in the universe. One of the most likely candidates for dark matter is a weakly interacting massive particle (WIMP), such as the lightest supersymmetric particle. XMASS searches for the WIMP-xenon nucleus interaction in liquid xenon. Liquid xenon has the following advantages to detect this interaction. Liquid xenon yields large amount of scintillation light (42,000 photons/MeV). This enables us to detect small energy signals such as dark matter recoil. Due to the high atomic number of xenon ($Z = 54$) and the high density of liquid xenon ($\sim 3\,\mathrm{g/cm^3}$), target volume can be small and external background gamma-rays can be absorbed within a short distance from the detector wall. With 20 cm self-shielding, external $^{238}$U background is expected to be reduced to less than $10^{-3}$ in the 5-50 keV electron recoil energy range from the simulation study. Figure 1 shows the expected sensitivity of the XMASS experiment. Our goal is to reach $10^{-45}$ cm$^2$.

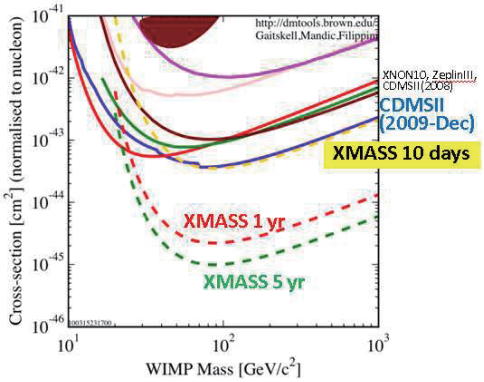


Fig. 1. XMASS sensitivity compared to other experiments. See http://dmtools.berkeley.edu/

Fig. 2. Hall-C. Water tank is left side.

The detector is being constructed at Hall-C in the Kamioka mine 1,000 m underneath the top of Mt. Ikenoyama. Figure 2 shows the photo of the Hall-C. The volume of the Hall-C is 15 m in width, 21 m in depth and 15 m in height. Most of the XMASS facilities are located at the Hall-C. In order to shield external gamma-rays and neutrons, the liquid xenon detector (inner detector: ID) is located at the center of the cylindrical water tank (outer detector: OD) which is 10.5 m in height and 10 m in diameter as shown in Figure 4. The water tank will be instrumented with 72 50-cm diameter inward facing PMTs to tag the incoming cosmic ray muons. The ID is in the liquid xenon copper vessel as shown in Figure 4. The ID PMTs are supported by the PMT holder and almost sphere shape of the 857 kg liquid xenon is filled inside the PMTs.

Dominant external background was expected to originate from the ID PMTs. We have developed the very low background PMT, Hamamatsu R10789 to reduce the radioactive contamination. In Table 1, history of the PMT development and achieved background level are shown. The background contribution from the PMTs is expected to be less than $10^{-4}$ count/day/keV/kg from the simulation study, that is better than our goal. Mass production of the PMTs had been completed and the PMTs were delivered by October 2009. We have checked all the PMTs. Dark noise rate at liquid xenon temperature was about 20 Hz, which is enough low for our measurement.

PMT installation to the holder started in December 2009

Fig. 3. Schematic view of the water tank and the liquid xenon vessel.


Fig. 5. Photo with the holder and PMTs.

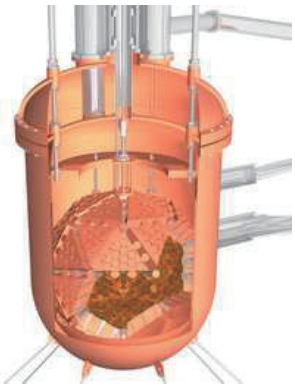

Fig. 4. Schematic view of the liquid xenon vessel and the PMT holder.

in the water tank. The residual dust in the ID becomes the radioactive background source. Moreover, high radon concentration in the air causes higher background from the PMTs Therefore, we have developed low dust and radon system in the water tank. The air in the water tank keep low radon concentration using radon free air. We made a clean booth inside the water tank and all the installation was done there. PMT installation and cabling has been completed in February 2010. Figure 5 shows the holder and PMTs after the installation. During the installation radon concentration is about 200 mBq/m$^3$ which is 1/100 of that in the atmosphere. Also the dust level is less than 1000 particles/ft$^3$ (Particle size is more than 0.5 $\mu$m).

PMT signals are sent to the top of the water tank and are recorded by ADC and FADC. Electronics hut was built on the top of the water tank in July 2009. All of the modules were installed for the data taking of 642 channel for the ID and 72 channel for the OD. We reuse the modules which had worked for the Super-K experiment.

Internal background needs to be removed before and also during the data taking. $^{85}$Kr in xenon is a potential source of the radioactive contamination. We have developed a distillation system to reduce the $^{85}$Kr contamination. We have tested the performance of the system in July 2009. The $^{85}$Kr concentration was reduced by $10^{-5}$ with a 4.7 kg Xe/hour process speed. With this speed, we can process one ton xenon in ten days. Though we don't need to remove the $^{85}$Kr in xenon during the data taking, radon needs to be removed before and during the data taking because radon is emanated from the surrounding material. We are now developing the radon removal system.

We will install the liquid xenon vessel and pipes and plan to start data taking in 2010.

Table 1. History of the ID PMT development. Background level was measured by Germanium detector (mBq/PMT is in unit.)

| PMT type | U | Th | $^{40}$K | $^{60}$Co |
|---|---|---|---|---|
| Proto-type (2000) | 50 | 13 | 610 | $<$1.8 |
| R8778 (2002) | 18$\pm$2 | 6.9$\pm$1.3 | 140$\pm$20 | 5.5$\pm$0.9 |
| R10789 (2009) | 0.7$\pm$0.28 | 1.5$\pm$0.31 | $<$5.1 | 2.9$\pm$0.16 |

**References**

1. Y. Suzuki et al., "Low energy solar neutrino detection by using liquid xenon", Aug. 2000, hep-ph/0008296.

2. S. Moriyama, "XMASS EXPERIMENT I", Proceedings of the International Workshop on Technique and Application of Xenon Detectors, Kashiwa, Japan, 3-4 Dec. 2001.

3. M. Yamashita, "XMASS at Kamioka: Large Scale Cryogenic detector in the underground laboratory", presentation at the WONDER 2010 Conference, Gran Sasso, Italy, 22-23 March 2010.

# HIGH ENERGY COSMIC RAY DIVISION

## Overview

Three major research activities of the High Energy Cosmic Ray Division are the study of very high energy gamma rays by the CANGAROO group, extremely high energy cosmic rays by the Telescope Array (TA) group, and very high energy cosmic rays and gamma rays by the Tibet AS$\gamma$ Collaboration. Other activities, such as experiments utilizing the Akeno observatory, the Norikura observatory, the Mt. Chacaltaya observatory (jointly operated with Bolivia), and the emulsion-pouring facilities are closely related to inter-university joint research programs. Also an all-sky high resolution air-shower detector (Ashra) has been installed on the Hawaii island. The High Energy Astrophysics Group was newly-created in this fiscal year and aims to explore various high energy astrophysical phenomena, mainly by theoretical approaches.

The CANGAROO project (Collaboration of Australia and Nippon for a GAmma-Ray Observatory in the Outback) is a set of large imaging atmospheric Cherenkov telescopes to make a precise observation of high-energy air showers originated by TeV gamma rays. It started as a single telescope with a relatively small mirror (3.8 m in diameter) in 1992. In 1999 a new telescope with a 7-m reflector has been built, and now it has a 10-m reflector with a fine pixel camera. The main purpose of this project is to explore the violent, non-thermal universe and to reveal the origin of cosmic rays. An array of four 10-m telescopes has been completed in March 2004 so that more sensitive observations of gamma rays are realized with its stereoscopic imaging capability of Cherenkov light. Several gamma-ray sources have been detected in the southern sky and detailed studies of these sources are now ongoing.

At the Akeno observatory, a series of air shower arrays of increasing geometrical sizes were constructed and operated to observe extremely high energy cosmic rays (EHECRs). The Akeno Giant Air Shower Array (AGASA) was operated from 1991 to January 2004 and covered the ground area of 100 $km^2$ as the world largest air shower array. In 13 years of operation, AGASA observed a handful of cosmic rays exceeding the theoretical energy end point of the extra-galactic cosmic rays (GZK cutoff) at $10^{20}$ eV. The Telescope Array (TA), a large plastic scintillator array with air fluorescence telescopes, has been constructed in Utah, USA, which succeeds AGASA and measures the EHECRs with an order of magnitude larger aperture than that of AGASA to unveil the origin of super-GZK cosmic rays discovered by AGASA. The full-scale TA has started taking data as the largest array viewing the northern sky.

An air shower experiment aiming to search for celestial gamma-ray point sources started in 1990 with Chinese physicists at Yangbajing (Tibet, 4,300 m a.s.l.) and has been successful. This international collaboration is called the Tibet AS$\gamma$ Collaboration. An extension of the air shower array was completed in 1995 and an emulsion chamber has been combined with this air shower array since 1996 to study the primary cosmic rays around the knee energy region. After successive extensions carried out in 1999, 2002 and 2003, the total area of the air shower array amounts to 37,000 $m^2$. The sun's shadow in cosmic rays affected by the solar magnetic field was observed for the first time in 1992, utilizing its good angular resolution at multi-TeV energy region. From this experiment with better statistics, we expect new information to be obtained on the large-scale structure of the solar and interplanetary magnetic field and its time variation due to the 11-year-period solar activities.

A new type of detector, called Ashra (all-sky survey high resolution air-shower detector), was developed. The first-phase stations were installed near the Mauna Loa summit in the Hawaii Island and high-efficiency observation is continuing. It monitors optical and particle radiation from high-energy transient objects with a wide field-of-view.

The High Energy Astrophysics group is conducting theoretical researches on fundamental processes responsible for nonthermal particle acceleration in various astrophysical environments, including first-order diffusive shock acceleration, second order stochastic acceleration in shock downstream regions, modification of shock structure by pick-up interstellar neutrals, as well as injection processes of suprathermal particles. In addition to these theoretical works, R/D studies for radio observations of pulsars and cosmic ray air showers are also being made.

## CANGAROO-III and TeV gamma-ray Project

[Spokespersons : R.W. Clay, R. Enomoto, and T. Tanimori]

Collaboration list:
Institute for Cosmic Ray Research, University of Tokyo, Chiba, Japan; School of Chemistry and Physics, University of Adelaide, Australia; Mt Stromlo and Siding Spring Observatories, Australian National University, Australia; Australia Telescope National Facility, CSIRO, Australia; Department of Radiological Sciences, Ibaraki Prefectural University of Health Sciences, Ibaraki, Japan; Faculty of Science, Ibaraki University, Ibaraki, Japan; School of Allied Health Sciences, Kitasato University, Kanagawa, Japan; Department of Physics, Konan University, Hyogo, Japan; Department of Physics, Kyoto University, Kyoto, Japan; Solar-Terrestrial Environment Laboratory, Nagoya University, Aichi, Japan; National Astronomical Observatory of Japan, National Institutes of Natural Sciences, Tokyo, Japan; Department of Physics, Tokai University, Kanagawa, Japan; Department of Physics, Yamagata University, Yamagata, Japan; Faculty of Management Information, Yamanashi Gakuin University, Yamanashi, Japan; Faculty of Medical Engineering and Technology, Kitasato University, Kanagawa, Japan; Department of Physics, Hiroshima University, Hiroshima, Japan; Department of Basic Physics, Tokyo Institute of Technology, Tokyo, Japan;

Dept. of Physics, College of Science and Engineering, Ritsumeikan University; Institute of Particle and Nuclear Studies, High Energy Accelerator Research Organization (KEK), Ibaraki, Japan [1].

## Status of the Project

CANGAROO is the acronym for the Collaboration of Australia and Nippon (Japan) for a GAmma Ray Observatory in the Outback. The collaboration started in 1992 with a single Imaging Atmospheric Cherenkov Telescope (IACT) of 3.8 m diameter called CANGAROO-I in the desert area near Woomera, South Australia (136°47′E, 31°06′S, 160 m a.s.l.). As its third-generation experimental setup, the CANGAROO-III stereoscopic IACT system has been in operation since March 2004 with four IACTs of 10 m diameter. Stereoscopic observations of atmospheric Cherenkov light images produced by particle showers caused by high-energy particles bombarding the earth allow effective discrimination of gamma rays from charged cosmic rays which are the overwhelming backgrounds. Two of the four telescopes (called T3 and T4 in the order of construction) have been used in observations , as the first and second telescopes have degraded. A stereoscopic triggering system was installed at the beginning of 2005 and has been working properly, rejecting most single muon events, which are the major background component at low energies. We are continuing observations of various candidates of celestial gamma-ray emitters on moonless, clear nights.

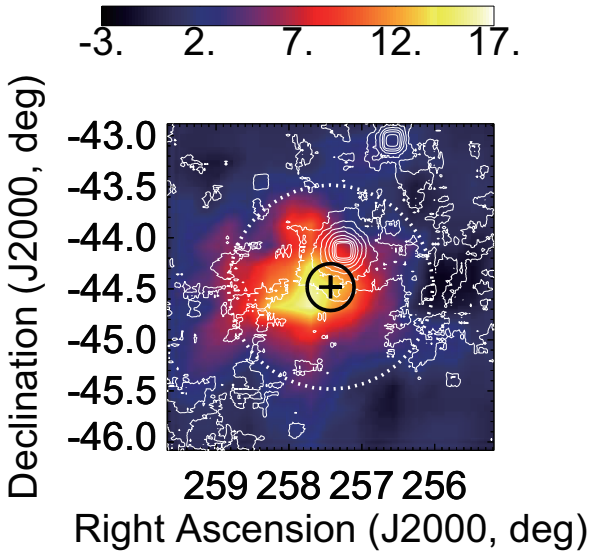


Fig. 1. Map of excess events of 2004 data by using the ON- and OFF source observations. The number of excess events per $0.2^o \times 0.2^o$ cell is plotted in the equatorial coordinate. The number of excess events was smoothed by taking the average of the 3 × 3 = 9 cells around each investigated direction. The black cross at the center of the map indicated the position of the pulsar PSR B1706-44, the radius of the black circle represents the point spread function (PSF) of $\delta\theta_0 = 0.24^o$, and the circle of white dotted line shows the region within $1^o$ radius from the pulsar. The inserted white contours are the hard-X-ray map obtained from the ROSAT satellite [3].

## CANGAROO-III Results

### Observation of TeV Gamma Rays from the vicinity of PSR B1 706−44[2]

Observations for about 50 hours have given an indication of extended emission of TeV gamma rays around the pulsar PSR B1706-44 as shown in Fig 1. The strength of the signal depends on how we estimate angular size of the extended emission. The total flux at 1 TeV is $(4.7 \pm 0.7) \times 10^{-11}(E/1\mathrm{TeV})^{-3.1\pm0.7}$ cm$^{-2}$s$^{-1}$TeV$^{-1}$, when integrated for incident angles within a circle of $1^o$ radius. This corresponds to $(4.9 \pm 0.7) \times 10^{-8}(E/1\mathrm{TeV})^{-3.1\pm0.7}$ cm$^{-2}$s$^{-1}$TeV$^{-1}$sr$^{-1}$ in unit of "per solid angle". After integration of the gamma-ray energy, $E$, it is $2.2\times 10^{-11}$ cm$^{-2}$s$^{-1}$ for $E >$1TeV, which is as large as the Crab flux of $1.8 \times 10^{-11}$ cm$^{-2}$s$^{-1}$. A best fit to the radial profile gives two components of diffuse emission, *i.e.*, 0.3 degree wide plus flat ones. The flux of the 0.3-degree source is sub-Crab level.

The intensity within the area corresponding to the point spread function, $\theta < 0.24^o$ from PSR B1706−44, is $(3.0 \pm 0.6) \times 10^{-12}$ cm$^{-2}$s$^{-1}$ for gamma-ray energy $E >$ 1 TeV. The flux corresponds to 17% of the Crab flux at 1 TeV, setting constraint on the emission from a compact source, which may underlie below the extended emission. The relative excess of this region compared with that of $0.4^o < \theta < 0.6^o$ is $6 \pm 4$ % Crab. These are the results from ON/OFF subtraction method.

On the other hand, a statistically significant result could not be obtained from method of the wobble and ring background analysis. The $2\sigma$ upper limit on the emission within $0.24^o$ radius from PSR B1706−44 is $1.8 \times 10^{-12}$ cm$^{-2}$s$^{-1}$ at 1 TeV, which corresponds to 10% of the Crab flux at 1 TeV.

The extended emission with two methods suggests complex structure of TeV gamma-ray emission existing in the vicinity of PSR B1706−44. A deeper investigation and further efforts for improving the technique of Imaging Air Cherenkov telescope remain to be pursued, in order to resolve and distinguish Galactic sources of TeV gamma-rays against the diffusive emission of the Galactic disk.

### HESS J1614–518 [4]

We report the detection with the CANGAROO-III imaging atmospheric Cherenkov telescope array of a very high energy gamma-ray signal from the unidentified gamma-ray source HESS J1614−518, which was discovered in the H.E.S.S. Galactic plane survey (see Fig. 2). Diffuse gamma-ray emission was detected above 760 GeV at the 8.9 $\sigma$ level during an effective exposure of 54 hr from 2008 May to August. The spectrum is represented with a power-law: $(8.2 \pm 2.2_{stat} \pm 2.5_{sys}) \times 10^{-12} \times (E/1\ \mathrm{TeV})^{-\gamma}$ cm$^{-2}$ s$^{-1}$ TeV$^{-1}$ with a photon index $\gamma$ of $2.4 \pm 0.3_{stat} \pm 0.2_{sys}$, which is compatible with that of the H.E.S.S. observations. By combining our result with multi-wavelength data, we discuss the possible counterparts for HESS J1614−518 and consider radiation mechanisms based on hadronic and leptonic processes for a supernova remnant, stellar winds from massive stars, and a pulsar wind nebula (see for example Fig. 3).

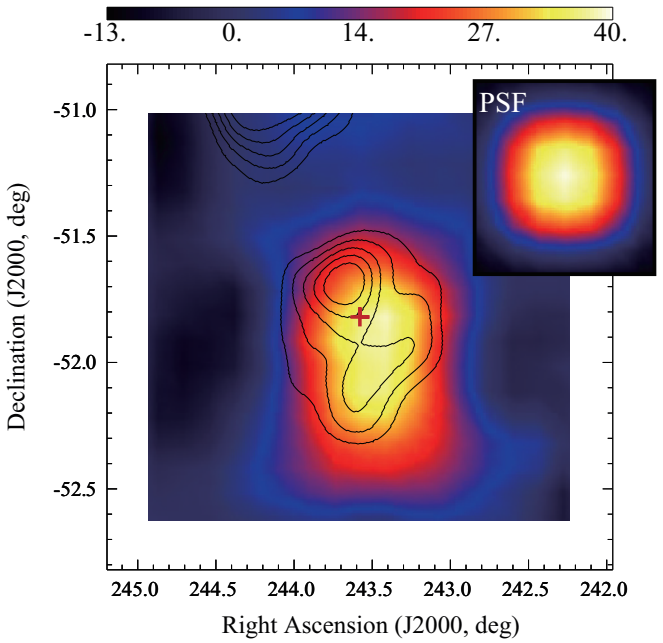


Fig. 2. Morphology of gamma-ray–like events. The number of excess events per $0^\circ.2 \times 0^\circ.2$ cell is smoothed and plotted in the equatorial coordinate. The black solid contours show the VHE gamma-ray emission seen by H.E.S.S. The red cross shows the center position of HESS J1614−518.

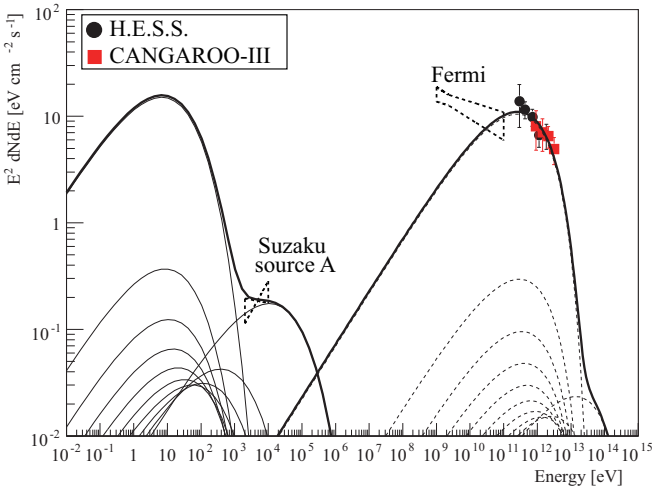


Fig. 3. SED with a time-evolving leptonic model curves for PSR J1614−5144. The thin solid and dotted lines show the synchrotron and IC component derived from the evolving electron per $3.3 \times 10^5$ yr ($0 < t < 3.3 \times 10^6$ yr), respectively. The bold solid and dotted lines show their total.

## Other Activities

For future project for TeV gamma-rays observation, we decided to join CTA (Cherenkov Telescope Array[5]). More than forty scientists, not only CANGAROO group, joined and formed a new group named CTA-Japan[6] and we signed up MOU[7] with CTA international consortium We are aiming at production of imaging cameras for this project and will start making a camera for the prototype 23m$^\phi$ telescope with a collaboration with Max Plank Institute, Munchen from 2010.

## Bibliography

[1] Collaboration website: `http://vesper.icrr.u-tokyo.ac.jp/`.

[2] R. Enomoto et al., *Astrophys. J.*, **703**, 1725 (2009).

[3] Skyview website: `http://skyview.gsfc.nasa.gov/`.

[4] T. Mizukami et al., submitted to *Astrophys. J.*.

[5] CTA website: `http://www.cta-observatory.org/`.

[6] CTA-Japan website: `http://cta.scphys.kyoto-u.ac.jp/`.

[7] memorandum of understandings.

## TA: Telescope Array Experiment

Spokespersons:

M. Fukushima / ICRR, University of Tokyo
P. Sokolsky / Dept. of Physics, University of Utah

Collaborating Institutions:

Chiba Univ., Chiba, Japan; Chungnam Nat. Univ., Daejeon, Korea; Ehime Univ., Matsuyama, Japan; Ewha W. Univ., Seoul, Korea; Hiroshima City Univ., Hiroshima, Japan; Hanyang Univ., Seoul, Korea; ICRR, Univ. of Tokyo, Kashiwa, Japan; INR, Moscow, Russia; Kanagawa Univ., Yokohama, Japan; KEK/IPNS, Tsukuba, Japan; Kinki Univ., Higashi-Osaka, Japan; Kochi Univ., Kochi, Japan; Musashi Inst. of Tech., Tokyo, Japan; Nat. Inst. of Rad. Sci., Chiba, Japan; Osaka City Univ., Osaka, Japan; Pusan Nat. Univ., Pusan, Korea; Rutgers Univ., Piscataway, NJ, USA; Saitama Univ., Saitama, Japan; Tokyo Inst. of Tech., Tokyo, Japan; Tokyo Univ. of Science, Noda, Japan; Univ. of Denver, Denver, CO, USA; Univ. of Utah, Salt Lake City, UT, USA; Univ. of Yamanashi, Kofu, Japan; Waseda Univ., Tokyo, Japan; Yonsei Univ., Seoul, Korea

## Overview and Status of TA

The TA [1] is the detector that consists of the surface array of plastic scintillator detectors (a la AGASA) and fluorescence detectors (a la HiRes). The aim of the TA is to explore the origin of extremely-high energy (EHE) cosmic rays by measuring energy, arrival direction and mass composition. It is located in the West Desert of Utah, 140 miles south of Salt Lake City (lat. 39.3°N, long. 112.9°W, alt. ∼1400 m). The construction of the TA was performed mainly by the Grants-in-Aid for Scientific Research (Kakenhi) of Priority Areas "The Origin of Highest Energy Cosmic Rays" (JFY2003-JFY2008) and the US National Science Foundation (NSF). All the three fluorescence stations started the observation in November 2007. Major construction of the surface detector array was completed in February 2007, and the array of the surface detectors started the full operation in March 2008. The TA is operated by the international collaboration of researchers from US, Russia, Korea and Japan. The main fund for the TA operation is the Grants-in-Aid for Scientific Research (Kakenhi) of Specially Promoted Research "Extreme

Phenomena in the Universe Explored by Highest Energy Cosmic Rays" (JFY2009-JFY2013).

### Surface Detector Array

The surface detector (SD) array consists of 507 plastic scintillators on a grid of 1.2 km spacing. It covers the ground area of about 700 km$^2$, which is about seven times larger than that of AGASA. The trigger efficiency is $\sim$100% for cosmic rays with energy above $10^{19}$ eV with zenith angle less than 45°.

The counter is composed of two layers of plastic scintillator overlaid on top of each other. The scintillator is 1.2 cm thick, 3 m$^2$ large and is read out by 104 wave length shifter fibers installed in grooves on the surface. Both ends of the fibers are bundled and optically connected to the photomultiplier.

Power of each SD is supplied by a solar panel and a battery, and the communication between SDs and the host at the communication tower is performed by wireless LAN.

### Fluorescence Telescope

The TA has three fluorescence detector (FD) stations. The fluorescence station in the southeast is called the Black Rock Mesa (BRM) site. The southwestern station is called the Long Ridge (LR) site and the station in the north is called the Middle Drum (MD) site.

Twelve reflecting telescopes were newly constructed and installed at each of the BRM and LR stations and cover the sky of 3°-34° in elevation and 108° in azimuth looking toward the center of the surface detector array.

The MD station was constructed using refurbished equipment from the old HiRes-I observatory at Dugway in Utah. HiRes mirrors are about 40% smaller in area than the mirrors in the BRM and LR FD stations. Fourteen reflecting telescopes cover the sky of 3°-31° in elevation and 114° in azimuth.

We also built a laser shooting facility (Central Laser Facility: CLF) in the middle of the array for atmospheric monitor. The CLF is located at an equal-distance (21 km) from three fluorescence stations. The Rayleigh scattering at high altitude can be considered as "standard candle" observable at all stations.

A LIDAR (LIght Detection And Ranging) system located at the BRM station is used for the atmospheric monitoring. It consists of a pulsed Nd:YAG laser and a telescope attached to an alto-azimuth. The back-scattered light is received by the telescope to analyze the extinction coefficient along the path of the laser.

For monitoring the cloud in the night sky, we installed an infra-red CCD camera at the BRM station, and take data of the night sky every hour during FD observation.

In order to confirm absolute energy scale of the fluorescence detector in situ, we plan to operate a compact electron linear accelerator (TA-LINAC) about 100 m away from the fluorescence station and inject an electron beam vertically up into the atmosphere. A beam of $10^9$ electrons with energy of 40 MeV and a duration of 1 $\mu$s well simulates a shower energy deposition of $\sim 4\times10^{16}$ eV 100 m away from the station, which corresponds to a shower of $\sim 4\times10^{20}$ eV 10 km away. The calibration is obtained by comparing the observed fluorescence signal with the expected energy deposition calculated by the GEANT simulation [2]. The accelerator was designed with a collaboration of KEK accelerator physicists and was assembled in KEK. We finished testing the basic performance of the accelerator in KEK by the end of 2008 and we obtained the total energy of injected electrons with an accuracy of 5%. The main accelerator part was installed in a 40-feet commercial container. We transported the accelerator system from Japan, and deployed it to the BRM site in March 2008 as shown in Fig. 1. We finished the installation of power facility to the TA-LINAC and the procedure of radiation safety. We began to start up the TA-LINAC in June 2010.

Fig. 1. The TA-LINAC that was installed in the BRM site. The accelerator part is in a 40-ft container, which is located 100 m in front of the fluorescence station. The photo of the accelerator taken from the electron-gun side is also shown.

The TA has 507 surface detectors, three FD stations, three communication towers, the CLF, and the cosmic ray center in the city to the east of the TA site. Since these facilities are distributed in the wide area, we developed wide area radio network by 2.4 GHz and 5.7 GHz wireless LAN modules.

### Status of TA Observation

Fig. 2 shows the fraction of operation of the surface detectors from May 2008 to June 2010. There were periods for which the fraction of operation decreased because of maintenance and bad weather. Recently the average fraction of operation is about 99%.

Fig. 3 shows the observation hours for the BRM and LR fluorescence detectors from November 2007 to April 2010. We observe during moonless night, and the observation time per night in winter is longer than that in summer.

## Results

The first TA results were presented at the International Cosmic Ray Conference that was held in Poland in July 2009 (ICRC09). We presented twelve oral talks including TA highlight talk and twelve posters. Using the surface detectors for the first half year or the fluorescence detectors for one year, we showed three presentations on arrival directions of ultra-high

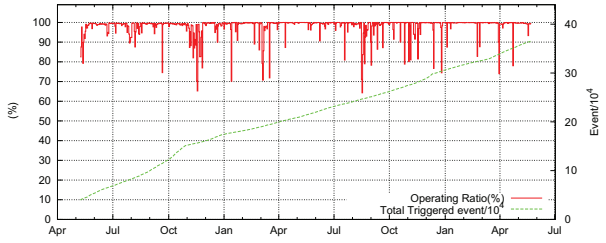


Fig. 2. The fraction of operation of the surface detectors in red and the integrated number of triggered air shower events in green.

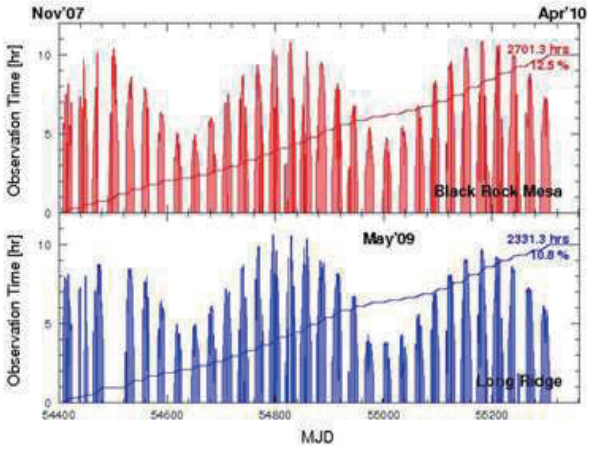


Fig. 3. Observation hours per night and integrated observation hours for the BRM (upper) and LR (lower) fluorescence detector site. The horizontal axes represent modified Julius day (MJD).

energy (UHE) cosmic rays, four presentations on air shower reconstruction and energy spectrum, one presentation on mass composition, one presentation on UHE photon search, three presentations on Monte Carlo simulation, and eleven presentations related to detector application in TA.

In the Japanese Physical Society meeting in March 2010, we presented new results. One is the measurement of energy spectrum by hybrid analysis for which information of the surface detectors are included in the analysis of the fluorescence detectors. The other is the measurement of mass composition by the analysis of the maximum depth ($X_{\max}$) of air showers. We also updated the result of the UHE photon search. The first two results became the first doctoral theses from the TA group [3, 4].

## Arrival directions of UHE cosmic rays

The search for anisotropy in the arrival directions of UHE cosmic rays has been a long-standing problem. We present the test of the autocorrelation between arrival directions of UHE cosmic rays by using surface detector data from May 2008 to November 2008. The selected surface detector data set consists of 13 events with energy above $10^{19.5}$ eV. Fig. 4 shows the arrival directions in galactic coordinates. No cluster candidates were found within the angle of 2°, with less than 0.3 expected events if the arrival directions are isotropic.

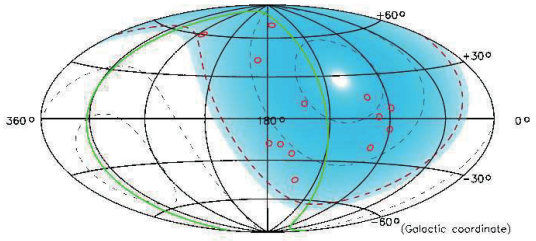


Fig. 4. The preliminary result of the distribution of arrival directions of 13 UHE cosmic rays with energy above $10^{19.5}$ eV in galactic coordinates.

## Measurement of energy spectrum by hybrid analysis

When we reconstruct air showers by monocular analysis for fluorescence detectors, the reconstruction of air showers is improved if we add the information of the surface detectors. We call this analysis hybrid analysis. Here timing information of one surface detector near shower core is used. If we use only data of the fluorescence detectors, the aperture depends on energy of primary cosmic rays, but hybrid analysis has the merit that the aperture is kept constant by the size of the surface detector array ( for energy above $10^{19}$ eV for the current TA operation ) and systematic error of the aperture becomes smaller.

We apply hybrid analysis to the data of fluorescence detectors in the BRM and LR sites and the surface detectors that were taken from May 2008 to September 2009 for one and a half years and measure the energy spectrum for energy above $10^{18.7}$ eV as shown in Fig. 5. It is consistent with the spectra from the HiRes detectors.

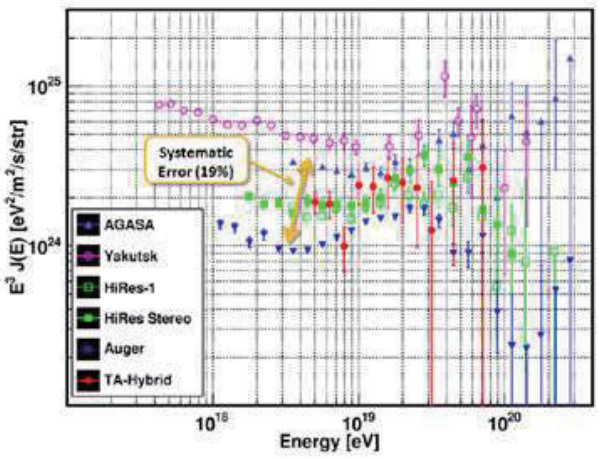


Fig. 5. Energy spectra of several experiments. Red symbols represent the preliminary energy spectrum obtained by TA hybrid analysis. Blue upward triangles represent AGASA result, pink symbols represent Yakutsk result, green symbols represent HiRes result, and blue downward triangles represent Auger result.

### Measurement of mass composition by shower maximum depth ($X_{\max}$)

It is important to measure mass composition of UHE cosmic rays and its energy dependence in order to understand the origin and propagation of UHE cosmic rays. Since the cross section of interaction of cosmic rays with nuclei in the atmosphere depends on particle species, the longitudinal shower profile depends on incident particle species. Mass composition of primary cosmic rays was studied by comparing the maximum shower depth ($X_{\max}$) distribution between data and MC. We obtain the $X_{\max}$ distribution for the data observed simultaneously by the BRM and LR fluorescence detectors, which are called stereo events. Since arrival directions of UHE cosmic rays are determined precisely by stereo events, longitudinal development of cosmic rays can be studied in detail.

Fig. 6 shows the $X_{\max}$ distributions for stereo events for energy above $10^{18.6}$eV that were taken from November 2007 to October 2009 for about two years. Fig. 6a, Fig. 6b, and Fig. 6c correspond to the $X_{\max}$ distributions for different hadronic interaction models (QGSJET-II, QGSJET-01, SIBYLL), respectively. Fig. 7 shows the average $X_{\max}$ as a function of energy of UHE cosmic rays. The result is that the $X_{\max}$ distribution of the TA data is consistent with the $X_{\max}$ distribution expected for protons.

### Measurement of energy spectrum by FD monocular analysis at the MD site

The HiRes telescopes were moved to the MD site. The FD monocular data at the MD site were analyzed from December 2007 to December 2008 by modifying the configuration of the telescopes and trigger condition in the HiRes analysis program. It allows a direct comparison of energy scales and energy spectra between the TA and HiRes detectors. The monocular energy spectrum from the MD fluorescence detector is shown in Fig. 8. It is consistent with the spectra from the two HiRes detectors.

### Search for UHE photons

Several models were proposed for the interpretation of the origin of highest energy cosmic rays. There is a possibility that cosmic rays were generated and accelerated in very active region such as active galactic nuclei (AGN) up to highest energy cosmic rays (bottom-up model), and were observed at the earth through GZK process [5, 6]. If highest energy cosmic rays are generated and accelerated at the sources such as AGN, there is a possibility that UHE photons with energy around $10^{19}$ eV are generated by resonant $\pi^0$ production in GZK-type process. It is also expected that large amount of UHE photons with energy above $10^{19}$ eV could be generated by non-accelerated model (top-down model) such as unknown super-heavy particles. It is expected that UHE photons with energy above $10^{19}$ eV interact in deeper atmosphere than UHE hadrons. Then the curvature of air shower front of photons around the ground is larger than that of hadrons.

Fig. 9 shows the curvature of air shower front for the data of the surface detectors taken from May 2008 to October 2009. We obtained the limit on the integral flux of photons

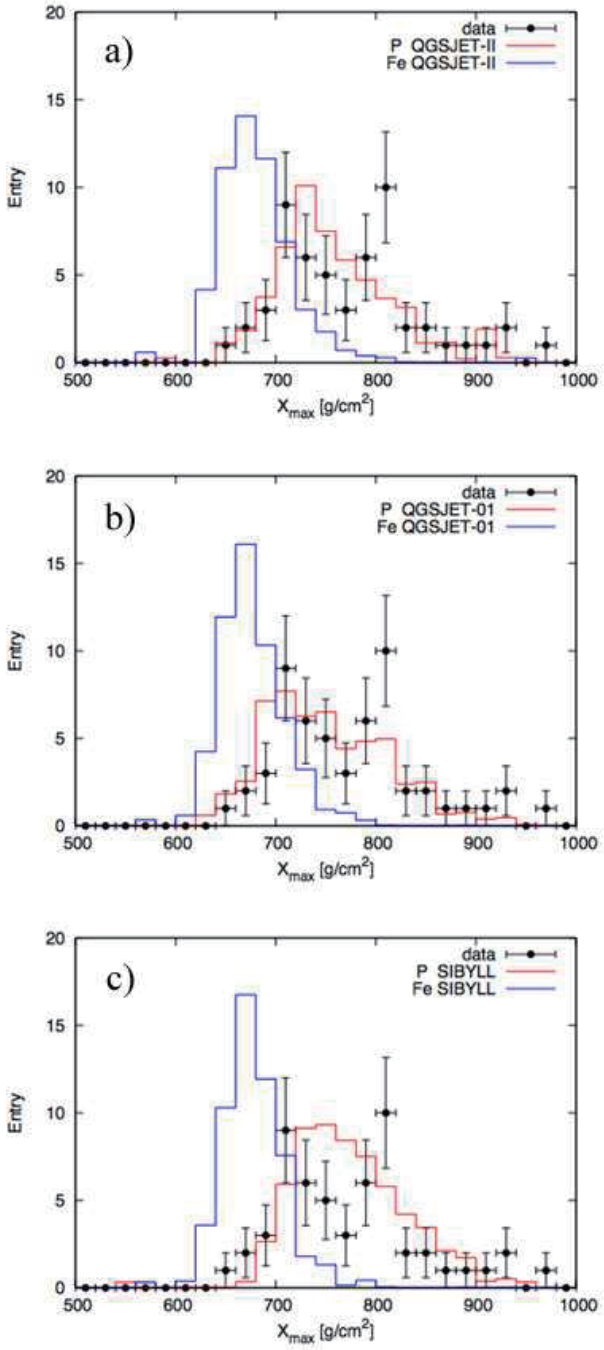


Fig. 6. The preliminary result of the distributions of the maximum depth ($X_{\max}$) of air showers obtained from the TA data. Black circles represent the TA result. Blue and red histograms correspond to the $X_{\max}$ distributions for protons and irons, respectively. a) for QGSJET-II, b) for QGSJET-01, and 3) for SIBYLL hadronic interaction models.

with energy above $10^{19}$ eV to be

$$3.3 \times 10^{-2}\ km^{-2} sr^{-1} yr^{-1}$$

at 95% confidence level as shown in Fig. 10.

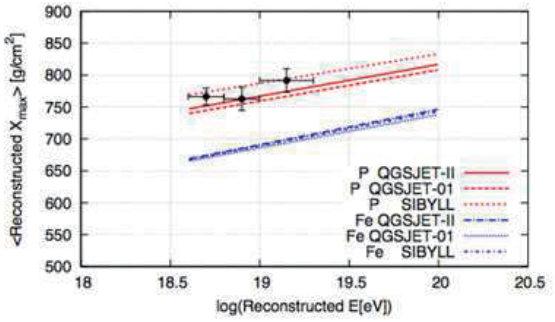


Fig. 7. The average $X_{\max}$ versus energy of UHE cosmic rays. The preliminary TA result is denoted by black circles. Red lines correspond to the predictions for protons for three hadronic interaction models. Blue lines correspond to the predictions for iron.

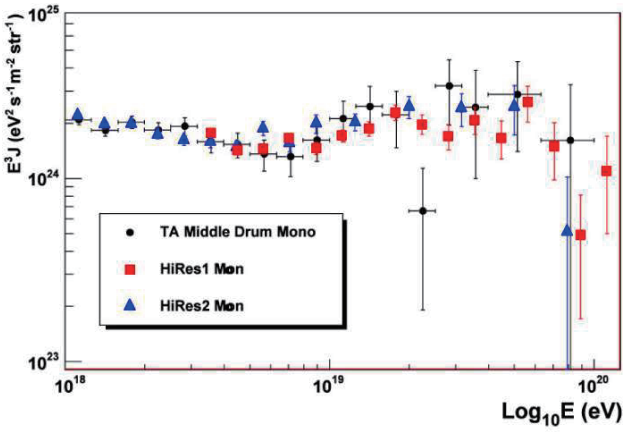


Fig. 8. The preliminary monocular energy spectrum from the TA MD fluorescence detector (black circles). Red circles and blue circles represent those for the HiRes-1 and HiRes-2 detectors, respectively.

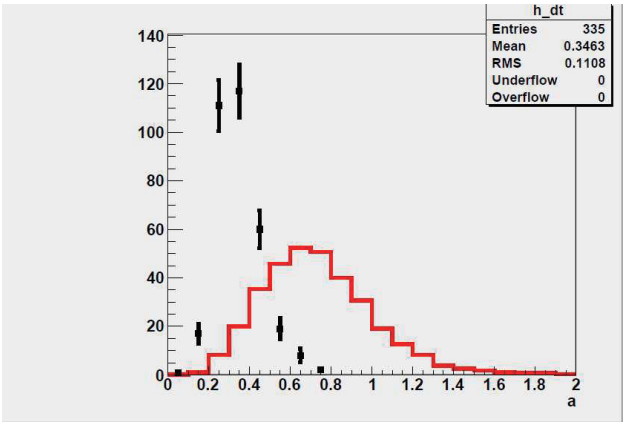


Fig. 9. The preliminary result of the distribution of the curvature of shower front of UHE cosmic rays (Linsley curvature parameter) for zenith angle from 45° to 60°. Black points denote the distribution of curvature of the TA data. The histogram corresponds to the expected distribution of the curvatures for the photons that are generated by the spectrum with power index of -2.

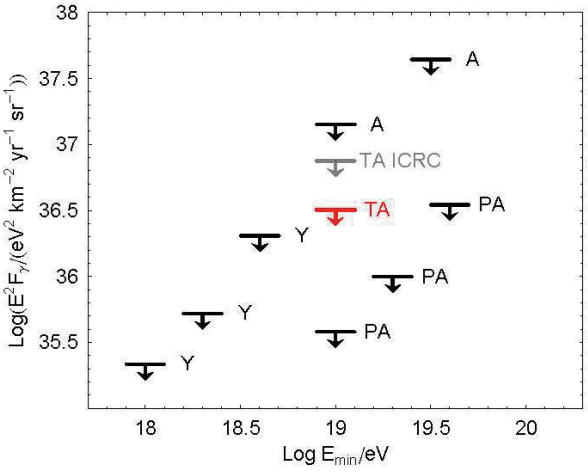


Fig. 10. Upper limits on the integral flux of UHE photons for different experiments: the latest preliminary TA result (TA) in red, TA at ICRC09 (TA ICRC) in gray, AGASA (A), Auger (PA), and Yakutsk (Y).

## Measurement of energy spectrum by using the data of the surface detectors

After ICRC09, we showed the energy spectrum of UHE cosmic rays by using the data of the surface detectors that were taken between May 2008 and November 2008. Energies of primary cosmic rays are measured from the particle density at a distance of 800 m from shower core by estimating the relation of conversion from particle density to primary energy using air shower MC and detector MC simulations. We evaluated the aperture for the selected events as a function of primary energy by using MC simulations. The energy spectrum by the surface detectors using "energy scaled to FD energy" is shown in Fig. 11, and it is consistent with that by MD FD monocular energy spectrum. We will perform the further study for the dependence of estimated energy on hadronic interaction models and mass composition of primary particle,

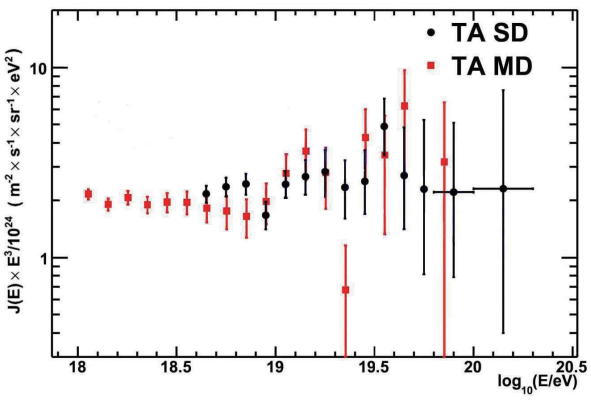


Fig. 11. Preliminary energy spectrum measured by the data of the surface detectors with "energy scaled to FD energy". Black points denote the result of the surface detectors and red points denote the result of the MD fluorescence detector.

## Prospects

The Auger group and the HiRes group published the results of energy spectrum, which are consistent with GZK cutoff with their energy scales determined by the method of fluorescence telescope [7, 8].

For the anisotropy, the Auger group claimed there is a correlation between the arrival directions of the highest energy cosmic rays and the positions of AGN [9] while the HiRes group reported that no correlations have been found [10].

For composition in EHE region, the Auger data suggests a change to a heavier composition [11] while the HiRes data is consistent with constant elongation rate which stays with proton [12].

Auger's claim from arrival direction suggests that UHE cosmic rays are protons which are in consistent with their result that UHE cosmic rays are irons from $X_{\max}$ study.

We have the data of the surface detectors for about two years and the exposure of the TA surface detectors correspond to almost total exposure taken by AGASA. Based on this data, we proceed the analyses for correlation with arrival direction of UHE cosmic rays, the measurement of energy spectrum including the issue of cutoff around $5\times10^{19}$eV by the TA surface detectors and the comparison of air shower reconstruction between atmospheric fluorescence telescope detectors and surface detectors.

In the near future, we determine energies of air showers within total uncertainty of about 10% and measure the spectrum of UHE cosmic rays precisely by using end-to-end absolute energy calibration of fluorescence telescopes with the TA-LINAC. The "ankle" around $10^{18.5}$eV is interpreted as the transition from galactic cosmic rays to extra-galactic cosmic rays or electron-positron pair production by the interaction of proton cosmic ray with cosmic background radiation photon. A construction of TALE, a Low Energy extension of TA with the energy range down to $10^{17}$ eV was proposed in the US fund to investigate the modulation of cosmic ray composition and spectrum expected by the galactic to extra-galactic transition of cosmic ray origins including "second knee" in the $10^{17}$ eV decade. By the TA+TALE project, comprehensive studies on UHE cosmic rays will be possible for wide energy range from $10^{17}$ eV to $10^{20}$ eV or above.

It is our belief that the characteristic features of the TA detector, the sampling of electromagnetic shower energy, the unique calibration of fluorescence generation, usage of HiRes-I telescopes in the TA site, and the measurement in the Northern Hemisphere, will make an essential contribution to the understanding of the intricate problem of GZK cutoff, anisotropy, and composition of EHE cosmic rays. We will analyze the increasing TA data and measure energy spectrum, particle composition including UHE photons and UHE neutrinos, anisotropy of arrival directions more in detail and explore the origin of UHE cosmic rays and understand the extreme phenomena of the universe.

## Bibliography


[1] http://www.telescopearray.org/

[2] T. Shibata *et al*., Ncul. Instr. and Meth. A597 (2008) 61-66.

[3] D. Ikeda, Ph.D. thesis, University of Tokyo, 2010.

[4] Y. Tameda, Ph.D. thesis, Tokyo Institute of Technology, 2010.

[5] K. Greisen, Phys. Rev. Lett. **16**, 748 (1966).

[6] G.T. Zatsepin and V.A. Kuz'min, JETP Lett. **4**, 78 (1966) [Pis'ma Zh. Eksp. Teor. Fiz. **4**, 114 (1966)].

[7] R.U. Abbasi *et al*. (HiRes Collaboration), Phys. Rev. Lett. 100 (2008) 101101.

[8] J. Abraham *et al*. (Pierre Auger Collaboration), Phys. Rev. Lett. 101 (2008) 061101.

[9] J. Abraham *et al*. (Pierre Auger Collaboration), Astropart. Phys. 29 (2008); J. Abraham *et al*. (Pierre Auger Collaboration), Science 318 (2007) 939;

[10] R.U. Abbasi *et al*. (HiRes Collaboration), Astropart. Phys. 30 (2008) 175-179.

[11] J. Abraham *et al* (Pierre Auger Collaboration), Phys. Rev. Lett. 104 (2010) 09110.

[12] R.U. Abbasi *et al*, (HiRes Collaboration), Phys. Rev. Lett. 104 (2010) 161101.


# Tibet AS$\gamma$ Project

## Experiment

The Tibet air shower experiment has been successfully operated at Yangbajing (90°31′ E, 30°06′ N; 4300 m above sea level) in Tibet, China since 1990. It has continuously made a wide field-of-view (approximately 2 steradian) observation of cosmic rays and gamma rays in the northern sky.

The Tibet I array was constructed in 1990 and it was gradually upgraded to the Tibet II by 1994 which consisted of 185 fast-timing (FT) scintillation counters placed on a 15 m square grid covering 36,900 $m^2$, and 36 density (D) counters around the FT-counter array. Each counter has a plastic scintillator plate of 0.5 $m^2$ in area and 3 cm in thickness. All the FT counters are equipped with a fast-timing 2-inch-diameter photomultiplier tube (FT-PMT), and 52 out of 185 FT counters are also equipped with a wide dynamic range 1.5-inch-diameter PMT (D-PMT) by which we measure up to 500 particles which saturates FT-PMT output, and all the D-counters have a D-PMT. A 0.5 cm thick lead plate is put on the top of each counter in order to increase the counter sensitivity by converting gamma rays into electron-positron pairs in an electromagnetic shower. The mode energy of the triggered events in Tibet II is 10 TeV.

In 1996, we added 77 FT counters with a 7.5 m lattice interval to a 5,200 $m^2$ area inside the northern part of the Tibet II array. We called this high-density array Tibet HD. The mode energy of the triggered events in Tibet HD is a few TeV.

In the late fall of 1999, the array was further upgraded by adding 235 FT-counters so as to enlarge the high-density area from 5,200 $m^2$ to 22,050 $m^2$, and we call this array and further upgraded one Tibet III. In 2002, all of the 36,900 $m^2$ area was

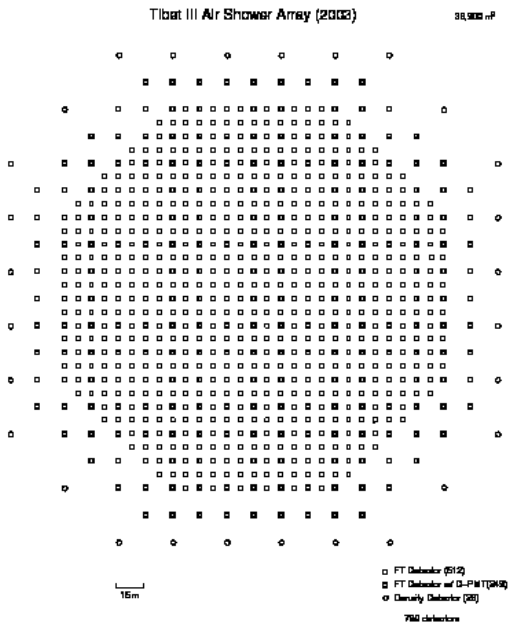


Fig. 1. Schematic view of the Tibet III array.

covered by the high-density array by adding 200 FT-counters more. Finally we set up 56 FT-counters around the 36,900 $m^2$ high density array and equipped 8 D-counters with FT-PMT in 2003. At present, the Tibet air shower array consists of 761 FT-counters (249 of which have a D-PMT) and 28 D-counters as in Fig. 1.

The performance of the Tibet air shower array has been well examined by observing the Moon's shadow (approximately 0.5 degrees in diameter) in cosmic rays. The deficit map of cosmic rays around the Moon demonstrates the angular resolution to be around $0.9^\circ$ at a few TeV for the Tibet III array. The pointing error is estimated to be better than $0^\circ.011$, by displacement of the shadow's center from the apparent center in the north-south direction, as the east-west component of the geomagnetic field is very small at the experimental site. On the other hand, the shadow center displacement in the east-west direction due to the geomagnetic field enables us to spectroscopically estimate the energy scale uncertainty less than $\pm 12$ %.

Thanks to high statistics, the Tibet air shower experiment introduces a new method for energy scale calibration other than the conventional estimation by the difference between the measured cosmic-ray flux by an air shower experiment and the higher-energy extrapolation of cosmic-ray flux measured by direct measurements by balloon-borne or satellite experiments.

## Physics Results

Our current research theme is classified into 4 categories:

(1) TeV celestial gamma-ray point/diffuse sources [3],

(2) Chemical composition and energy spectrum of primary cosmic rays in the knee energy region [4],

(3) Cosmic-ray anisotropy in the multi-TeV region with high precision,

(4) Global 3-dimensional structure of the solar and interplanetary magnetic fields by observing the Sun's shadow in cosmic rays.

We will introduce a part of the results obtained in this fiscal year.

The *Fermi Gamma-ray Space Telescope* (*Fermi*), successor of the Energetic Gamma Ray Experiment (EGRET), was launched in June 2008 to measure the energy range between 20 MeV and 300 GeV, approximately a hundred times sensitive than EGRET. The Large Area Telescope (LAT) on board the *Fermi* surveys the entire sky for 3 months, after which the 205 most significant sources were published as a bright source list above 100 MeV at a significance greater than $\sim 10\sigma$. This survey detected many new $\gamma$-ray pulsars. A typical 95% uncertainty radius of source position in this list is approximately 10 arcmin and the maximum is 20 arcmin; these values are greatly improved compared to those of EGRET. This provides a more accurate, unbiased search for common sources across multi wavelengths, compared with the EGRET era. Recently, the Milagro experiment observed 14 of the 34 *Fermi* sources selected from the list at a false-positive significance of $3\sigma$ or more at the representative energy of 35 TeV. Accordingly, we search for TeV $\gamma$-ray sources in the *Fermi* bright source list with the Tibet-III air shower array. Using the Tibet-III air shower array, we search for TeV $\gamma$-rays from 27 potential Galactic sources in the early list of bright sources obtained by the *Fermi* Large Area Telescope at energies above 100 MeV. Among them, we observe 7 sources instead of the expected 0.61 sources at a significance of $2\sigma$ or more excess. The chance probability from Poisson statistics would be estimated to be $3.8\times10^{-6}$, as is seen in Fig. 2 If the excess distribution observed by the Tibet-III air shower array has a density gradient toward the Galactic plane, the expected number of sources may be enhanced in chance association. Then, the chance probability rises slightly, to $1.2\times10^{-5}$, based on a simple Monte Carlo simulation. These low chance probabilities clearly show that the *Fermi* bright Galactic sources have statistically significant correlations with TeV $\gamma$-ray excesses. We also find that all 7 sources are associated with pulsars, and 6 of them are coincident with sources detected by the Milagro experiment at a significance of $3\sigma$ or more at the representative energy of 35 TeV. The significance maps observed by the Tibet-III air shower array around the *Fermi* sources, which are coincident with the Milagro $\geq 3\sigma$ sources, are consistent with the Milagro observations. This is the first result of the northern sky survey of the *Fermi* bright Galactic sources in the TeV region.

Around the *Fermi* Galactic bright sources with $\geq 2\sigma$ significance by the Tibet-III data and $\geq 3\sigma$ by the Milagro data except for the Crab, we compare significance maps between the Tibet-III air shower array (a)–(d) and the Milagro exper-

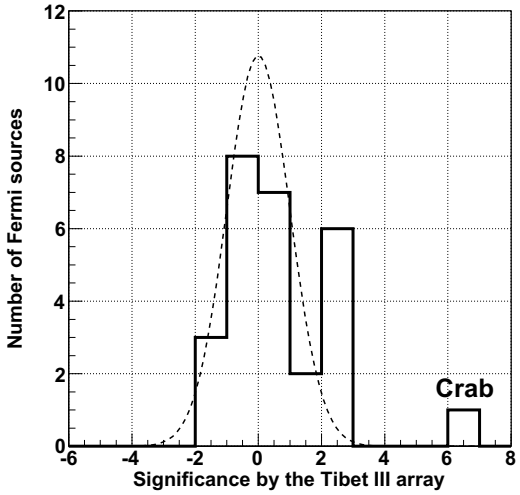


Fig. 2. From [1]. Shown are histograms of significance distribution of the *Fermi* bright sources observed by the Tibet-III air shower array. The dashed curve is the expected normal Gaussian distribution.

iment (a')–(d') in Fig. 3. Each image has a (5 degrees × 5 degrees) region including one or two *Fermi* sources. It is remarkable that the Tibet-III air shower array obtains images consistent with those observed in the Milagro experiment. Besides, the maximum significance positions obtained by both the Tibet-III air shower array and the Milagro experiment might be shifted from the pulsar positions. In fact, recent imaging air Cherenkov telescopes also discovered many candidates for TeV pulsar wind nebulae (PWNe), which are displaced within a few tenths of degree from the pulsars in the southern sky. Thus, these observations would imply that the excesses are possible candidates for TeV PWNe. The correlation between TeV and GeV $\gamma$-rays is being realized by the wide sky survey instruments, such as the Tibet-III air shower array and the Milagro experiment, in the early *Fermi* era.

Recently, the Milagro experiment reported a yearly variation in the so-called LOSS-CONE dip amplitude of cosmic ray anisotropy at sidereal time frame around 6 TeV. Figure 4(b) compares the single-band valley depths (SBVDs) reported by the Milagro experiment and those observed by the Matsushiro underground muon observatory (corresponding to primary energy around 0.6 TeV), during the identical seven-year period from 2000 to 2007. The SBVD by Matsushiro in this figure is multiplied by three in order to roughly compensate the attenuation of the amplitude in the sub-TeV region. Adjusting to the analysis period in Milagro), the yearly mean SBVD by Matsushiro from 12 month data between June and July was calculated. The steady increase in the SBVD reported by the Milagro experiment is not seen in the Matsushiro record. Also calculated was SBVD every year in the entire period of the observation by Matsushiro and confirmed that the long-term variation of the SBVD is similar to the variation of the amplitude of the sidereal diurnal anisotropy which shows no significant correlation again with the solar activity and magnetic cycles.

Meanwhile, we plot the yearly variation in the LOSS-CONE amplitude observed by the Tibet-III air shower array

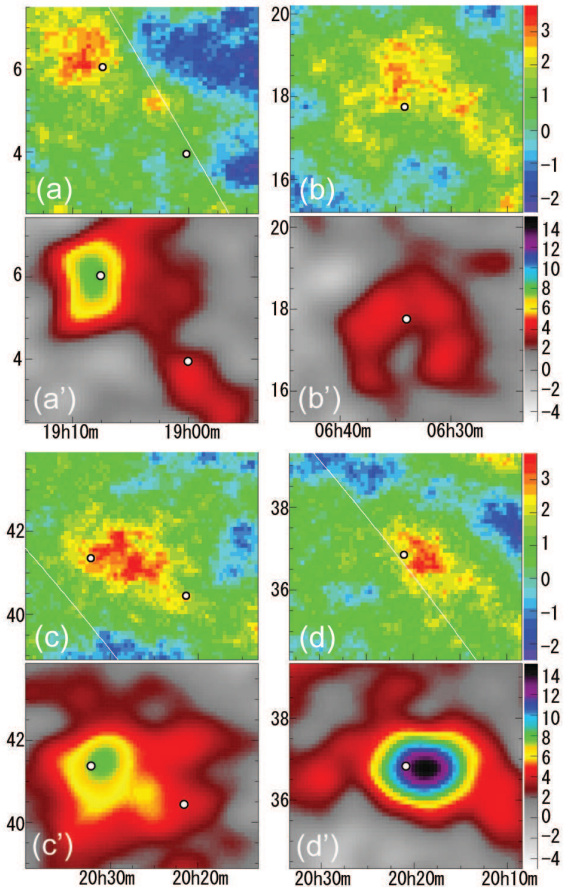


Fig. 3. From [1]. Comparisons of significance maps around the *Fermi* sources between the Tibet-III air shower array (a)–(d) and the Milagro experiment (a')–(d'). Selected are *Fermi* sources with $\geq 2\sigma$ significance by the Tibet-III air shower array and $\geq 3\sigma$ by the Milagro experiment except for the Crab. White points in each image show the *Fermi* source positions: (a)(a') J1907.5+0602/J1900.0+0356; (b)(b') J0634.0+1745 (Geminga); (c)(c') J2021.5+4026/J2032.2+4122; (d)(d') J2020.8+3649. The horizontal axis, vertical axis, and color contours indicate the right ascension, declination, and significance, respectively. For more detail and references, see [1].

(in this analysis, corresponding to 4.4, 6.2, 12 TeV representative primary energy), as is shown in Fig. 4(a). The distribution is consistent with a constant amplitude, there being no evidence for yearly variation in the LOSS-CONE amplitude[2]. It is concluded, therefore, that the steady increase of the SBVD reported by the Milagro experiment is, most likely, not due to the decreasing solar modulation in the declining phase of the 23rd solar activity cycle.

The solar activity in Cycle 23 gradually changes to final minimum phase. The Sun's shadow generated by multi-TeV cosmic-ray particles has been continuously observed with the Tibet-II and Tibet-III air shower array in 1996 through 2008 during almost whole period of the Solar Cycle 23. We have shown that the Sun's shadow is strongly affected by the solar and interplanetary magnetic fields changing with the solar activity. We present yearly variation of the Sun's shadow above 10 TeV in association with the Solar Cycle 23, in unit of deficit significance in Fig. 5 and in unit of deficit intensity in Fig. 6, respectively. We observe the solar minimum still continue in 2008, as is indicated by the corresponding sunspot number ob-

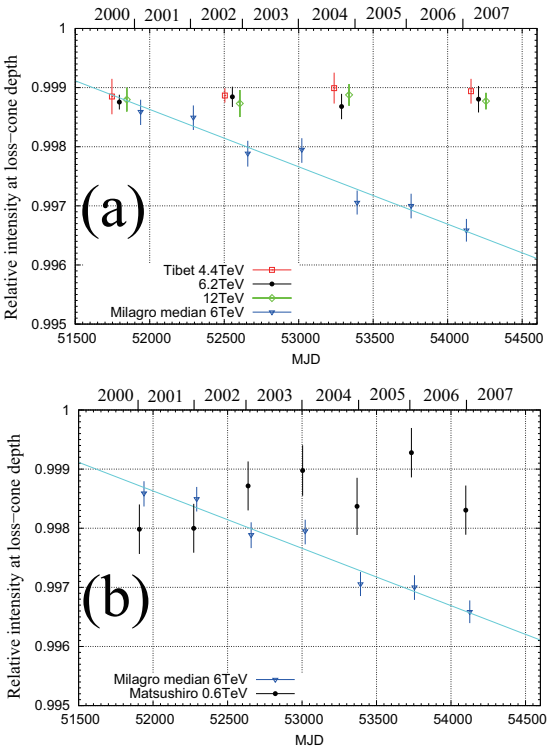


Fig. 4. Time dependence of the maximum depth of the LOSS-CONE observed by the Tibet-III air shower array (a) and the Matsushiro underground muon observatory (b) [see, K.Munakata et al., ApJ, 712, 1100-1106, 2010], along with the time dependence observed by the Milagro experiment. The LOSS-CONE depth and its error by the Matsushiro underground muon observatory are multiplied by a factor of three, to compensate for the attenuation of the amplitude in the sub-TeV energy region.

servation. Although the Sun shadow 2009 is under analysis, we keep an eye on it to see whether it will still remain at high significance or not.

## Other Activities

This group has developed and completed several automatic measuring systems that are powerful for analyzing cosmic ray tracks or air shower spots, that is, automatic microdensitometers, precise coordinate-measuring systems and image scanners controlled by a computer. Enormous data recorded on nuclear emulsion plates or X-ray films are rapidly and precisely measured by the use of these measuring systems.

The emulsion-pouring facilities can meet the demands for making any kind of nuclear emulsion plates which are used for cosmic ray or accelerator experiments. The thermostatic emulsion-processing facilities are operated in order to develop nuclear emulsion plates or X-ray films. Using these facilities, it is also possible to make and develop emulsion pellicles in 600 $\mu$m thickness each. In this way, these facilities are open to all the qualified scientists who want to carry out joint research program successfully.

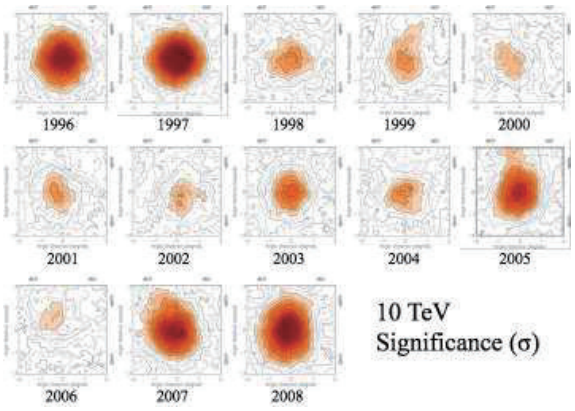


Fig. 5. Observed yearly variation of the Sun's shadow depth (significance map.

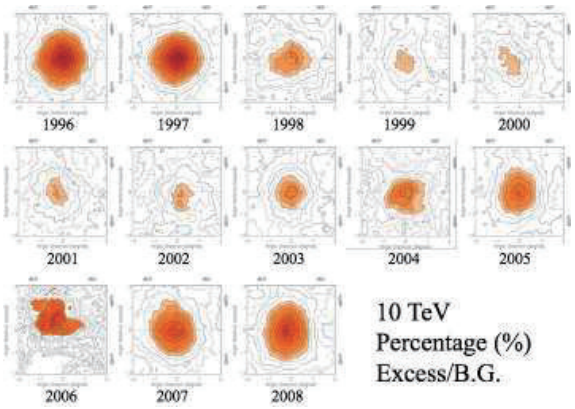


Fig. 6. Observed yearly variation of the Sun's shadow depth, (intensity map).

## Future Plans

### (1) Gamma-ray astronomy in the 100 TeV region

We have a plan to construct a large ($\sim 10,000$ m$^2\times$1.5m deep) underground ($\sim$ 2.5 m soil+concrete overburden) water Cherenkov muon detector array (Tibet MD) around an extended version (Tibet AS, $\sim$83,000 m$^2$) of Tibet III. By Tibet AS + MD, we aim at background-free detection of celestial point-source gamma rays in the 100 TeV region (10 TeV – 1000 TeV) with world-best sensitivity and at locating the origins of cosmic rays accelerated up to the knee energy region in the northern sky. The measurement of cut off energies in the energy spectra of such gamma rays in the 100 TeV region may contribute significantly to understanding of the cosmic-ray acceleration limit at SNRs. Search for extremely diffuse gamma-ray sources by Tibet AS + MD, for example, from the galactic plane or from the Cygnus region may be very intriguing as well. Above 100 TeV, the angular resolution of Tibet AS with 2-steradian wide field of view is 0.2° and the hadron rejection power of Tibet MD is 1/10000. The proposed Tibet AS + MD, demonstrated in Fig. 7, has the world-best sensitivity in the 100 TeV region, superior to HESS above 10-20 TeV and to CTA above 30-40 TeV.

Then, how many unknown/known sources do we expect to detect by Tibet AS + MD, assuming the energy spectra of the gamma-ray sources extend up to the 100 TeV region? Eleven of the HESS new 14 sources discovered by the galac-

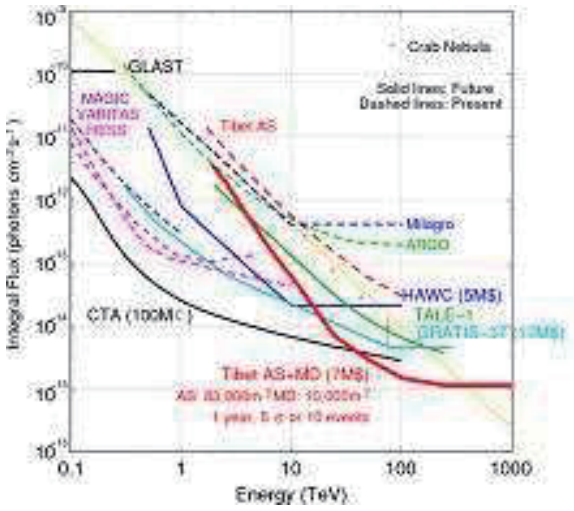


Fig. 7. Tibet AS + MD (red curve) integral flux sensitivity ($5\sigma$ or 10 events/1yr) for a point source.

tic plane survey in the southern sky would be detected by Tibet AS + MD, if it were located at the HESS site. As no extensive search has been done by an appratus with sensitivity comparable to HESS (1 % in unit of RX J1713.7-3946/50-hour observation) in the northern sky, we expect to discover some 10 new gamma-ray sources in the northern sky. In addition to unknown point-like sources, we expect to detect established sources in the 100 TeV region: TeV J2032+4130, HESS J1837-069, Crab, some new Milagro sources, Mrk421, Mrk501 are sufficiently detectable and Cas A, HESS J1834-087,LS I+63 303, IC443 and M87 are marginal.

Furthermore, our integral flux sensitivity to diffuse gamma rays will be the world-best as well. The diffuse gamma rays from the Cygnus region reported by the Milagro group and also diffuse gamma-rays from the galactic plane will be clearly detected. Diffuse gamma-rays of extragalacitic origin may be an interesting target as well.

In fall, 2007, a prototype underground muon detector, composed of two 52m$^2$ water pools, was successfully constructed in Tibet to demonstrate the technical feasibility, cost estimate, validity of our Monte Carlo simulation, as is shown in Figs. 8 and 9.

Single muon peak is clearly observed in the prototype muon detectors as shown in Fig.10.

Preliminary analysis indicates that our MC simulation reproduces real data quite reasonably, as is demonstrated in Fig. 11 and Fig. 12.

### (2) Chemical composition of primary cosmic rays making the knee in the all-particle energy spectrum

We have measured the energy spectra of primary cosmic-ray protons, heliums, all particles around the knee energy region. The main component responsible for making the knee structure in the all particle energy spectrum is heavier nulei than helium. The next step is to identify the chemical component making the knee in the all particle energy spectrum. We have a plan to install an air shower core detector array (1000

Fig. 8. Prototype muon detector viewed from outside, just before being covered with soil.

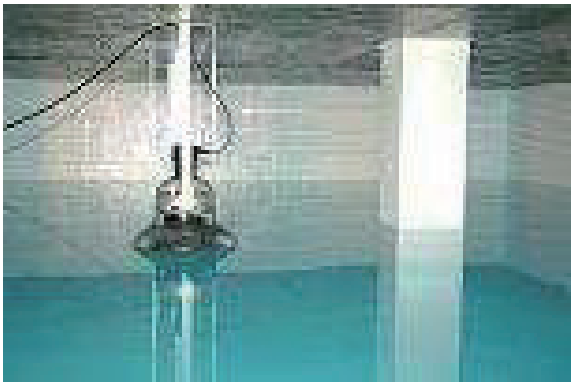

Fig. 9. Prototype muon detector viewed from inside.

to 5000 m$^2$ in area) around the center of Tibet III, as is illustrated in Fig. 13 to distinguish the heavy component making the knee by measuring the difference in lateral distribution of energetic air shower cores.

This will be the first experiment to selectively measure the energy spectrum of the heavy component in the knee energy region and will demonstrate that the knee of the all particle energy spectrum is really composed of heavy nuclei. Figure 14 shows the expected energy spectra of cosmic-ray iron nuclei depending on theoretical models. Tibet AS + YAC has a strong model discrimination power. Sixteen YAC detectors were set up at Yangbajing in 2009 and preliminary analysis is under way.

## Tibet AS$\gamma$ collaboration

ICRR, Univ. of Tokyo, Kashiwa, Chiba 277-8582

In collaboration with the members of:
Hirosaki Univ., Hirosaki, Japan; Saitama Univ., Urawa, Japan; IHEP, Beijing, China; Yokohama National Univ., Yokohama, Japan; Hebei Normal Univ., Shijiazhuang, China; Tibet Univ., Lhasa, China; Shandong Univ., Jinan, China; South West Jiaotong Univ. Chengdu, China; Yunnan Univ., Kunming, China; Kanagawa Univ., Yokohama, Japan; Faculty of Education, Utsunomiya Univ., Utsunomiya, Japan; ICRR, Univ. of Tokyo, Kashiwa, Japan; Konan Univ., Kobe, Japan; Shibaura Inst. of Technology, Saitama, Japan; Department of Physics,

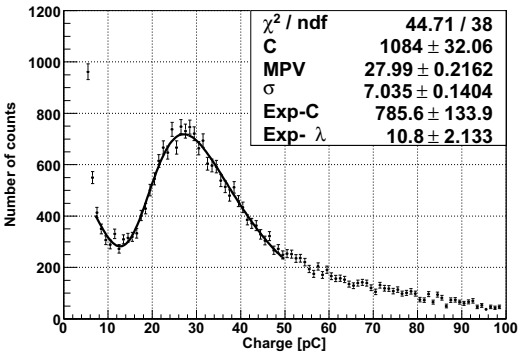


Fig. 10. Single muon peak in the prototype muon detector. Charge distribution recorded by the sum of two PMTs in a cell of the prototype muon detector. A peak of charge distribution is defined as one muon.

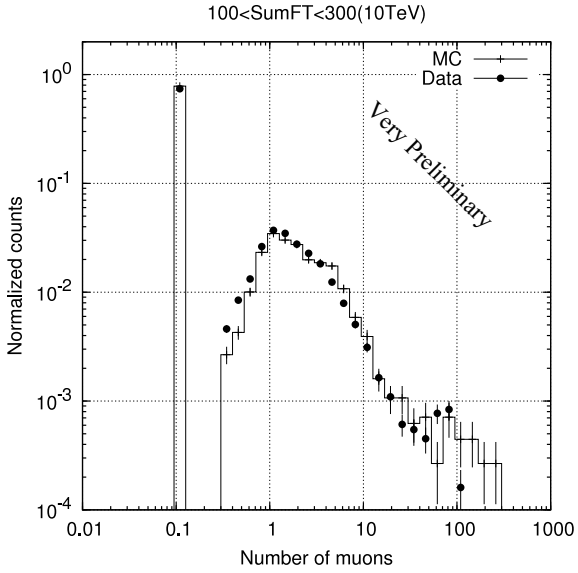


Fig. 11. Number of muons recorded by the prototype muon detector in an air shower at 10 TeV region ($100<\Sigma\rho<300$). The filled diamonds indicate experimental data, while the solid histograms are the MC simulation. Air showers with null muons detected by the muon detector are plotted at number of muons of 0.1.

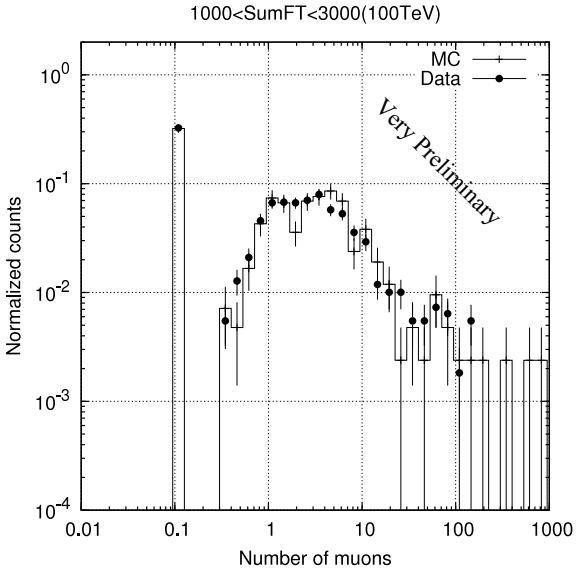


Fig. 12. Number of muons recorded by the prototype muon detector in an air shower at 100 TeV region ($1000<\Sigma\rho<3000$). The filled diamonds indicate experimental data, while the solid histograms are the MC simulation. Air showers with null muons detected by the muon detector are plotted at number of muons of 0.1.

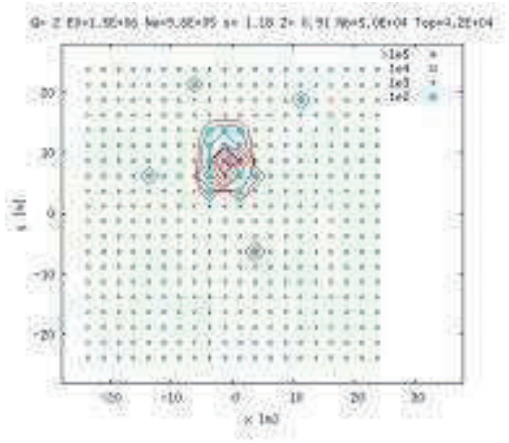

Fig. 13. Illustration of YAC array.

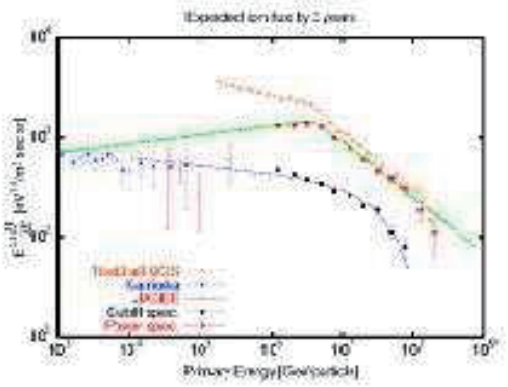

Fig. 14. Expected cosmic-ray iron energy spectra with Tibet AS + YAC.

Shinshu Univ., Matsumoto, Japan; Center of Space Science and Application Research, Beijing, China; Tsinghua Univ., Beijing, China; Waseda Univ., Tokyo, Japan; NII, Tokyo, Japan; Sakushin Kakuin Univ., Utsunomiya, Japan; AMNC, Utsunomiya Univ., Utsunomiya, Japan; Tokyo Metropolitan Coll. of Industrial Technology, Tokyo, Japan; Shonan Inst. of Technology, Fujisawa, Japan; RIKEN, Wako, Japan; School of General Education, Shinshu Univ. Matsumoto, Japan; Nihon University, Narashino, Japan.

## Bibliography

### Papers in refereed journals

[1] "Observation of TeV Gamma Rays from the Fermi Bright Galactic Sources with the Tibet Air Shower Array ", M. Amenomori *et al.*, ApJ **709** L6–L10, (2010).

[2] "On Temporal Variations of the Multi-TeV Cosmic Ray Anisotropy Using the Tibet III Air Shower Array", M. Amenomori *et al.*, ApJ, **711** 119–124, (2010).

[3] "Recent results on gamma-ray observation by the Tibet air shower array and related topics", M. Amenomori *et al.*, J. Phys. Soc. Jpn.,**78**, 88–91 (2009).

[4] "Chemical Composition of Cosmic Rays around the Knee Observed by the Tibet Air-Shower-Core Detector", M. Amenomori *et al.*, J. Phys. Soc. Jpn.,**78**,206–209 (2009).

### Papers in conference proceedings

[5] "A northern sky survey for PeV gamma rays using the Tibet air shower array with water-Cherenkov-type underground muon detector"s, M. Amenomori et al. (The Tibet AS$\gamma$ Collaboration), Proceedings of the 31st International Cosmic Ray Conference, Lodz, Poland, 7-15 July 2009, OG.2.2 (ID: 293), (2009).

[6] "Tibet AS+MD Project", M. Amenomori et al. (The Tibet AS$\gamma$ Collaboration), Proceedings of the 31st International Cosmic Ray Conference, Lodz, Poland, 7-15 July 2009, OG.2.7 (ID:297), (2009).

[7] "Demonstration of hadronic cosmic-ray rejection power by a water Cherenkov underground muon detector with the Tibet air shower array", M. Amenomori et al. (The Tibet AS$\gamma$ Collaboration), Proceedings of the 31st International Cosmic Ray Conference, Lodz, Poland, 7-15 July 2009, OG.2.7 (ID: 810), (2009).

[8] "Interpretation of the cosmic-ray energy spectrum and the knee inferred from the Tibet air-shower experiment", M. Amenomori et al. (The Tibet AS$\gamma$ Collaboration), Proceedings of the 31st International Cosmic Ray Conference, Lodz, Poland, 7-15 July 2009, HE.1.2 (ID: 294), (2009).

[9] "Large-scale sidereal anisotropy of multi-TeV galactic cosmic rays and the heliosphere", M. Amenomori et al. (The Tibet AS$\gamma$ Collaboration), Proceedings of the 31st International Cosmic Ray Conference, Lodz, Poland, 7-15 July 2009, SH.3.2 (ID: 296), (2009).

[10] "New estimation of the power-law index of the cosmic-ray energy spectrum as determined by the Compton-Getting anisotropy at solar time frame", M. Amenomori et al. (The Tibet AS$\gamma$ Collaboration), Proceedings of the 31st International Cosmic Ray Conference, Lodz, Poland, 7-15 July 2009, SH.3.3 (ID: 303), (2009).

[11] "Sun's Shadow in changing phase from the Solar Cycle 23 to 24 Observed with the Tibet Air Sower Array", M. Amenomori et al. (The Tibet AS$\gamma$ Collaboration), Proceedings of the 31st International Cosmic Ray Conference, Lodz, Poland, 7-15 July 2009, SH.3.4 (ID: 751), (2009).

[12] "The sidereal anisotropy of multi-TeV cosmic rays in an expanding Local Interstellar Cloud", M. Amenomori et al. (The Tibet AS$\gamma$ Collaboration), Proceedings of the 31st International Cosmic Ray Conference, Lodz, Poland, 7-15 July 2009, SH.3.2 (ID: 388), (2009).

## The Ashra Project

### Overview

Ashra (*All-sky Survey High Resolution Air-shower detector*) [1, 2, 3] is a project to build an unconventional optical telescope complex that images very wide field of view, covering 77% of the sky, yet with the angle resolution of a few arcmin, sensitive to the blue to UV light with the use of image intensifier and CMOS technology. The project primarily aims to observe Cherenkov and fluorescence lights from the lateral and longitudinal developments of very-high-energy cosmic-ray air showers in the atmosphere. It can also be used to monitor optical transients in the wide field of sky. The observatory will firstly consist of one main station having 12 detector units and two sub-stations having 8 and 4 detector units. One detector unit has a few light collecting systems with segmented mirrors. The main station was constructed on Mauna Loa (3,300 m) on Hawaii Island in 2007.

We started observation of optical transients and pilot observation of Cherenkov tau neutrinos with some of the light collectors in 2008. By analyzing the accumulated data from these observations, we have already searched for optical and VHE-neutrino emissions, for example, in the field of GRB081203A around the Swift/BAT-triggered GRB time [4, 5, 6].

### Project

The observatory will firstly consist of one main station having 12 detector units and two sub-stations having 8 and 4 detector units. One detector unit has a few light collecting systems with segmented mirrors. The features of the system were studied with a prototype detector unit located on Haleakala. The main station was constructed on Mauna Loa (3,300 m) in 2007.

The key technical feature of the Ashra detector rests on the use of electrostatic lenses to generate convergent beams rather than optical lens systems. This enables us to realize a high resolution over a wide field of view. This electron optics requires:

- *image pipeline;* the image transportation from imaging tube (image intensifier) to a trigger device and image sensors of fine pixels (CCD+CMOS), with high gain and resolution, and
- *parallel self-trigger:* the systems that trigger separately for atmospheric Cherenkov and fluorescence lights.

### Observational Objectives

*optical transients;* Ashra will acquire optical image every 6 s after 4-s exposure. This enables us to explore optical transients, possibly associated with gamma ray bursts (GRBs), flares of soft gamma-ray repeaters (SGRs), supernovae explosion, and so on, in so far as they are brighter than $B \simeq 13$

| Opt. Transients | TeV-$\gamma$ | Mountain-$\nu$ | Earth-skimming-$\nu$ | EeV-CR |
|---|---|---|---|---|
| B-UV | Cherenkov | Cherenkov | Fluorescence | Fluorescence |
| $\lambda$=300$\sim$420nm | several TeV | a few 100 TeV | a few 10 PeV | a few 100 PeV |
| 15 mag./4s @3$\sigma$ | 5% Crab/1yr@5$\sigma$ | 5 WB-limit/1yr | 2 WB-limit/1yr | 1600/1yr >10 EeV |
| 2 arcmin | 6 arcmin | unknown | 3 arcmin @ 100 PeV | 1 arcmin @ 10 EeV |

Table 1. Summary of performance with the full configuration (Ashra-2) of three Ashra sites. Detected light, energy threshold, sensitivity limit, and angular resolution are listed from top down for each objective. For EeV-CRs, trigger requirement is two or more stations. Waxman and Bahcall have calculated a neutrino flux upper limit from astrophysical transparent source, here referred to as the WB-limit. For the observation time for objectives other than optical transients, the realistic detection efficiency is taken into account.

mag, for which we expect 3-$\sigma$ signals. The unique advantage is the on-time detection of the events without resorting to usual satellite alerts. 10$\sim$20 events per year are expected in coincidence with the Swift gamma-ray events. The field of view that is wider than satellite instruments allows to detect more optical transients, including an interesting possibility for an optical flash, not visible with gamma rays.

*TeV gamma rays;* Atmospheric Cherenkov radiation will be imaged by Ashra. Requiring the signal-to-noise ratio (SNR) >5, the system will allow to explore VHE gamma-ray sources with the energy threshold of several TeV at the limiting flux sensitivity of 5% Crab for 1-year observation.

*EeV cosmic rays;* For fluorescence lights from VHE cosmic rays the effective light gathering efficiency is comparable with that of the High Resolution Fly's Eye detector (HiRes). The arcmin pixel resolution of Ashra provides finer images of longitudinal development profiles of EeV cosmic ray (EeV-CR) air showers. The resolution of arrival direction with the stereo reconstruction is thus significantly improved and it is better than one arcmin for the primary energy of EeV and higher [7]. This is useful to investigate events clustered around the galactic and/or extragalactic sources. This in turn would give us information as to the strength and coherence properties of the magnetic field.

*PeV-EeV neutrinos;* Ashra may detect Cherenkov and/or fluorescence signals generated from tau-particle induced air-showers that is generated from interactions of tau neutrinos with the mountain and/or the earth. This is identified by peculiar geometry of the air-shower axis. The 1-year detection sensitivity with the full configuration of Ashra is 5 and 2 times larger than the Waxman-Bahcall limit for mountain-produced event (Cherenkov) and earth-skimming event (fluorescence), respectively. The most sensitive energy of around 100 PeV is suitable for the GZK neutrino detection.

The expected performance for each observational object is summarized in Table 1. An example of a 42-degree FOV image taken by the Ashra light collector is shown in Figure 1.

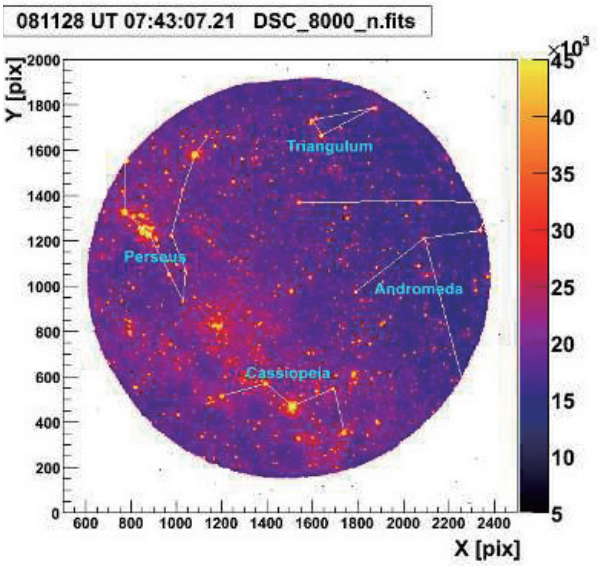


Fig. 1. Example of a 42-degree FOV image taken by the Ashra light collector. The solid lines are drawn to indicate constellations.

## Site Preparation

After finishing the grading work for the area of 2,419 m$^2$ at the Mauna Loa site at the end of July 2005, installation of electrical power lines and transformers was performed until the beginning of September. We started the construction of the detector in October 2005 after receiving materials from Japan. By the middle of December 2005, the first shelters having motorized rolling doors, acrylic plate windows to maintain air-tightness, and heat-insulating walls and floors have been constructed and positioned on eight construction piers of concrete blocks at the Mauna Loa site. In the shelters, the optical elements of the light collectors have been already installed. The optical performance were checked and adjusted to be optimum with star light images from the pilot observation.

In December 2005, we evaluated the night sky background flux on Mauna Loa using the Ashra light collector installed and aligned in a shelter. The result is fairly consistent with the background in La Palma and Namibia by the HESS group From the star light observations, our understanding of the light correction efficiency to be accurate within 5% level.

The civil engineering construction of light collectors in shelters at the Mauna Loa site was completed in August 2007. Figure 2 shows a picture of the constructed Mauna Loa stations. In this Ashra-1 experiment, we are performing device installation and specific observation in a step-by-step way to enhance the scientific impacts.

| Satellite | Trigger Number | GRB Name | Trigger Time | Observed Period [sec] |
|---|---|---|---|---|
| Swift | 322590 | N/A | 080828 UT 08:15:09.33 | $-2.3\times10^3 - 1.1\times10^4$ |
| Swift | 324362 | N/A | 080910 UT 12:52:21.68 | $-4.3\times10^3 - 7.7\times10^3$ |
| Swift | 336489 | GRB081203A | 081203 UT 13:57:11.57 | $-1.2\times10^4 - 5.6\times10^3$ |
| Fermi | 262607680 | GRB090428 | 090428 UT 10:34:38.46 | $-8.1\times10^3 - 5.9\times10^3$ |
| Fermi | 262701807 | GRB090429C | 090429 UT 12:43:25.70 | $-4.1\times10^3 - 7.1\times10^3$ |
| Swift | 373674 | GRB091024 | 091024 UT 08:56:01.26 | $-1.6\times10^3 - 3.3\times10^2$ |
| Fermi | 282484409 | N/A | 091214 UT 11:53:27.83 | $-5.4\times10^3 - 4.0\times10^3$ |
| Fermi | 288007622 | GRB100216A | 100216 UT 10:07:00.19 | $-4.0\times10^3 - 1.1\times10^4$ |

Table 2. Summary of coincidence events with satellite GRB triggers[8][9]. Listed events are those which GRB trigger position are within our FOV at the GRB trigger time.

Fig. 2. The Ashra main and sub stations at the Mauna Loa sites.

## Observation

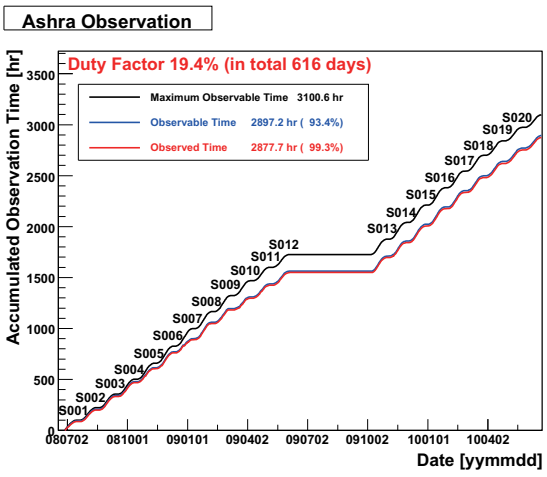


Fig. 3. Summary of Ashra optical transient observation time.

As a first step, we have started the observation of optical transients. During observation, Optical images were constantly collected every 6 s after 4-s exposure. Figure 3 summarizes our observation statistics up to now. Maximum observable time is defined by the following condition:

- *Sun condition;* the altitude of the sun must be lower than $-18$ degree.
- *Moon condition;* the altitude of the moon is lower than 0 degree, or the moon fraction is less than 0.2.

We have accumulated more than 2900 hours of observation time within two years of observation. Good weather rate of 93% shows the superiority of our site and operation efficiency of 99% demonstrates the stability of our operation, where good weather rate is defined by observable time divided by maximum observation time and operation efficiency is defined by observed time divided by observable time. Table2 summarizes coincidence events with satellite GRB triggers[8][9]. In those events, our wide field covers the GRB position at the GRB trigger time. Observed period shows the time period relative to GRB trigger time. In this time period, the GRB position is within our filed of view.

The next step is to start observation of Cherenkov air showers using the light collector towards Mauna Kea. It may detect Cherenkov signals originated from tau neutrinos which interacts with the mountain and/or the earth as described in the section below. We prepared the optical and photoelectric image pipeline system in that light collector. The installation of trigger and DAQ system was performed. Pilot observation to confirm the detection principle of tau neutrino has been carried out [6].

## Search for early optical transients

We constructed a 2/3-scale prototype Ashra detector on Haleakala to verify the optical performances. From October 2004 to August 2005 at the observatory, We made good observations for 844 hours out of 1,526 hours of the moonless nighttime. The fine resolution (arc-minutes) in the ultra wide field of view (0.5 sr) has already been demonstrated using a 2/3-scale model. Our wide field observation covered the HETE-2 WXM error box at the time of GRB041211. 2,000 images were taken every 5 s with 4-s exposure from the time 1h7m before GRB041211 to 1h41m after GRB041211. We detected no objects showing time variation in the WXM error box. It indicates the 3-sigma limiting magnitudes of B$\sim$11.5 magnitude [10]. This is compared with other observations [11, 12]. We also successfully performed two more observations coincident with Swift: GRB050502b [13] and GRB050504 [14].

The Ashra-1 light collector unit on Mauna Loa has the achieved resolution of a few arcmin, viewing 42 degree circle region of which center is located at Alt = 11.7 deg, Azi = 22.1 deg. The sensitive region of wavelength is similar with the B-band. Utilizing this light collector, we have searched for optical counterpart in the field of GRB081203A [15] around

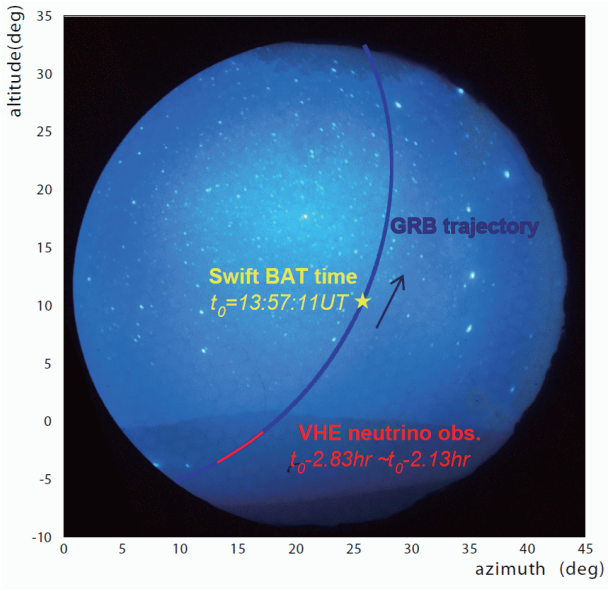


Fig. 4. Trajectory of the GRB081203A counter part in the field of view.

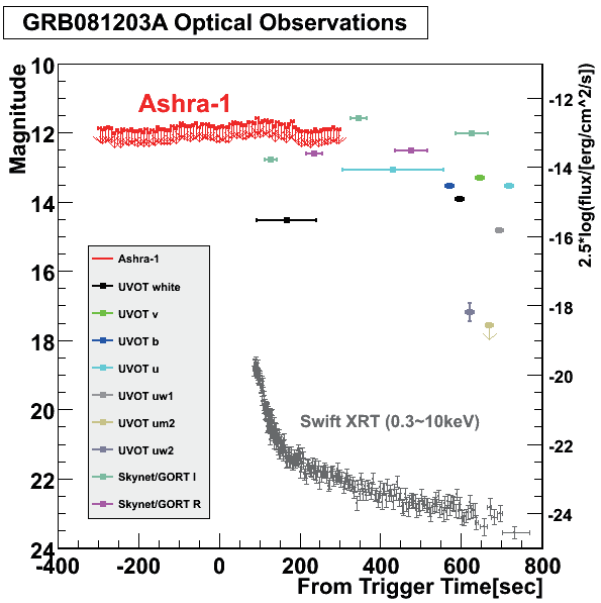


Fig. 5. Summarized lightcurve for GRB081203A around the trigger time. 3-sigma limiting magnitudes of our observation (labeled as Ashra-1) and other observations are compared as a function of time after GRB. The horizontal axis is in linear scale. The vertical axis in the right is only for the data by Swift XRT (gray data), where the scale is arbitrary.

the Swift/BAT-triggered GRB time (T0). Figure 4 shows the trajectory of the GRB position in our field of view. We preliminary analyzed 83 images covering the field of GRB081203A every 7.2s with 6s exposure time respectively during the observation between T0-300s and T0+300s. We detected no new optical object within the PSF resolution around the GRB081203A determined by Swift-UVOT [16]. Around the Swift-BAT trigger time, we have obtained data in every 7.2 seconds with 6sec exposure. The examples of obtained preliminary S/N (signal to noise ratio) maps including the trigger time can be found at [1]. As a result of our preliminary analysis, the following 3-sigma limiting magnitudes are derived. The limiting magnitudes were estimated in comparison with stars in Tycho-2 Catalog to be distributed between 11.7 and 12.0. Figure 5 shows limiting optical magnitudes vs time comparing with the other measurements [4].

## Search for Cherenkov tau neutrinos

We used a detection technique called 'the Earth-skimming neutrino'. This detection technique was originally proposed in 1990's [17] and already used by other observations. The essence of this technique is separation of target and detection. Small cross section of first interaction of neutrino favors dense material, while fine imaging of the interaction does not. If the first interaction is separated from the following interactions, we can evade from the above contradiction.

Reaching the Earth, a neutrino enters into the Earth's crust and mountains, interacts with materials via charged current interaction, and produces a lepton. The lepton propagates in the crust with loss of its energy. If it is a tau lepton, it decays after exit to the atmosphere, and generates detectable air shower. The length of the propagation of tau lepton in the rock makes a cluster around a few 10 km above $10^{17}$eV due to the energy loss. Hence we can detect tau neutrinos of decades of energies with a fixed geological formation.

This detection technique has a maximum sensitivity around 100 PeV. Using this technique, we aim to connect PeV to EeV by lowering the energy threshold of neutrino observation with air light. PeV is the energy range where ice and water Cherenkov experiments have their maximum sensitivities, while EeV is the energy range where experiments with air shower have. For that aim, we think that detection of Cherenkov radiation from air shower is important. In order to detect Cherenkov radiation emitted forward, shower front must be directed to the detector. Therefore, we chose a geometry widely viewing rock of over 10km thickness, that is, mountain. We designed an observation facing the mountain (Figure 6). In this observation, we used a light collector toward Mauna Kea.

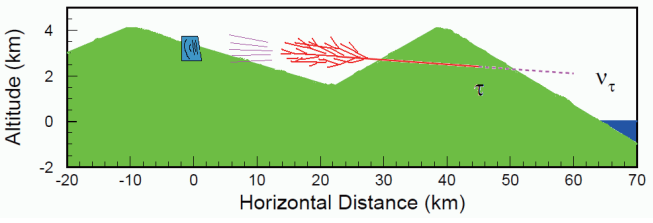


Fig. 6. Conceptual figure of this observation (the Earth-skimming neutrino detection technique). The right mountain is Mauna Kea and the left is Mauna Loa.

## Cherenkov tau shower observation

We intended an observation in order to study neutrino emissions from transient objects. Also, performance check of our trigger system is another aim of this observation.

Before the observation, we simulated neutrino signals

generated by tau leptons emerging from Mauna Kea (Figure 7). Then, we calibrated the detector with artificial sources, such as an LED and a radiant source. Furthermore, we verified the system's performance by an observations of cosmic rays (protons). Cosmic-ray observation was carried out with an FOV closer to the zenith than in the neutrino observation. Figure 8a shows an example of obtained image of Cherenkov radiation from air-showers, and Figure 8b shows a simulated event by CORSIKA. We can see that the obtained data resembles the simulated event. It demonstrates well the strength of the high angular resolution of our detector. As shown by the comparison of Figure 7 with the data (Figure 8a), our detector has an ability of detecting air showers from neutrinos.

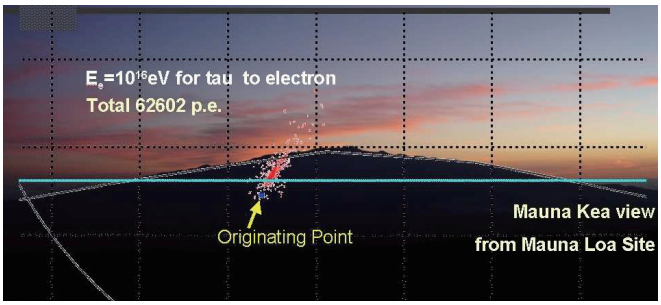


Fig. 7. Example of simulated neutrino event.

The observation for neutrino emission was executed in a duration from October to December in 2008 (Table 3). Fortunately we accomplished highly efficient observation. As a result we observed a GRB, GRB081203A, in a period before and after its occurrence, tens of GRBs after their occurrence, and tens of active galactic nuclei (AGN).

The obtained data were analyzed. In order to estimate the sensitivity we must take into account spurious events generated by background cosmic rays. In principle, the Earth-skimming neutrino detection technique is free from background events, thanks to the screening effect of the Earth's rock. Also, the FOV of this observation is nearly horizontal, hence thick atmosphere screens the normal cosmic-ray events. We studied the screening effects and confirmed the absence of background events from background sources. Then, the most frequent background was Cherenkov radiation from muons that interact with the detector itself. We simulated the radiation, and carefully removed them from the data.

### Results of tau neutrino search

We did not discover any candidate of neutrino emission in the range from tens of PeV to EeV. We set preliminary upper limits to the fluence and flux of source models, related to the mechanism for the particle acceleration in transient objects. All the following limits are derived with 95% confidence level.

For GRB081203A precursor, we set a limit $E\phi(E) < 5.4 \times 10^{-8}$ [cm$^{-2}$], assuming a spectrum extended up to 5 EeV. For GRB081203A late prompt emission, the obtained limit is $E^2\phi(E) < 4.3$ [erg cm$^{-2}$]. Combination of the two observations for GRB081203A, the upper limit for neutrino emission [6] and the optical observation with our detector [5], leads to the conclusion that it is not contradictory to the normal particle acceleration. This discussion can be considered as a beginning of 'multi-particle astronomy'[18]. For GRB afterglow, the limit leads $E^2\phi(E) < 19$ [erg cm$^{-2}$]. Note that this limit is set by the source integrated analyses. Furthermore, neutrino emission from AGN was studied. The limit for diffuse flux is about 2nd order of magnitude larger than that by other experiments, but better than Auger experiment at 100 PeV. In addition to that, we set a meaningful upper limit, $E^{1.4}\phi(E) < 1.3 \times 10^{-12}$[cm$^{-2}$s$^{-1}$PeV$^{0.4}$], based on a source model assuming proton synchrotron emission. This limit corresponds to a diffuse flux rejected by experiments. However, it should be noted that our result is not affected by the source distribution in the universe because of a limit for point sources.

By means of Cherenkov tau shower observation, our detector is sensitive to neutrinos with energies of $1 \sim 100$ PeV. This energy range is just between the maximum sensitivities of ice experiments and other air-shower experiments. For future neutrino experiments, pointing accuracy in this region will become more important, in order to localize transient objects and investigate the mechanism of the particle acceleration in individual sources. The Ashra detector may be considered as a promising candidate to realize 'multi-particle astronomy'[18], which is necessary to understand particle acceleration in the universe.

## Bibliography

[1] http://www.icrr.u-tokyo.ac.jp/∼ashra

[2] Sasaki, M., 2003, "Very High Energy Particle Astronomy with All-sky Survey High Resolution Air-shower Detector (Ashra)", *Progress of Theoretical Physics Supplement,* vol. 151, pp. 192–200.

[3] Sasaki, M., et al., 2008, "The Ashra Project" Proc. 30th Intl. Cosmic Ray Conf. Merida 3, 1559.

[4] Aita, Y., et al., 2008, GCN Circ. 8632.

[5] Ogawa, S., et al., 2009, "Ashra Optical Transient Observation", 31th Intl. Cosmic Ray Conf. (Lodz), ID1410.

[6] Noda, K., et al., 2009, "VHE neutrino pilot observation with the Ashra detector", 31th Intl. Cosmic Ray Conf. (Lodz), ID313.

[7] Sasaki,M., et al., 2002, "Design of UHECR telescope with 1 arcmin resolution and 50° field of view", *Nucl. Instrum. Methods,* vol. A492, pp. 49–56.

[8] http://gcn.gsfc.nasa.gov/swift_grbs.html

[9] http://gcn.gsfc.nasa.gov/fermi_grbs.html

[10] Sasaki, M., et al., 2004. GCN Circ. 2846.

[11] Sasaki, M., et al., 2005. "Status of Ashra project," Proc. 29th Intl. Cosmic Ray Conf. Pune 8, 197–200.

[12] Sasaki, M., et al., 2005. "Observation of Optical transients with the Ashra Prototype," Proc. 29th Intl. Cosmic Ray Conf. Pune 5, 319–322.

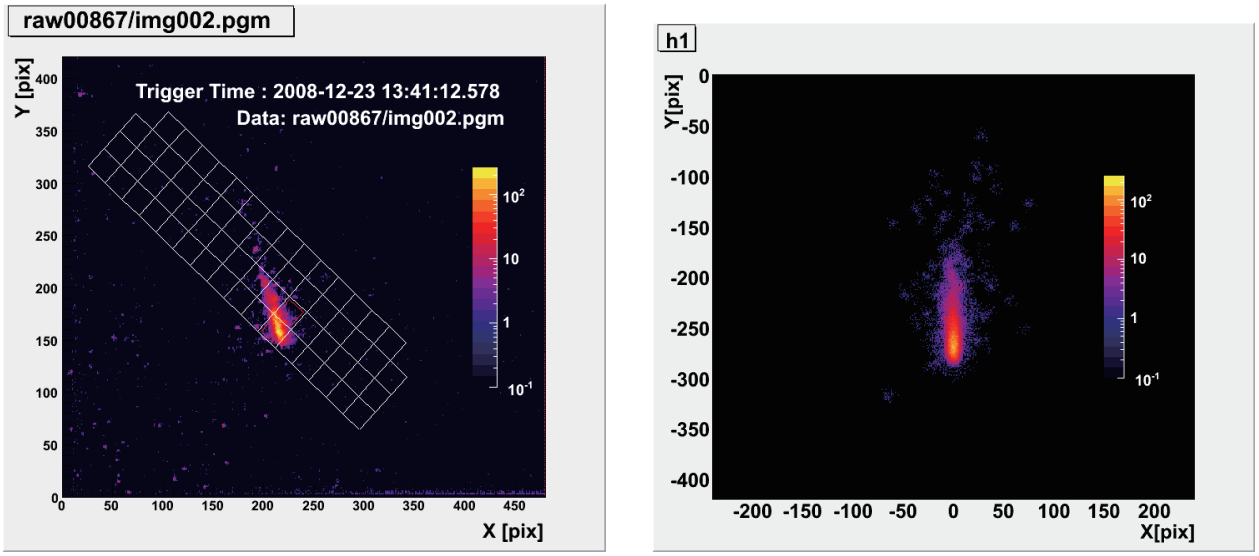


(a) data (b) simulated event

Fig. 8. Example of air-shower image from the cosmic-ray observation. The conditions for simulated event are as follows; proton, energy = 1EeV, core distance = 266m, angular resolution = 9 arcmin, and thinning = $10^{-6}$. The color shows pixel value (max. is 255 counts).

Table 3. Observation time for Cherenkov tau neutrinos. Duty factor is defined by the observed time divided by the total time including daytime and full moon periods.

| Period (UT) | Max. Observable Time [hr] | Observed Time [hr] (duty factor) |
|---|---|---|
| 2008/10/28 – 11/11 | 95.5 | 75.3 (17%) |
| 2008/11/15 – 12/10 | 164.6 | 140.5 (20%) |

[13] Sasaki, M., et al., 2005. GCN Circ. 3499.

[14] Sasaki, M., Manago, N., Noda, K., Asaoka, Y., 2005. "GRB050502b: Early Observation," GCN Circ. 3421.

[15] Parsons, A. M., et al., GCN Circ. 8595

[16] De Pasquale, M., et al.,GCN Circ. 8603.

[17] Fargion, D., 2002, ApJ **570** 909 (arXiv:astro-ph/9704205).

[18] Sasaki, M., 2000, in Proc. of ICRR workshop "ICRR2000 Satellite Symposium: Workshop of Comprehensive Study of the High Energy Universe".

## High Energy Astrophysics Group

[Spokesperson: T. Terasawa]

ICRR, Univ. of Tokyo, Kashiwa, Chiba 277-8582

### Overview

The high energy astrophysics group was created recently in December 2009, to aim at making theoretical and observational studies of violent astrophysical phenomena in which nonthermal cosmic ray particles are being accelerated. Targets of the group's study include high energy astrophysical objects such as supernova explosions/pulsar magnetospheres, giant flares and repeating bursts of magnetars, jets from active galactic nuclei (AGN), star-burst galaxies, mysterious gamma ray bursts (GRB), as well as galaxy clusters.

In addition, studies have been made also for nonthermal phenomena within the heliosphere, such as interplanetary shocks and the earth's bow shock [1], magnetic reconnection, the interaction processes between the solar wind and the lunar surface. While these heliospheric phenomena are limited in their energy coverage, their studies have been proved to give a theoretical basis to interpret distant high energy phenomena.

### Research topics: 1. Reevaluation of acceleration processes

While the diffusive shock acceleration process has been accepted as the standard model of astrophysical particle acceleration, interests are being renewed on other processes such as second order stochastic acceleration in relativistic turbulences behind relativistic shocks formed in GRBs and AGNs. We have presented a new result on the contribution of the second order acceleration to the formation of the X-ray photon spectrum from GRBs [3] (Figure 1). Modification of the supernova shock structure by the pick-up interstellar neutrals is also studied [4] (Figure 2).

### Research topics: 2. Injection/preacceleration process

How to 'inject', or preaccelerate particles to suprathermal energy before the start of the diffusive shock process is an important unsolved problem. To answer the electron injection problem, the origin of whistler waves, which are responsible

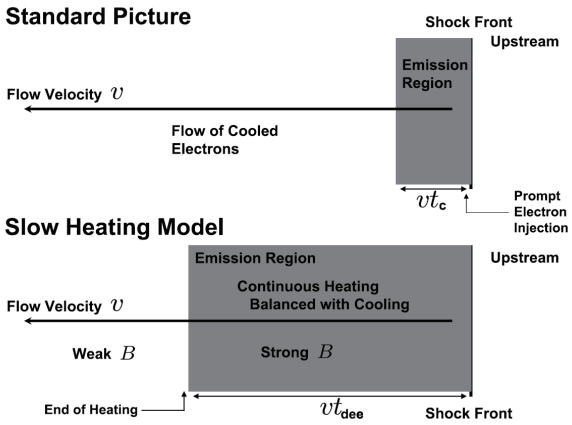


Fig. 1. Schematic illustrations of standard GRB model and a new GRB model [3] in which the second order acceleration works efficiently.

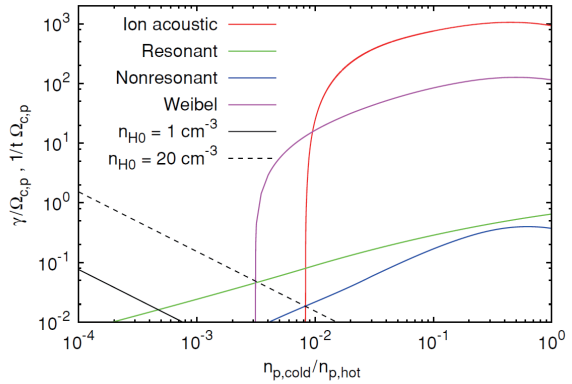


Fig. 2. Comparison of the growth rates of various plasma instabilities in the downstream region of a supernova shock where pick-up interstellar neutral particles play an essential role [4].

for the scattering of suprathermal electrons, should be studied. Based on the whistler wave observation in the upstream regions of strong interplanetary shocks, we are approaching this long-standing issue. The preliminary results are consistent with the idea of nonlinear cascade from low frequency ion-excited Alfvén waves toward higher frequency whistler waves [Oka, Terasawa, et al., in preparation].

It is expected that the interactions between fast plasma flows with surfaces of solid bodies play an important role for particle injection in some astrophysical environments. The nearest example found recently is in the solar-wind-moon interaction (Figure 3), where efficient acceleration of solar wind ions reflected by the lunar surface is found from the SELENE project [5-9].

**Research topics: 3. Magnetars and pulsars**

The magnetosphere around neutron stars are candidate sites for efficient particle acceleration. Magnetars, slowly-rotating neutron stars with strong magnetic field of $10^{13-15}$ G, occasionally show a giant-flare (GF) activity, in which the

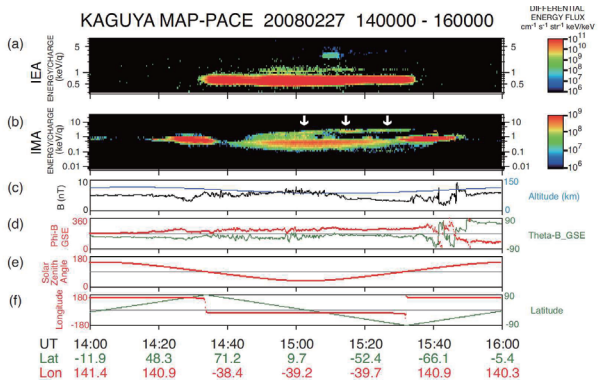


Fig. 3. An example of solar wind ions scattered/accelerated on the lunar surface (white arrows). Panels (a) and (b) are omini-directional energy-versus-time spectrogram of ion sensors. Panels (c) and (d) are magnetic field intensity and direction in the geocentric solar ecliptic coordinate. Panels (e) and (f) show the solar zenith angle and the latitude/longitude of the position of SELENE [9].

peak gamma-ray luminosity reaches to $10^{47}$ erg s$^{-1}$ [Terasawa et al., 2005], which is as strong as the luminosity of AGNs. In addition to giant flares, magnetars also show burst activities, much weaker than GFs but repeating many times. Recently we have discovered ionospheric disturbances caused by repeating bursts of the magnetar SGR J1550-5418 in January 2009. Such ionospheric disturbance can be used as a new monitoring method for magnetars [10].

Crab pulsar, the remnant of the supernova explosion in 1054 A.D., is one of the well-known neutron stars. While its physical properties have been studied for more than 40 years since its discovery, there remains an enigma about the origin of giant radio pulses (GRPs). We have recently observed GRPs from Crab pulsar with a high time resolution at 1.4GHz ($\sim$30 ns), and discovered the existence of sub-microsecond structure of GRPs (Figure 4). It is expected that this structure would provide a new clue to solve the emission/propagation mechanism of GRPs as well as the relating particle acceleration mechanism. This observation of Crab pulsar has been conducted under a collaboration project with NICT (National institute of Information and Communications Technology).

**Research topics: 4. R/D study for radar detection of UHECR**

Wide attention has been attracted to the detection of ultra high energy cosmic rays (UHECR) with radio techniques, either passive and active, towards future large-scale UHECR observatory on the ground. Collaborating with the TA group of ICRR, we have made a R/D study of the active method, namely, the detection of radar echoes from extensive air showers of UHECRs (EAS echoes, hereafter) utilizing the MU radar system (Figure 5).

We have found an EAS echo candidate at the direction of the zenith angle $\theta = 12^{\circ}$ and the azimuthal angle $\varphi = 185^{\circ}$ as shown in Figure 6a (indicated by an arrow), The other fainter peaks seen in Figure 6a are explained in terms of the antenna side lobe effect as simulated in Figure 6b. The time variation of echo signal is shown in Figure 6c, where the duration of

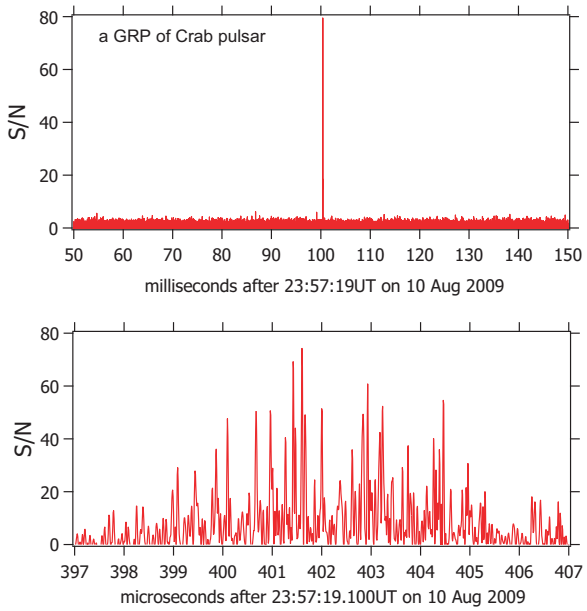


Fig. 4. (a) upper panel: A GRP of Crab pulsar observed on 10 August 2009 in the 1405-1435 MHz band, where 1 $\mu$sec average is taken. (b) lower panel: The same as (a), but with the highest time resolution 1/128 $\mu$sec.

Fig. 5. The MU radar in Shigaraki, Japan. This is a high-power (peak:1MW, average:50kW) mono-static pulse Doppler radar with the central frequency $f$=46.5MHz operated by the Research Institute for Sustainable Humanosphere (RISH) of Kyoto University.

the echo was 4-6$\mu$s, which is close to the duration expected for EAS echoes.

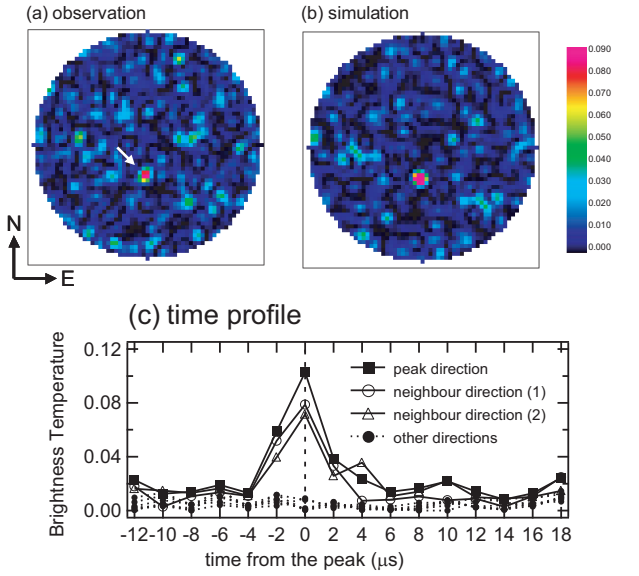


Fig. 6. An EAS echo candidate [2]. (a) upper left panel: The sky map of the brightness temperature (in an arbitrary unit) for the zenith angle $\theta \leq 50^{o}$. (b) upper light panel: The same as (a) but for a simulated sky map. (c) lower panel: The time variation of the brightness temperature.

## Bibliography


### Papers in conference proceedings

1. "Shocks in the heliosphere", Terasawa, T., an invited review paper at *International Association of Geomagnetism and Aeronomy*, Sopron, 29 August 2009, in press, 2010.

2. "Search for radio echoes from EAS with the MU radar, Shigaraki, Japan", Terasawa, T., T. Nakamura, H. Sagawa, H. Miyamoto, H. Yoshida, M. Fukushima, Proceedings of 31st International Cosmic Ray Conference, session H.E.1.6, paper #0199, 2009.

### Papers in refereed journals

3. "Slow heating model of gamma-ray burst: Photon spectrum and delayed emission", K. Asano and T. Terasawa, Astrophys. J. 705:1714-1720, 2009.

4. "Plasma instabilities as a result of charge exchange in the downstream region of supernova remnant shocks", Ohira, Y., T. Terasawa, and F. Takahara, Astrophys. J. Lett. 703:L59-L62, 2009.

5. "First direct detection of ions originating from the Moon by MAP-PACE IMA onboard SELENE(KAGUYA)", Yokota, S., Y. Saito, K. Asamura, T. Tanaka, M. N. Nishino, H. Tsunakawa, H. Shibuya, M. Matsushima, H. Shimizu, F. Takahashi, M. Fujimoto, T. Mukai, and T. Terasawa, Geophys. Res. Lett. 36:L11201.1-4, 2009.

6. "Pairwise energy gain-loss feature of solar wind protons in the near-Moon wake", Nishino, M. N., K. Maezawa, F. Fujimoto, Y. Saito, S. Yokota, K. Asamura, T. Tanaka, H. Tsunakawa, M. Matsushima, F. Takahashi, T. Terasawa, H. Shibuya, H. Shimizu, Geophys. Res. Lett. 36:L12108.1-4, 2009.

7. "Solar-wind proton access deep into the near-Moon wake", Nishino, M. N., Fujimoto, M., Maezawa, K., Saito, Y., Yokota, S., Asamura, K., Tanaka, T., Tsunakawa, H., Matsushima, M., Takahashi, F., Terasawa, T., Shibuya, H., and Shimizu, H., Geophys. Res. Lett. 36:L16103.1-4, 2009.

8. “First in situ observation of the Moon-originating ions in the Earth’s Magnetosphere by MAP-PACE on SELENE(KAGUYA)” Tanaka, T., Y. Saito, S. Yokota, K. Asamura, M. N. Nishino, H. Tsunakawa, H. Shibuya, M. Matsushima, H. Shimizu, F. Takahashi, M. Fujimoto, T. Mukai, and T. Terasawa, Geophys. Res. Lett. 36:L22106.1-4, 2009.

9. In-flight performance and initial results of Plasma energy Angle and Composition Experiment (PACE) on SELENE (KAGUYA), Saito, Y., S. Yokota, K. Asamura, T. Tanaka, M. N. Nishino, T. Yamamoto, Y. Terasawa, M. Fujimoto, H. Hasegawa, H. Hayakawa, M. Hirahara, T. Mukai, T. Nagai, T. Nagatsuma, T. Nakagawa, M. Nakamura, K.I. Oyama, E. Sagawa, S. Sasaki, K. Seki, I. Shinohara, T. Terasawa, H. Tsunakawa, H. Shibuya, M. Matsushima, H. Shimizu, F. Takahashi, Space Sci. Rev., in press, 2010.

10. First VLF detection of short repeated bursts from magnetar SGR J1550-5418, Tanaka, Y. T., J.-P. Raulin, F. C. P. Bertoni, P. R. Fagundes, J. Chau, N. J. Schuch, M. Hayakawa, Y. Hobara, T. Terasawa, and T. Takahashi, Astrophys. J. Lett., in press, 2010.

# ASTROPHYSICS and GRAVITY DIVISION

## Overview

Astrophysics and Gravity Division consists of Gravitational Wave Group, The Sloan Digital Sky Survey Group ,Theory Group and Primary Cosmic Ray Group. The Gravitational Wave Group conducts R&Ds for LCGT project jointly with researchers of gravitational wave experiment and theory in Japan. The main items of those R&Ds are TAMA project and CLIO project. The Sloan Digital Sky Survey Group continues accumulating data of images and spectroscopic observation of galaxies and publishing papers in collaboration with worldwide researchers. Theory Group conducts both theoretical study of the Universe and astroparticle physics. Primary Cosmic Ray Group started the research on the history of solar activity.

## Gravitational Wave Group

### Introduction

A gravitational wave is a physical entity in space-time predicted by Einstein's theory of general relativity. Its existence was proven by the observation of PSR1913+16 by Taylor and Hulse [1], who won the Nobel prize in 1993. However, nobody has succeeded to directly detect gravitational waves. The theory of gravitation can be tested by the detection of gravitational waves. A gravitational wave detector is the last tool of mankind to inspect the universe. In order to directly observe gravitational waves, we aim to construct the Large scale Cryogenic Gravitational wave Telescope (LCGT). For the first step of constructing sensitive laser interferometer, we developed a 300 m baseline interferometric gravitational wave detector, TAMA, at the Mitaka campus of the National Astronomical Observatory of Japan (NAOJ) and nine observation runs had been conducted[1]. TAMA project started in April, 1995, as a five-year project and it was extended by two years after 1999. TAMA was organized by researchers belonging to universities and national laboratories. The observation runs spanned from two to eight weeks, the last one of which ended in 2004[2, 3]. We presented the development of Seismic Attenuation System (SAS) installed for four main mirrors[4] and tried to achieve its design sensitivity of TAMA[5]. We finally found that the sensitivity at low frequencies is limited by so-called up-conversion noise possibly arising from the suspension and actuation system and could not be improved anymore without a drastic change of the suspension system utilizing more sophisticated actuator[6, 7]. In regard with CLIO project, the construction of which was started in 2003 and ended in March, 2007, we succeeded to break the room temperature limit by cryogenic mirror system that was operated at cryogenic temperature at first in the world[9].

We submitted the budget request of LCGT project for FY 2010 and also we applied to a funding program promoting advanced sciences in 2009. Although we passed to have chance of hearing by the government panel for this program, LCGT was not nominated in 2009 and was not approved for FY2010. In this year, we studied how to improve the sensitivity of LCGT by utilizing the recent development of interferometer technologies on bandwidth and we determined not to adopt the suspension point interferometer for the final design of LCGT.

*1 J. H. Taylor and J. M. Weisberg, Astrophysical J., **345** (1989) 434.

## LCGT Project

[Spokesperson : Kazuaki Kuroda]

ICRR, Univ. of Tokyo, Kashiwa, Chiba 277-8582

In collaboration with the members of:
National Astronomical Observatory (NAOJ), High Energy Accelerator Research Organization (KEK), Department of Physics (University of Tokyo, abbreviated as UT hereafter), Research Center for the Early Universe (UT), Institute for Laser Science (University of Electro-Communications), Department of Advanced Materials Science (UT), Earthquake Research Institute (UT), Department of Astronomy (UT), Department of Physics (Osaka City University), Faculty of Engineering (Hosei University), Metrology and Measurement Science (National Institute of AIST), Space-Time Standards Group (National Institute of Information and Communication Technology), Department of Earth and Space Science (Osaka University), Department of Physics (Kyoto University), Yukawa Institute for Theoretical Physics (Kyoto University), Graduate School of Humanities and Sciences (Ochahnomizu University), Advanced Research Institute for the Sciences and Humanities (Nihon University), Department of Advanced Physics (Hirosaki University), Astronomical Institute (Tohoku University), Department of Physics (Niigata University), Department of Physics (Rikkyo University), Department of Physics (Waseda University), College of Industrial Technology (Nihon University), School of Engineering (Nagaoka University of Technology), Department of Physical Science (Hiroshima University), Faculty of Science (University of the Ryukyu), Max Planck Institute for Gravitational physics (AEI), California Institute of Technology, Department of Physics (University of Western Australia), Department of Physics (Louisiana State University), Center for Computational Relativity and Gravitation (Rochester Institute of Technology), Department of Physics (Glasgow University), Columbia Astrophysics Laboratory (Columbia University in the city of New York), Department of Physics (Birmingham University), Department of Astronomy (Beijing Normal University), Inter University Center for Astronomy & Astrophysics (Pune University), Sternberg State Astronomical Institute (Moscow University), LATMOS (CNRS), Center for Astrophysics (University of Science and Technology of China), Center for Astrophysics (Tsinghua University), Institute of High Energy Physics (Chinese Academy of Sciences), Center for Gravitation and Cosmology (Purple Mountain Observatory), Center for Measurement Standards (Indus-

trial Technology Research Institute), Goddard Space Flight Center (NASA), ARTEMIS (CNRS)

## Objective of LCGT

After the discovery of the highly relativistic binary neutron star system [2], a new young binary pulsar has been detected [3]. The former discovery had increased the coalescence rate from $10^{-6}$ to $10^{-5}$ a year in a galaxy as big as our Galaxy [4] and the latter pushes up by another factor of six. Although it was good news for the detection of gravitational waves, we still needed to wait for long time to detect by the presently existing detectors. This was the reason why we needed to construct LCGT (Large-scale Cryogenic Gravitational wave Telescope). The objective of LCGT is to detect at least one gravitational wave event in a year. There are many other possible gravitational wave sources in the universe other than the coalescence of binary neutron stars. However, the coalescence of binary neutron stars differs completely from other sources in the sense that its wave form is precisely predicted, and its existence has certainly been confirmed.

## Status of LCGT Project

The target sensitivity of LCGT is to observe binary neutron star coalescence events occurring at 250 Mpc with S/N=8 in its optimum configuration[10]. This is ten-times more sensitive than that of the LIGO (initial LIGO), and by two orders more than that of TAMA at their most sensitive frequencies. This will be attained by the laser interferometer located underground, using three-kilometer length baseline, cooling mirrors at cryogenic temperature, and a high-power laser source employing 150 W output. The optical configuration is a power recycled Fabry-Perot-Michelson interferometer with the resonant-sideband-extraction (RSE) scheme (in Fig. 1). The detailed design of the control system was tested for the resonant sideband extraction scheme[11]. Table 1 lists the important parameters of LCGT, which were revised three times from the original design[12]. Ultimate sensitivity of a laser interferometer is determined by seismic noise at low frequencies (10-30 Hz) (which is reduced by improving the vibration isolation system), and it is limited by photon shot noise at higher frequencies (more than 300 Hz), which can be improved only by increasing the light power in the main cavities. The sensitivity of middle frequencies (30-300 Hz) is limited by the photon recoil force noise. This requires that thermal noise is reduced both by decreasing the temperature and by decreasing the internal mechanical loss (*i.e.*, increasing the mechanical Q of vibration modes). The source of thermal noise comes from both mirror internal vibration, mechanical loss of the optical coating and swing noise of the pendulum suspending the mirror. The reduction of thermal noise is attained by cooling both the mirror, itself, and the suspension system that suspends the mirror.

Figure 2 compares the sensitivity curve of LCGT with those of TAMA, CLIO (a 100 m prototype cryogenic interferometer placed underground of Kamioka mine, described later), LIGO (initial LIGO) and the room temperature limit of CLIO. The sensitivity at low frequencies of LCGT is attained by SAS, which has been developed by TAMA. That of higher frequencies is attained by higher laser power, which has been basically shown by TAMA. The mid-frequency region is improved by cryogenic mirror and suspension system, which has been proven by CLIO. Although the improvement, especially two orders of magnitude at low frequencies, is adventurous, it is not impossible by our expertise and high moral to attain the goal.

Table 1. LCGT design parameters to detect binary neutron-star coalescence events in 250 Mpc.

| Item | Parameter |
|---|---|
| Baseline Length | 3 km |
| Interferometer | One set |
| | Power recycled Fabry-Perot |
| | -Michelson with RSE |
| Optical Power | Laser:150 W; Finesse:1550 |
| | Input power at BS: 825 W |
| | Cavity power 780 kW |
| Beam radius at End | 3 cm |
| Main Mirror | Sapphire 30 kg, 20 K |
| | Diameter 25 cm |
| | Mechanical Q:$10^8$ |
| Suspension | Frequency: 1 Hz; Q:$1 \times 10^8$ |
| pendulum | 10 K |
| Vacuum | $\leq 10^{-7}$ Pa |

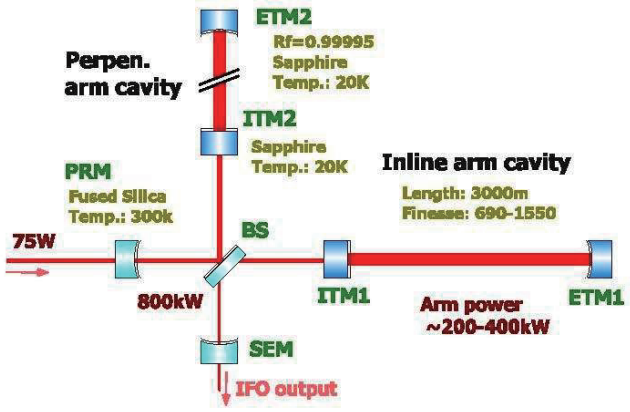


Fig. 1. Basic optical design of LCGT. The optical configuration is a power recycled Fabry-Perot-Michelson interferometer with the resonant-sideband-extraction (RSE) scheme.

## Cryogenic Mirror development

The original design of the cryogenic mirror system is shown in Fig. 3. The mirror is suspended by two loops of sapphire fibers connected to an auxiliary mirror that is a part of suspension point interferometer (SPI). This mirror is also suspended from an alignment control platform that is suspended

*2 M. Burgay, *et al.*, Nature, **426** (2003) 531.
*3 D.R. Lorimer, *et al.*, Astrophysical J. **640**(2006) 428.
*4 C. Kim, V. Kalogera and D. R. Lorimer, Astrophysical J. **584** (2003) 985.

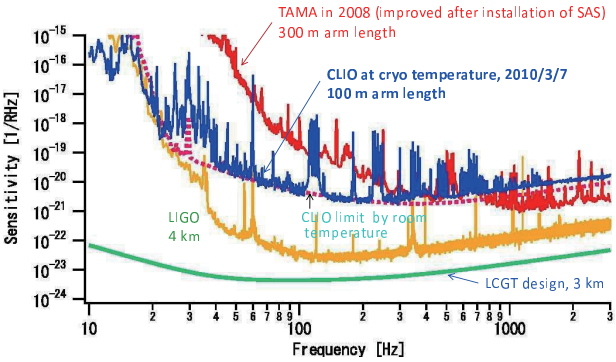


Fig. 2. LCGT design sensitivity compared with those of TAMA (red line), CLIO (a 100m prototype cryogenic interferometer placed underground of Kamioka mine, blue line), LIGO (initial LIGO, yellow line) and the CLIO limit at room temperature (red broken line). The horizontal axis is frequency [Hz] and the vertical axis represents sensitivity spectrum for gravitational waves [1/$\sqrt{}$Hz].

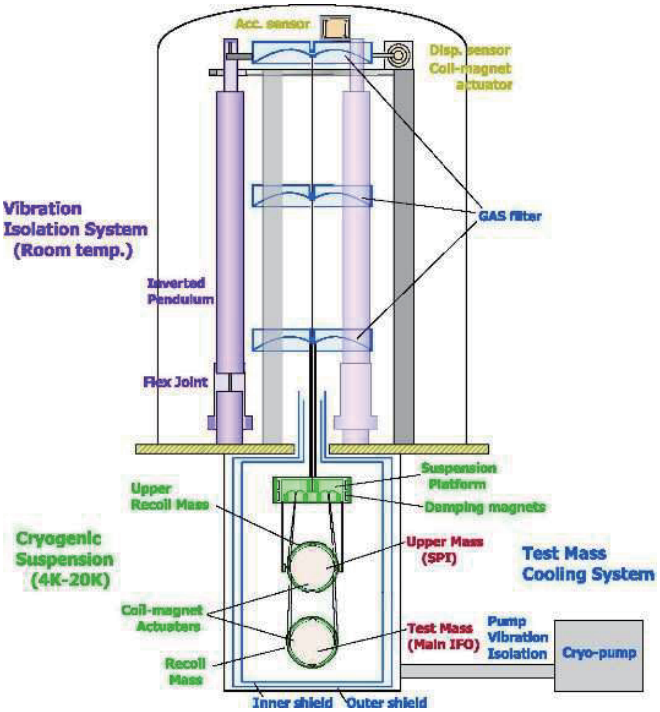


Fig. 3. Schematic design of the original cryogenic suspension system. The mirror is suspended by sapphire fibers connected to an auxiliary mirror, which is suspended by metal wires from a platform that has a heat link to a 4 K heat anchor inside the vacuum. The platform is also suspended with an insulator rod connected through the holes of radiation shields to an isolation table suspended by a seismic attenuation system placed at room temperature in the common high vacuum. Since the auxiliary mirror will be replaced by other intermediate mass due to the abortion of the SPI system, the conceptual design of cryogenic suspension remains the same.

with an insulator rod connected through the center holes of the radiation shields to an isolation table suspended by a low-frequency vibration isolator, which is placed at room temperature. The auxiliary mirror has a heat link to the platform and another heat link connects the platform and a heat anchor point (4 K) inside the vacuum located just above the platform.

Since the SPI will be replaced by an alternative system as is described in the end of this LCGT section, the auxiliary mirror will be replaced by an appropriate intermediate mass, which functionally works for heat path. However, the basic concept of the cryogenic suspension system is maintained in this alternation.

Both the cryogenic system and the vibration isolator are put inside a common high-vacuum chamber.

To realize this concept, the following research subjects were conducted and reported:

1. Removal of heat produced by high-power laser illumination (annual report 1997-1998 and also in references [13])
2. Holding the high Qs of the mirror internal modes and suspension pendulum [14]
3. Reducing the contamination of mirror surfaces (annual report 2000-2001 and also in [15]).
4. Estimating heat production by optical loss in the mirror [16].
5. Alignment control of mirrors in a cryogenic environment [17]
6. Low mechanical loss of the optical coating (annual report 2003-2004 and also in reference [18])

As for item 5, we confirmed that a superconducting film could be used for the receptor of the magnetic force in place of permanent bar magnets that are normally used in the existing detectors. The film can be easily sputtered on the mirror surface without harmfully degrading the mechanical Q of the mirror. With respect to the last item, we reported on a measurement of the bulk substrate of the mirror at cryogenic temperature in the annual report (2003–2004). We could correctly estimate the thermal vibration noise of the optical coating while considering the inhomogeneous loss that had been neglected at an early stage of interferometer development. The substrate of the cryogenic mirror is sapphire, which has a large thermo-elastic thermal noise at room temperature. However, since the thermal-expansion ratio of sapphire at cryogenic temperature goes down to nearly 0 and the heat conductivity becomes greater, the thermo-elastic noise drastically reduces at the cryogenic temperature. Thermal noise estimated from the Q of the coating was well below the design sensitivity of LCGT, which means that this coating noise does not limit the sensitivity, whereas, the sensitivity of a room-temperature mirror is limited by this effect. This is the significant merit of the cryogenic mirror system.

## Byproduct of cryogenic mirror

A serious problem was pointed by Braginskii[5]. Large power density of Fabry-Perot cavity may cause so-called para-

*5 Braginskii, *et al.*, Physics Lett. A **305** (2002)111.

metric instability, which is produced by the coupling between optical cavity modes with elastic vibration modes of the mirror substrate. Since the sapphire has larger elastic wave velocity, the number density of elastic modes is fewer than that of synthesized silica mirror, which is the case of advanced LIGO. And also the coupling constant between optics and mechanics is smaller in LCGT than in advanced LIGO due to the smaller beam size of LCGT. This merit comes from the adoption of cryogenics of LCGT[19]. Recent publication shows the effective suppression of the increase of the instability by adopting a negative feedback directly applied to the mirror[20].

### Towards CLIO

All of the above R&D confirmed the feasibility of reducing the thermal noise of the interferometer in the middle-frequency region. This research underlines the basis of LCGT. However, for a practical cryogenic detector, more practical R&Ds will be needed for the installation of cryogenic mirrors. One of the earliest R&D activities along this line was the Kashiwa cryogenic interferometer system reported in the annual report (2000–2001; 2002–2003; 2003–2004). By this Kashiwa cryogenic interferometer, we learned the necessity of several practical R&D items and began to construct the CLIO interferometer in Kamioka to establish techniques for the cryogenic interferometer (refer to the section of CLIO).

### Practical R&Ds

#### Measurement of the optical qualities of sapphire

LCGT adopts cryogenic mirrors to reduce thermal noise in place of expanding laser beam radius that is planed both in the Advanced LIGO and the Advanced Virgo. $Al_2O_3$ monocrystal is selected as the cryogenic mirror substrate because it has excellent mechanical and thermal properties. However, there were some optical problems to be solved. High optical absorption and in-homogeneity of refractivity are concerned with rather difficult reproducibility of large ingots exceeding 20 cm. While some small-sized $Al_2O_3$ crystal substrates had good absorption quality and better homogeneity enough to satisfy the LCGT requirement, larger samples (10cm in diameter, 6cm in length) had less quality [21]. Moreover, we know that the fabrication technology of $Al_2O_3$ crystal to date is not mature enough to consistently produce large substrates of adequate quality. In order to inspect optical homogeneity of large pieces of $Al_2O_3$ crystal for the production of better quality, we developed a scanning technique of birefringence measurement with high sensitivity and reported the determination of the optical axis of the uni-axial crystal and the measurement of the fluctuation of birefringence. Although we have not obtained a large pieces satisfying the requirement of LCGT, we established a tool to distinguish the quality required to pass the specification of LCGT by this R&D in the annual report (2007-2008) and in reference[23].

### Other R&Ds

Apart from the above R&D issues, a high power laser system that produces more than 100 W is continually being developed by a group in Advanced Material Science, School of New Frontier Science, University of Tokyo[24]. Also, researchers at KEK tested the mechanical strength of suspension fiber of sapphire crystal [25] and the result of heat radiation leaking from room temperature tube to the cryogenic chamber was quantitatively measured as reported in the section of CLIO[16]. We steadily advance towards the realization of LCGT by these R&D activities.

### Study on the Bandwidth Optimization of LCGT

A broad band RSE (resonant-sideband extraction) configuration was selected as a default LCGT optical design since 2004. With recent progresses in technology, it appears that we have a chance to enhance the sensitivity of LCGT by selecting more suitable optical parameters. We started to establish a working group to discuss and optimize the optical configuration including a possibility of the detuned RSE which has a narrower bandwidth but a better sensitivity in total. The purpose of this working group is to investigate and to make recommendations on the interferometer optical configuration design of LCGT and its observation band for gravitational waves.

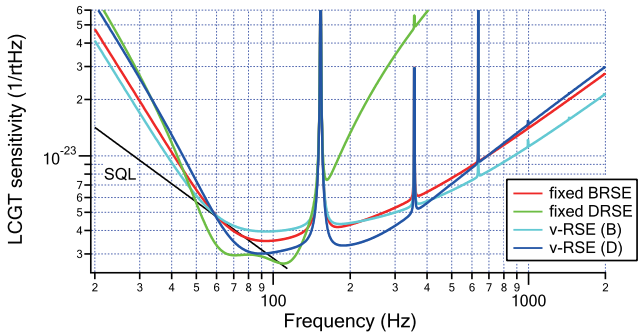


Fig. 4. Sensitivity curves of the candidate configurations: BRSE (red curve), DRSE (green curve), and VRSE (B/D) with sky-blue/blue curves.

It is possible to optimize and tune the observation frequency band for target gravitational-wave sources, by choosing suitable optical parameters. So as to determine the optical parameters, we define three candidate parameter sets: broad-band RSE (**BRSE**), detuned RSE (**DRSE**), and variable RSE (**VRSE**) configurations. VRSE is designed to have good sensitivity both with tuned and detuned operation, and to switch observation bands depending on the observation purposes and targets. The detector sensitivity curves are estimated with the current best-estimated boundary conditions of LCGT: an input laser power, suspension and mirror thermal noises, seismic noise, and optical readout noises. The estimated sensitivity curves are shown in Fig. 4. and Table 2 shows brief summary of optical parameters.

The DRSE configuration (green curve) has the best floor-level sensitivity at around 100 Hz, and the best observable distance of 132 Mpc for neutron-star inspiral events (SNR=8, sky averaged). The BRSE configuration (red curve) has wider observation band to cover various sources, and moderate observable range of 114 Mpc for neutron-star inspirals. The blue and sky-blue curves are for the VRSE configuration with a

Table 2. Setup parameters, inspiral range (IR), and strain sensitivity at 1 kHz of each configuration. The first number in each IR column is with the assumption that wave come from the optimal direction for LCGT, and each number in parenthesis is with the average over whole sky.

| | $T$ (Finesse) | $T_s$ | $\phi$ [deg] | $\zeta$ [deg] | IR [Mpc] | Sensitivity [$\mathrm{Hz}^{-1/2}$] |
|---|---|---|---|---|---|---|
| BRSE | 0.004 (1550) | 0.23 | 90 | 127.6 | 259 (114) | $1.4 \times 10^{-23}$ |
| DRSE | 0.009 (690) | 0.08 | 74.6 | 103.8 | 299 (132) | $2.1 \times 10^{-22}$ |
| VRSE (B) | 0.004 (1550) | 0.15 | 90 | 121.8 | 255 (112) | $1.1 \times 10^{-23}$ |
| VRSE (D) | 0.004 (1550) | 0.15 | 86.5 | 134.7 | 281 (123) | $1.5 \times 10^{-23}$ |

detuned mode **VRSE (D)** and with a broadband mode **VRSE (B)**, respectively. They have slightly narrower and wider observation bands than the BRSE (red curve) configuration, respectively.

Scientific outcomes obtained from GW observation highly depend on the sensitivity and observation band of a detector. We surveyed possible GW sources which would be targets of LCGT, and discussed advantages and disadvantages of each candidate interferometer configurations.

The most important criteria in the comparison is to increase the possibility to achieve the minimum success of LCGT: detect at least a few GW events within one year operation. The primary target of LCGT is coalescences of neutron-star binaries. We estimated the observable range, expected event rates, required observation period for the first detection, and measurement accuracy of binary mass parameters for these sources. Figure 5 shows the expected detection rate as a function of sky average detection range. Then we surveyed scientific outcomes from the other GW sources: black-hole binaries, black-hole ringdown, supernovae with stellar-core collapses, pulsars. We also compare the candidate configurations from a viewpoint of international observation network. Here, we show Table 3 summarizing the range for black-hole binaries, etc.

The working group concluded the following interferometer design and observation strategy as a part of new default LCGT design.

- The optical configuration of LCGT should be VRSE: a RSE (resonant-sideband extraction) with variable observation band.
- In the first observation phase, LCGT interferometer should be operated with a detuned mode, VRSE (D), for earlier detection of gravitational-wave signals. After the first detections, the variable configuration provides the option to change the observation band to broadband, VRSE (B), so as to obtain more scientific information.

### Study report on Elimination of Suspension Point Interferometer

Suspension point interferometer (SPI) is an active vibration isolation scheme for interferometric gravitational wave detectors. As a part of the default design of LCGT, it was thought that the SPI would be used in the LCGT, which was discussed since 2004. The SPI makes use of an auxiliary interferometer to monitor the seismic vibration transmitted through the suspension wires. The seismic vibration is actively suppressed by an appropriate feedback control using the signal from the auxiliary interferometer. However it was pointed out that the SPI would have too complicated structures, and designing the SPI to align main mirrors properly would be not easy by the complication.

The LCGT SPI special working group is charged with the investigations on the necessity and feasibility of the suspension point interferometer for LCGT. The biggest question to be answered is whether LCGT need to have an SPI or not. For this purpose, the working group examined the necessity of the SPI mainly from two aspects: (1) the reduction of the vibration introduced from heat-link wires and (2) the reduction of RMS mirror motion for robust lock acquisition. They also investigated alternative techniques which can replace or supplement the SPI.

Simulation results showed that the target sensitivity of LCGT would not be compromised by the heat-link vibration even without an SPI. The seismic noise would be limited by the vertical vibration coupling from the heat-links in the observation band. Since vertical vibrations cannot be suppressed by an SPI, an improvement of the seismic noise safety factor cannot be expected from SPI. Requirement of LCGT for the RMS displacement noise (0.1 m above 0.1 Hz) is satisfied without an SPI in the normal seismic period. Almost the same effect as the RMS reduction by the SPI can be achieved by a carefully designed hierarchical control.

The working group concluded the following actions to be taken regarding the LCGT SPI.

- We shall not install an SPI for LCGT.
- We shall continue to put R&D efforts on the alternative techniques, such as cryogenic active vibration isolation stage, hierarchical control, offset lock and green laser pre-lock.
- In order to keep the possibility of retrofitting an SPI in the future, we recommend to keep the vacuum tube size large enough (1 m). The beam height of the main laser in the vacuum tube shall be offset from the center to accommodate the SPI beam in the future.

## Bibliography

[1] H. Tagoshi it et al., Phys. Rev. D **63**(2001)062001-1-5.

[2] H. Tagoshi *et al.*, "Results of Searches for inspiraling compact star binaries from TAMA 300fs observation in 2004-2004", TAUP 2007, September 11-15, 2007, Sendai.

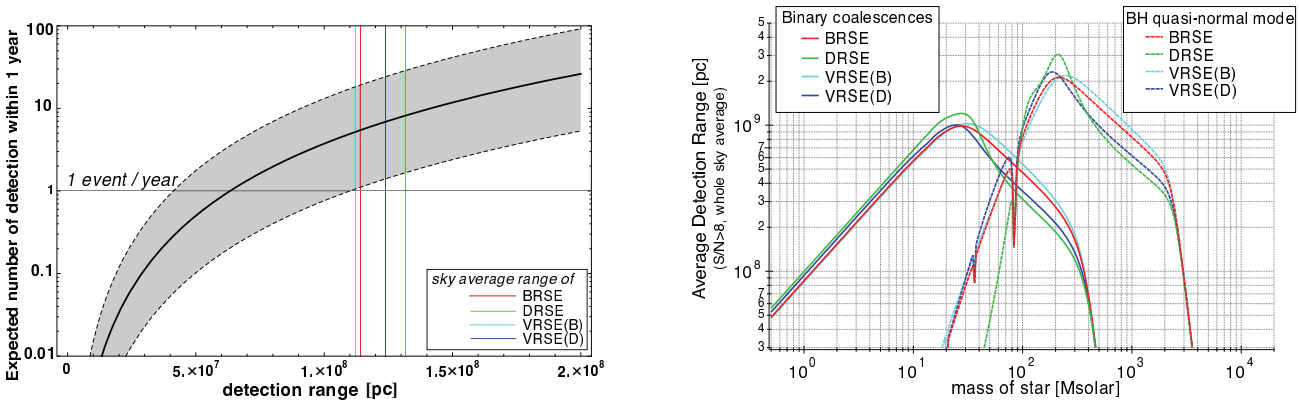


Fig. 5. *Left*: Solid thick black line is Expected event rate as a function of sky average detection range, and gray shaded zone is a confidence band of 95%. Solid thin lines show the range for binary coalescence. Colors are corresponding to the IFO configurations. *Right*: Sky-averaged detection ranges as a function of total mass of the source. Solid lines show the range for binary coalescence. Dashed lines show the range for ringdown GW from black-hole quasi-normal mode. Colors are corresponding to the IFO configurations.

Table 3. BH observations. In this estimation, we assume the amplitude of ringdown GW corresponding to 3% of mass.

| | IFO configurations | | | |
|---|---|---|---|---|
| | BRSE | VRSE (B) | VRSE (D) | DRSE |
| Binary coalescences NS-BH (1.4-10$M_\odot$) | | | | |
| Detection range $d_{\rm avg}$ [Mpc] | 240 | 235 | 261 | 278 |
| Expected event rate [events/yr] | | 0.006 – 6 | | |
| Binary coalescences BH-BH (10-10$M_\odot$) | | | | |
| Detection range $d_{\rm avg}$ [Mpc] | 570 | 557 | 615 | 677 |
| Expected event rate [events/yr] | | 0.07 – 7 | | |
| Quasi-normal mode : | | | | |
| Detection range $d_{\rm avg}$ [Gpc] for 200 $M_\odot$ | 2.1 | 2.0 | 2.3 | 3.0 |
| Survey mass region at 1 Gpc [$M_\odot$] | 110 - 910 | 115 - 760 | 100 - 490 | 100 - 450 |


[3] N. Kanda *et al.*,"Short gravitational wave signal searches in TAMA 300 data: stellar collapse and black hole", TAUP 2007, September 11-15, 2007, Sendai.

[4] R. Takahashi *et al.*, Class. Quantum Grav. **25** (2007) 114036.

[5] K. Agatsuma *et al.*, J. Phys.:Conference Series **122** (2008) 012013.

[6] K. Arai*et al.*, "Recent Progress of TAMA 300", TAUP 2007, September 11-15, 2007, Sendai.

[7] D. Tatsumi *et al.*, "TAMA 300 interferometer development", TAUP 2007, September 11-15, 2007, Sendai.

[8] M. Ohashi *et al.* "Status of LCGT and CLIO", TAUP 2007, September 11-15, 2007, Sendai.

[9] T. Uchiyama *et al.* in preparation for publication.

[10] K. Kuroda (on behalf of the LCGT Collaboration), "Status of LCGT", Class. Quantum Grav. **27** (2010) 084004.

[11] F. Kawazoe *et al.*, J. Phys.: Conference Series **122** (2008) 012017.

[12] K. Kuroda *et.al.*, Int. J. Mod. Phys. **D 8** (1999) 557; K. Kuroda,*et al.*, Class. Quantum Grav. **19** (2002) 1237; T. Uchiyama, *et al.*, Class. Quantum Grav. **21** (2004) S1161.

[13] T. Uchiyama, *et.al.*, Phys. Lett. **A 242** (1998) 211.

[14] T. Uchiyama, *et.al.*, Phys. Lett. **A 261** (1999) 5;*ibid* **A273**(2000)310.

[15] S. Miyoki, *et al.*, Cryogenics **40** (2000) 61: *ibid* **41** (2001) 415.

[16] T. Tomaru, *et al.*, Phys. Lett. **A 283** (2001) 80.

[17] N. Sato, *et al.*, Cryogenics **43** (2003) 425.

[18] K. Yamamoto, *et al.*, Class. Quantum Grav. **21** (2004) S1075.

[19] K. Yamamoto, *et al.*, J. Phys.: Conference Series **122** (2008) 012015.

[20] M. Evans, presented at GWADW meeting, Florida, May 10-15, 2009.

[21] M. Tokunari *et al.*, J. Phys.: Conference Series 32 (2006) 432.

[22] Z. Yan, *et al.*, Applied Optics **40**(2006) 1.

[23] M. Tokunari *et al.*, Class. Quantum Grav. *in press*.

[24] N. Mio, H. Takahashi and S. Moriwaki, J. Phys.: Conference Series **122** (2008) 012014.

[25] T. Suzuki *et al.*, presented at Amaldi 7 meeting, Sydney, July 8-14, 2007.

[26] T. Tomaru *et al.*, J. Phys.: Conference Series **122** (2008) 012009.

## CLIO Project

[Spokesperson : Masatake Ohashi]

ICRR, Univ. of Tokyo, Kashiwa, Chiba 277-8582

In collaboration with members of: KEK, Tsukuba; Kyoto-U, Kyoto; ERI of UT, Tokyo

CLIO (Cryogenic Laser Interferometer Observatory) is a 100 m-baseline underground cryogenic interferometer at the Kamioka Mine. CLIO forms a bridge connecting the CLIK (7 m prototype cryogenic interferometer at Kashiwa campus) and the planed LCGT (3 km cryogenic interferometer at Kamioka). The site of CLIO, near the Super-Kamiokande neutrino detector, is shown in Fig. 6. The tunnel was dug in 2002, and a strain meter for geophysics was installed in 2003 [1]. The construction of CLIO began in late 2003, and installation of the mode cleaner vacuum system was reported in the annual report (2003–2004). Four sets of cryostats and whole vacuum system were installed (annual report 2004–2005). We started the operation of CLIO in 2006 (annual report 2006).

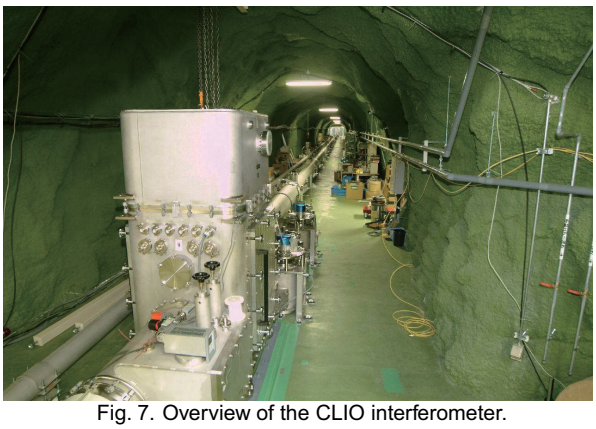

Fig. 7. Overview of the CLIO interferometer.

The prime purpose of CLIO is to demonstrate mirror thermal noise reduction with cryogenic mirrors. We achieved the design sensitivity at the room temperature after noise hunting taken in 2008 (Annual report 2008) [2]. After then, we started out cooling the mirrors and noise hunting with the mirrors under 20K had been done. We firstly observed the sensitivity improvement due to the mirror thermal noise reduction.

CLIO sensitivity curve with cooled mirrors (cryogenic sensitivity) and without cooling (300K sensitivity) are shown in fig. 9 with estimation curves of the mirror thermal noise. The 300K sensitivity and the cryogenic sensitivity were measured at 2008/11/5 and at 2010/03/20, respectively. When the cryogenic sensitivity was measured, two front mirrors were cooled and the rest of two end mirrors were at the room temperature. Temperature of the front mirrors were 17K and 18K. Modifications those are possible to affect the sensitivity at the cryogenic sensitivity measurement are exchange of final suspension wires and addition of heat link wires to the suspension systems. Cooling the mirror took about 250 hours and vacuum pressure was better than $10^{-4}$Pa for both sensitivity measurements.

The noise floor level of the cryogenic sensitivity from 90Hz to 240Hz is below the 300K sensitivity. Observation range for GWs from neutron star binary coalescence was also improved to 159kpc from 148kpc for the optimum direction. This is the first observation of sensitivity improvement by the cryogenic mirrors. The noise floor at 165Hz was reduced to $2.2 \times 10^{-19}\,\mathrm{m}/\sqrt{\mathrm{Hz}}$ from $3.1 \times 10^{-19}\,\mathrm{m}/\sqrt{\mathrm{Hz}}$ after cooling of the front mirrors. Amount of this noise floor reduction is consistent with the estimation of mirror thermal noise reduction due to cooling.

Along with the cryogenic sensitivity measurement, a few other studies corresponding to CLIO and LCGT have been done at the CLIO site. A digital control system developed in LIGO laboratory, USA was installed as a part of international collaboration, and lock acquisition test using the CLIO interferometer was successfully completed. One set of Local Suspension Point Interferometer (LSPI) was installed in a CLIO suspension system. Purpose of LSPI is an active control system of a mirror suspension system using an interferometer. The Pound-Drever-Hall (PDH) method[3] is generally used for obtaining control signal for a Fabry-Perot cavity. We have proposed a new solutions for expanding the linear signal range of the PDH method and it has just accepted for the publication[4].

Fig. 8. a sapphire mirror and cryogenic suspension system.

## Bibliography

[1] S. Takemoto, *et al.*, Journal of Geodynamics **41** (2006) 23.

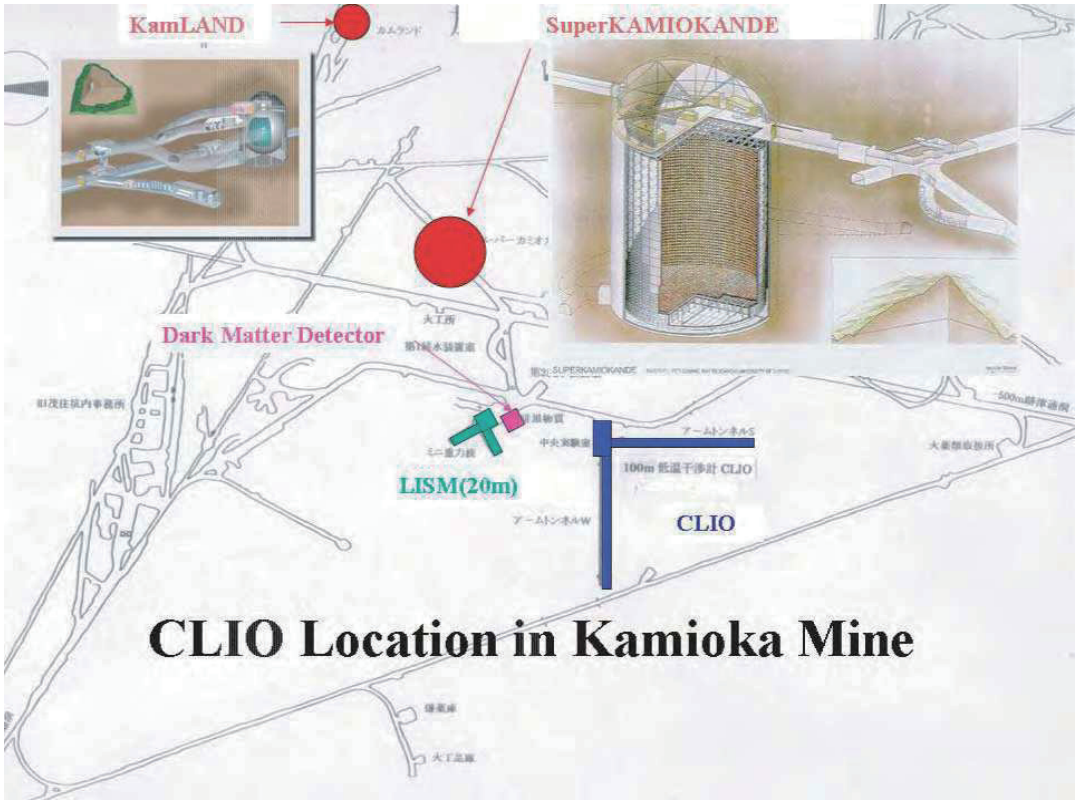


Fig. 6. Location of the CLIO interferometer.

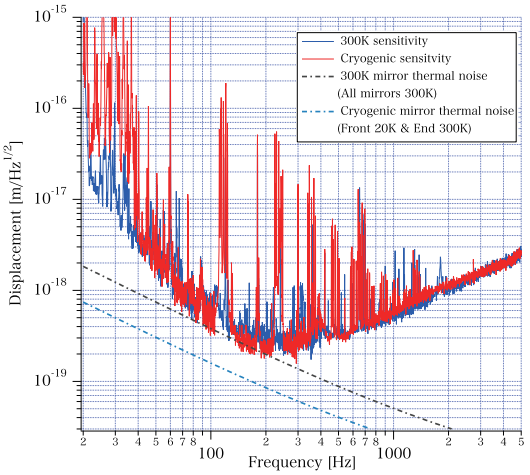


Fig. 9. Comparison of CLIO sensitivity curves. 300K sensitivity (solid blue line) and Cryogenic sensitivity (solid red line) show CLIO sensitivity curves without cooling mirrors measured at 2008/11/05 and with front mirrors under 20K measured at 2010/03/20, respectively. 300K mirror thermal noise (dot dash gray line) and Cryogenic mirror thermal noise (dot dash blue line) show estimation curve of mirror thermal noise corresponding to the each sensitivity measurements.

[2] S. Miyoki, *et al.*, Journal of Physics: Conference Series **203** (2010) 012075.

[3] R. W. P. Drever, *et al.*, Appl. Phys. B **31** (1983) 97-105.

[4] S. Miyoki, *et al.*, Accepted by Applied Optics.

## Sloan Digital Sky Survey

[Spokesperson : Masataka Fukugita]

ICRR, University of Tokyo, Kashiwa, Chiba 277-8582

In collaboration with the members of:
University of Tokyo, 7-3-1 Hongo, Bunkyo-ku, Tokyo 113-0033, Japan; Nagoya University, Chikusa, Nagoya 464-8602, Japan; National Astronomical Observatory of Japan, 2-21-1 Osawa, Mitaka, Tokyo 181-8588, Japan; Tohoku University, Aramaki, Aoba, Sendai 980-8578, Japan; Japan Women's University, 2-8-1, Mejirodai, Bunkyo-ku, Tokyo, 112-8681, Japan; The University of Chicago, 5640, South Ellis Ave., Chicago, IL 60637, USA; Fermi National Accelerator Laboratory, P.O. Box 500, Batavia, IL 60510, USA; Institute for Advanced Study, Einstein Drive, Princeton, NJ 08540, USA; Johns Hopkins University, Baltimore, MD 21218, USA; Los Alamos National Laboratory, Los Alamos, NM 87545, USA; Max-Planck-Institute for Astronomy, Königstuhl 17, D-69117 Heidelberg, Germany; Max-Planck-Institute for Astrophysics, Karl Schwarzschildstrasse 1, D-85748 Garching, Germany; New Mexico State University, P.O. Box 30001, Dept 4500, Las Cruces, NM 88003, USA; University of Pittsburgh, 3941 O'Hara St., Pittsburgh, PA 15260, USA; Princeton University, Princeton, NJ 08544, USA; United States Naval Observatory, P.O. Box 1149, Flagstaff, AZ 86002-1149; University of Washington, Box 351580, Seattle, WA 98195, USA

The survey operation of the SDSS has ended in June 2008, and all the primary data have been reduced and catalogued

as SDSS Data Release 7 (Abazajian et al. 2009). The catalogue contains images and parameters of 360 million objects over 911663 square degrees of sky and spectra of 1.62 million objects over 9380 square degree, approximately 1/4 the entire sky. Primary science analyses were also carried out, which fulfilled more than 95% of the science goals contemplated in the beginning of the survey, all satisfied at a satisfactory level. In addition we obtained some significant results that were not anticipated in the beginning, including the discovery of baryon acoustic oscillation, discovery of reionisation of the Universe,gravitational weak-lensing estimates of the mass distribution, and evidence for continued formation of the Milky Way. In short it has made a great contribution that tightens our understanding of the Universe and its evolution, summarised as establishing "the Standard Cosmology". The data are, and will be, used as the fundamental data-base to study a variety of the astrophysical science, perhaps as long as for a century.

Our work has continued that is categorised into three parts. (i) the characterisation of the instrument and the survey data. We have done this work all the time during the survey, from the commencement of the survey till the end. The results acquired have been communicated from time to time to the project team, but a summary of the entire data are now given as publications (Doi et al. 2010; Fukugita et al. 2010). (ii) The work of SDSS so far published is *first-stage-analyses*, the most recent example including upgrades of the two-point correlation function and baryon acoustic oscillation (Percival et al. 2009; Reid et al. 2009), production of the enlarged sample of quasars (Schneider et al. 2010) and of strong lensing (Inada et al. 2010). More elaborated analyses were needed to exploit fully the available data. The example includes the discovery of dust in galactic haloes, perhaps expelled from galaxies. The analysis rested on the unique feature of SDSS, very large data sets and extremely accurate photometry, as one has to resolve variations of brightness at an unprecedented accuracy of 0.003 magnitude (Ménard et al. 2010). Work for galaxy properties, a long term project of the Japanese group, was also published (Oohama et al. 2009). (iii) Taking the SDSS results as fiducial at the present-day Universe, we attempt to understand the evolution of galaxies. This is the work in progress.

Brief history of the work by the Japanese team for the SDSS is reviewed in Fukugita, Butsuri: Bull Phys, Soc, Japan, 2010, **65**, 524. Now, the work is planned for the continued SDSS project, termed as SDSS-III, and the work has been taken up by a team of IPMU. Software preparation and preliminary science work are being done by the IPMU team members, who include current and former members of the SDSS team of ICRR.

## Bibliography


[1] Cross-correlation weak lensing of SDSS galaxy clusters I: measurements, E. S. Sheldon, D. E. Johnston, R. Scranton, B. P. Koester, T. A. McKay, H. Oyaizu, C. Cunha, M. Lima, H. Lin, J. A. Frieman, R. H. Wechsler, J. Annis, R. Mandelbaum, N. A. Bahcall, M. Fukugita Astrophys. J. **703**, 2217 (2009).

[2] The seventh data release of the Sloan Digital Sky Survey, K. N. Abazajian et al. (SDSS Collaboration) Astrophys. J. Suppl. **182**, 543 (2009).

[3] The greater impact of mergers on the growth of massive galaxies: implications for mass assembly and evolution since z$\sim$1, K. Bundy, M. Fukugita, R. S. Ellis, T. A. Targett, S. Belli and T. Kodama, Astrophys. J. **697**, 1369 (2009).

[4] Measuring the galaxy-mass and galaxy-dust correlations through magnification and reddening, B. Ménard, R. Scranton, M. Fukugita and G. Richards, Mon. Not. Roy. astr. Soc. **405**, 1025 (2010).

[5] Luminosity functions of Type Ia supernovae and their host galaxies from the Sloan Digital Sky Survey, N. Yasuda & M. Fukugita Astron, J. **139**, 39 (2010).

[6] Cosmological constraints from the clustering of the Sloan Digital Sky Survey DR 7 luminous red galaxies, B. A. Reid et al, Mon. Not. Roy. astr. Soc. **404**, 60 (2010).

[7] Baryon acoustic oscillation in the Sloan Digital Sky Survey data release 7 galaxy sample, W. J. Percival et al., Mon. Not. Roy. astr. Soc. **401**, 2148 (2010).

[8] Properties of disks and bulges of spiral and lenticular galaxies in the Sloan Digital Sky Survey, N. Oohama, S. Okamura, M. Fukugita, N. Yasuda and O, Nakamura, Astrophys. J. **705**, 245 (2009).

[9] Photometric response functions of the Sloan Digital Sky Survey imager, M. Doi, M. Tanaka, M. Fukugita, J. E. Gunn, N. Yasuda, Ž. Ivezić, J. Brinkmann, E. de Haars, S. J. Kleinman, J. Krzesinski and R. French Leger, Astron. J. **139**, 1628 (2010).

[10] The Sloan Digital Sky Survey quasar catalog V. Seventh data release, D. P. Schneider et al. Astron. J. **139**, 2360 (2010)

[11] Effects of massive neutrinos on the structure formation of the universe, M. Fukugita Prog. in Particle and Nucl. Phys. **64**, 360 (2010)

[12] The Milky Way tomography with SDSS: III. Stellar kinematics, N. A. Bond et al. Astrophys. J. **716**, 1 (2010).

[13] The Sloan Digital Sky Survey quasar lens search. IV: Statistical lens sample from the fifth data release, N. Inada et al., Astron. J. **140**, 403 (2010).

[14] Characterisation of Sloan Digital Sky Survey Stellar Photometry, M. Fukugita, N. Yasuda, M. Doi, J. E. Gunn and D. G. York, arXiv 1008.0510 [astro-ph]

## Primary Cosmic Ray Group

[Spokesperson : H. Miyahara]
ICRR, Univ. of Tokyo, Kashiwa, Chiba 277-8582

## Probing solar activity during the past millennium with cosmogenic nuclide

In collaboration with the members of Univ. of Tokyo, Hirosaki Univ. and Australian National Univ.

History of solar activity has been actively examined based on the changes in the abundance of cosmogenic nuclides in decadal tree rings and ice cores, especially for the past millennium. However, the reconstructed variations are often contaminated by climate change as well as the changes in geomagnetic field intensity. We have therefore conducted the measurements of cosmogenic nuclide in tree rings with annual resolution, and have reconstructed the characteristics of each decadal solar cycle in the past. It will allow us to probe the changes of absolute state of solar magnetic activity at each stage with absolute age. It will also be a clue for understanding the mechanism of long-term changes in solar activity, and for constructing a methodology of forecasting near future solar activity. Since solar activity is one of the primal external forcings of climate change, history of solar activity should be precisely determined also in terms of validating climate models for the future climate projection. For this study, trees from Yaku Island, Nara prefecture, Aomori prefecture and Shizuoka Prefecture have been used. We have conducted the measurements of carbon-14 content using the Accelerator Mass Spectrometers at the University of Tokyo and The Australian National University. We have so far successfully reconstructed solar activity at several extreme events such as the Maunder Minimum (AD 1645-1715), the Spoerer Minimum (AD1416-1534), the Early Medieval Maximum Period (the 9-10th century), and several other long-term activity maxima and minima in the past 7,200 years (Miyahara et al., 2004, 2006, 2008a, 2008b). In 2009, we have conducted the measurements mainly focusing on the period around 7200 BP. We have detected the deviations of solar cycle lengths from 11 years in association with the long-term changes in solar activity level. We have also conducted measurements for around the onset of long-term sunspot absence. It has been also clarified that solar cycle is likely to show characteristic precursory features leading up to intervals of sunspot absence lasting several decades, and that they can be differentiated by events of different durations (Miyahara et al., 2010). It implies that there is a possibility of predicting future long-term decrease of solar activity level, which may bring severe climate change.

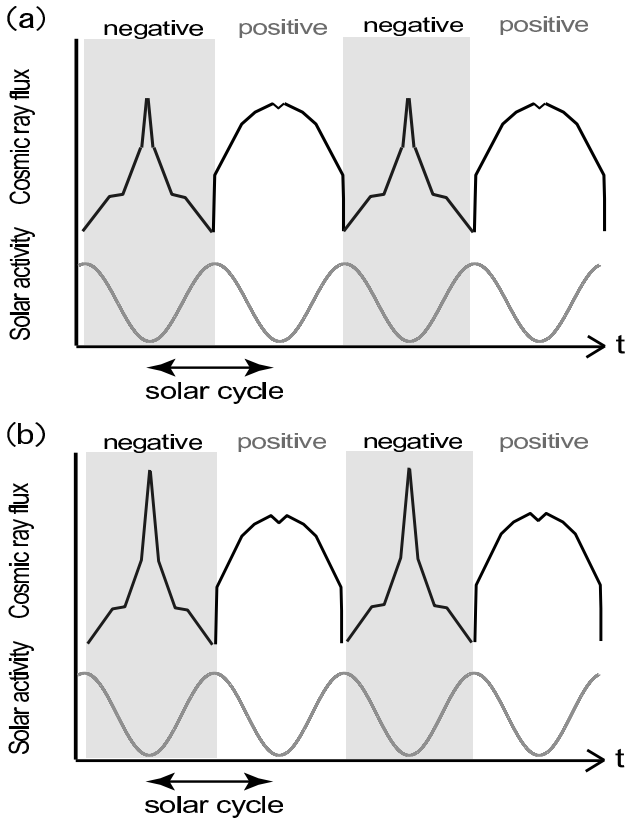


Fig. 1. Model of cosmic ray variations at (a) presentand and (b) the Maunder Minimum (Miyahara et al., 2009) estimated based on the results of numerical simulation of solar modulation by Kota and Jokipii (2001). At the Maunder Minimum, the variability of cosmic rays at negative solar polarity has been anomalously increased, resulting in the amplification of the 22-year cosmic-ray cycles.

### Bibliography

[1] H. Miyahara, K. Masuda, Y. Muraki, H. Furuzawa, H. Menjo, and T. Nakamura, Solar Physics, **224** (2004) 317.

[2] H. Miyahara, K. Masuda, Y. Muraki, H. Kitazawa, and T. Nakamura, J. Geophys. Res. , **111** (2006) A03103.

[3] H. Miyahara, K. Masuda, T. Nakamura, H. Kitazawa, K. Nagaya, and Y. Muraki, Quaternary Geochronology, **3** (2008a) 208.

[4] H. Miyahara, Y. Yokoyama, and K. Masuda, Earth and Planetary Science Letters, **272** (2008b) 290.

[5] H. Miyahara, K. Kitazawa, K. Nagaya, Y. Yokoyama, H. Matsuzaki, K. Masuda, T. Nakamura, and Y. Muraki, Journal of Cosmology, **8** (2010) 1970.

## Long-term changes in solar modulation of galactic cosmic rays in the heliosphere

In collaboration with the members of Univ. of Tokyo, Hirosaki Univ. and National Institute of Polar Research.

We have investigated the solar modulation of galactic cosmic rays around the Maunder Minimum, by measuring beryllium-10 content in annually separated layers of ice core obtained at the Dome Fuji station, East Antarctica. Variation of beryllium-10 content at the Maunder Minimum provides the information on the state of solar modulation of cosmic rays at sunspot absence, and thus the state of solar magnetic field and the heliosphere. The record will also be a basis for examining the cosmic-ray forcing of climate change for this peculiar period. We have been analyzing the ice core

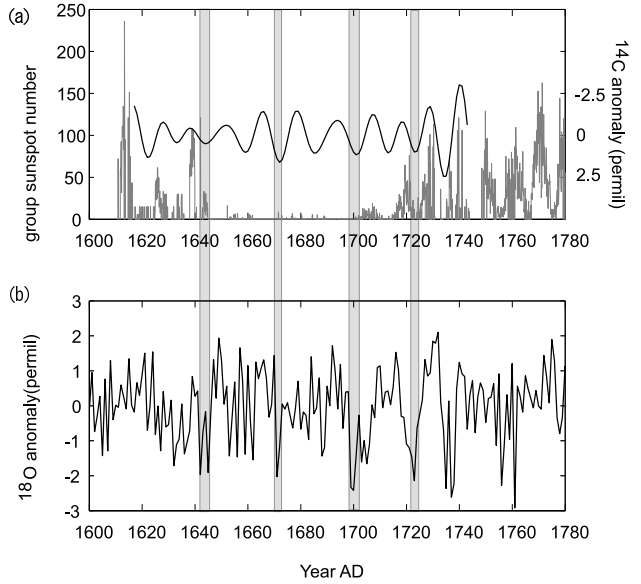


Fig. 2. Comparison of solar cycle with reconstructed temperatures around the Maudner Minimum (Miyahara et al., 2009). (a) Reconstructed Schwabe cycle based on the band-pass filtered carbon-14 record, together with the group sunspot numbers. (b) Reconstructed temperature based on oxygen-18/oxygen-16 ratio in the Greenland ice core by Vinther et al. (2003). The shaded areas correspond to the solar cycle minima of polarity negative determined by carbon-14 record.

for AD1600-1750 using the Accelerator Mass Spectrometer at the University of Tokyo. Our record will enable for the first time the direct comparison of beryllium-10 record from Antarctica with the record from Greenland that has been already obtained, which allow us to extract the signal of cosmic ray variations. We have suggested the possible variation of cosmic rays at this period (Miyahara et al., 2009) (Fig. 1), which shall be clarified by the records from both polar regions.

## Bibliography

[1] J. Kota, and J. R. Jokipii, Adv. Space Res. 27, (2001) 529.

[2] H. Miyahara, Y. Yokoyama, and Y. T. Yamaguchi, Proceedings of the IAU symposium No. 264, (2009) 427.

## Solar and Cosmic-Ray forcing of climate change

In collaboration with the members of Univ. of Tokyo and Nagoya Univ.

It has been suggested that cosmic rays play important role in cloud formation and thus in climate change. However, the relationship between cosmic rays and climate change has not been well understood as well as the mechanisms of their connection. We have therefore examined the possible influence of cosmic rays on climate change during the Maunder Minimum. It is generally expected that the long-term decrease of solar activity had been the possible cause of the Little Ice Age around the 14-19th century. We have examined whether cosmic rays had mediated the Sun-Climate relationship at the Little Ice Age. We have revealed that the drift of cosmic rays in the heliosphere had resulted in anomalous 22-year cycle during the Maunder Minimum, and that the intensified 22-year cycle had played important role in climate change at decadal to multi-decadal time scales (Miyahara et al., 2009, 2010). It was revealed that northern hemispheric temperature tends to be lower when the polarity of solar dipole magnetic field is negative (Fig. 2). We have suggested that the complex changes of solar magnetic field, heliospheric magnetic field, and consequent changes in cosmic rays are the possible origin of complexity of climate change at decadal to multi-decadal time scales.

## Bibliography

[1] H. Miyahara, Y. Yokoyama, Y. T. Yamaguchi, Proceedings of the IAU symposium No. 264, (2009) 427.

[2] H. Miyahara, Journal of Geography **119** (2010) 510.

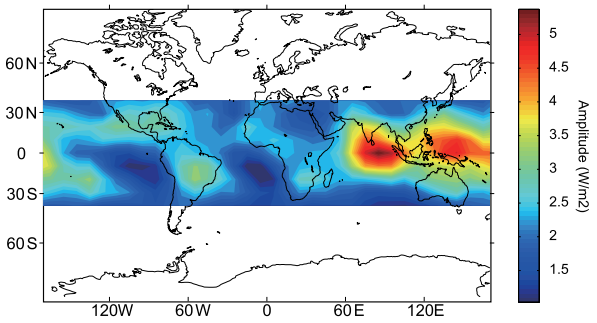


Fig. 3. Power of the 27-day periodicity in cloud activity at solar maximum.

## Cloud formation and the 27-day rotation of the Sun

In collaboration with the members of Univ. of Tokyo and Hokkaido Univ.

We have examined the influence of the 27-day rotation of the Sun on cloud formation. Total solar Irradiance (TSI), solar ultraviolet (UV), and galactic cosmic rays change in association with the 27-day rotation of the Sun. We have found that the 27-day solar rotational period affect cloud activity around the Western Pacific Warm Pool (WPWP). Only at solar maxima, when 27-day variation manifests in solar related parameters, the 27-day period is detected in cloud activity monitored by outgoing longwave radiation (OLR). Mechanism of the generation of 30-60 day period in cloud activity called as Madden-Julian Oscillation (MJO) in tropic region has not been well understood. We suggest that its rhythm is under the control of periodic variation of solar related parameters. Our study suggests that the area cosmic rays affect on cloud formation is localized (Fig. 3). The consequences of its affect should be clarified; it would help in understanding the response of complex climate system to the changes in incident cosmic rays at the earth.

## Bibliography

[1] Y. Takahashi, Y. Okazaki, M. Sato, H. Miyahara, K. Sakanoi, and P. K. Hong, Atmospheric Chemistry and Physics **10** (2010), 290.

## Reconstruction of climate change based on stable isotopes in tree rings

In collaboration with the members of Univ. of Tokyo, Nagoya Univ. and Tokyo Institute of Technology.

We are now conducting the measurements of multiple stable isotopes in tree rings from Japan in order to reconstruct the climate changes during the past two millenia in Japan. We have mainly conducting measurements using the 1850-year old cedar tree from Yakushima (Fig. 4) as well as the recent 150-year trees from the same area for the calibration.

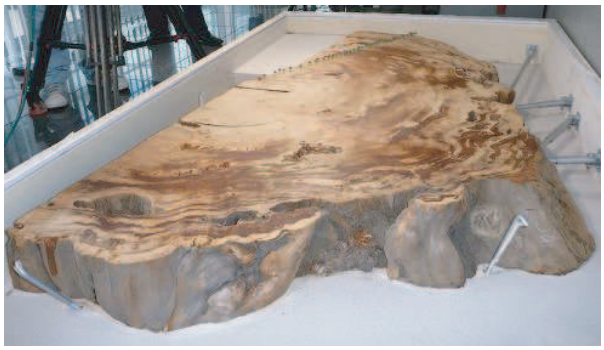

Fig. 4. Japanese cedar tree used in this study. The tree has been obtained from the Yaku Island.

## Deriving Historical Total Solar Irradiance from Lunar Borehole Temperatures

In collaboration with the members of JAXA and NASA/Goddard Space Flight Center.

As the Moon lacks atmosphere as well as any influence of human activities, lunar borehole temperatures are primarily driven by changes in solar irradiance. Variations of total solar irradiance (TSI), directly measured by radiometers flown onboard several satellites in recent decades, have provided a reliable short-term record of variations since 1978. However, this instrumental record has not yet led to a consensus result for solar variations on multi-decadal and longer timescales. It is important to clarify the actual variability of TSI in terms of distinguishing the contribution of change in TSI to the Little Ice Age. We have conducted the re-analysis of thermal properties of lunar regolith obtained by the Apollo Heat Flow Experiments, and conducted numerical simulations of heat flow in the regolith. We have shown that the historical changes in Total Solar Irradiance can be distinguished by small but potentially detectable differences in temperature, on the order of 0.01 K and larger depending on latitude, within 10 m depth of the Moon's surface (Fig. 5). In order to accomplish this experiment, we are now conducting discussions on the possible future missions. We are now discussing the potential preliminary mission for shallower depth at the next Japanese lunar landing mission.

## Bibliography

[1] H. Miyahara, G. Web, and R. F. Cahalan, Geophysical Research Letters **35** (2008), L02716.

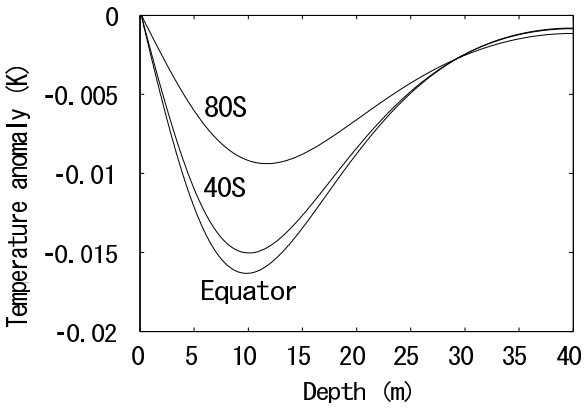


Fig. 5. Temperature anomalies in lunar regolith as response to 2 W/m2 difference in total solar irradiance at the Maunder Minimum, at the equator, mid-latitude (40S) and near the south pole (80S) (Miyahara et al., 2008).

# Theory Group

## Particle Phenomenology

[Spokesperson : J. Hisano]

## Waiting for $\mu \to e\gamma$ from the MEG Experiment

In collaboration with the members of ICRR Tohoku Univ. and Technische Universitat Munchen.

The Standard Model (SM) predictions for the lepton flavor-violating (LFV) processes like $\mu \to e\gamma$ are well far from any realistic experimental resolution, thus, the appearance of $\mu \to e\gamma$ at the running MEG experiment would unambiguously point towards a New Physics (NP) signal. In this article, we discuss the phenomenological implications in case of observation/improved upper bound on $\mu \to e\gamma$ at the running MEG experiment for supersymmetric (SUSY) scenarios with a see-saw mechanism accounting for the neutrino masses. We outline the role of related observables to $\mu \to e\gamma$ in shedding light on the nature of the SUSY LFV sources providing useful tools *i)* to reconstruct some fundamental parameters of the neutrino physics and *ii)* to test whether an underlying SUSY Grand Unified Theory (GUT) is at work. The perspectives for the detection of LFV signals in $\tau$ decays are also discussed.

## Bibliography

[1] J. Hisano, M. Nagai, P. Paradisi and Y. Shimizu, JHEP **0912**, 030 (2009) [arXiv:0904.2080 [hep-ph]].

## Implications of CDMS II result in supersymmetric model

In collaboration with the members of ICRR.

We studied implications of two dark matter candidate events at CDMS-II on the neutralino dark matter scenario in the supersymmetric standard model, in light of the recent lattice simulation on the strange quark content of a nucleon. The scattering rate of neutralino-nucleon is dominated by Higgs exchange processes and the mass of heavy Higgs boson is predicted for the neutralino of Bino-Higgsino mixing state [1]. In the work [2], we proposed an extended version of the gauge-mediated SUSY breaking models where extra $SU(2)_L$ doublets and singlet field are introduced. In this paper, we discuss direct detection of the dark matter and the collider signatures of the model.

## Bibliography

[1] J. Hisano, K. Nakayama and M. Yamanaka, Phys. Lett. B **684** (2010) 246

[2] J. Hisano, K. Nakayama, S. Sugiyama, T. Takesako and M. Yamanaka, arXiv:1003.3648 [hep-ph].

## Upward muon signals at neutrino detectors as a probe of dark matter properties

In collaboration with the members of ICRR.

We study upward muon flux at neutrino detectors such as Super-Kamiokande resulting from high-energy neutrinos produced by the dark matter annihilation/decay at the Galactic center. In particular, we distinguish showering and non-showering muons as their energy loss processes inside the detector, and show that this information is useful for discriminating dark matter models.

## Bibliography

[1] J. Hisano, K. Nakayama and M. J. S. Yang, Phys. Lett. B **678**, 101 (2009) [arXiv:0905.2075 [hep-ph]].

## Diffuse gamma-ray background and cosmic-ray positrons from annihilating dark matter

In collaboration with the members of ICRR and Tohoku Univ..

We study the annihilating dark matter contribution to the extra-galactic diffuse gamma-ray background spectrum, motivated by the recent observations of cosmic-ray positron/electron anomalies. The observed diffuse gamma-ray flux provides stringent constraint on dark matter models and we present upper bounds on the annihilation cross section of the dark matter. It is found that for the case of cored dark matter halo profile, the diffuse gamma-rays give more stringent bound compared with gamma-rays from the Galactic center. The Fermi satellite will make the bound stronger.

## Bibliography

[1] M. Kawasaki, K. Kohri and K. Nakayama, Phys. Rev. D **80** (2009) 023517 [arXiv:0904.3626 [astro-ph.CO]].

## Diffuse gamma-ray background and cosmic-ray positrons from annihilating dark matter

In collaboration with the members of ICRR and Tohoku Univ..

We study the annihilating dark matter contribution to the extra-galactic diffuse gamma-ray background spectrum, motivated by the recent observations of cosmic-ray positron/electron anomalies. The observed diffuse gamma-ray flux provides stringent constraint on dark matter models and we present upper bounds on the annihilation cross section of the dark matter. It is found that for the case of cored dark matter halo profile, the diffuse gamma-rays give more stringent bound compared with gamma-rays from the Galactic center. The Fermi satellite will make the bound stronger.

## Bibliography

[1] M. Kawasaki, K. Kohri and K. Nakayama, Phys. Rev. D **80** (2009) 023517 [arXiv:0904.3626 [astro-ph.CO]].

## Effects of Dark Matter Annihilation on the Cosmic Microwave Background

In collaboration with the members of ICRR.

We study the effects of dark matter annihilation during and after the cosmic recombination epoch on the cosmic microwave background anisotropy, taking into account the detailed energy deposition of the annihilation products. It is found that a fairly stringent constraint on the annihilation cross section is imposed for TeV scale dark matter masses from WMAP observations.

## Bibliography

[1] T. Kanzaki, M. Kawasaki and K. Nakayama, arXiv:0907.3985 [astro-ph.CO], to appear in Prog. Theor. Phys.

# Astrophysics and Cosmology

[Spokesperson : M. Kawasaki]

## Towards Inflationary Cosmology in String Theory

In collaboration with the members of IPMU.

We have worked towards realizing inflationary cosmology in the framework of string theory. We studied inflation driven by D-branes moving rapidly in warped extra dimensions, which is in contrast to well-studied slow-roll inflation models[1, 2]. We also proposed a curvaton model from type IIB string theory compactified on a warped throat region with approximate isometries, where the D-brane's position in the isometry directions plays the role of curvatons[3]. Furthermore, we explored a possibility where light fields other than

the inflaton source the primordial perturbations, while minimally affecting the inflaton dynamics. The results were applied to study effects of oscillation modes of wrapped D-branes in monodromy-driven large-field inflation models[4].

### Bibliography

[1] T. Kobayashi and S. Mukohyama, Phys. Rev. D **79** (2009) 083501 [arXiv:0810.0810 [hep-th]].

[2] T. Kobayashi, S. Mukohyama and B. A. Powell, JCAP **0909** (2009) 023 [arXiv:0905.1752 [astro-ph.CO]].

[3] T. Kobayashi and S. Mukohyama, JCAP **0907** (2009) 032 [arXiv:0905.2835 [hep-th]].

[4] T. Kobayashi and S. Mukohyama, Phys. Rev. D **81** (2010) 103504 [arXiv:1003.0076 [astro-ph.CO]].

## Phenomenological Aspects of Horava-Lifshitz Cosmology

In collaboration with the members of ICRR, IPMU and Nagoya Univ.

We show that, assuming the dispersion relation proposed recently by Horava in the context of quantum gravity, radiation energy density exhibits a peculiar dependence on the scale factor; the radiation energy density decreases proportional to $a^{-6}$. This simple scaling can have an impact on cosmology. As an example, we show that the resultant baryon asymmetry as well as the stochastic gravity waves can be enhanced. We also discuss current observational constraint on the dispersion relation.

### Bibliography

[1] S. Mukohyama, K. Nakayama, F. Takahashi and S. Yokoyama, Phys. Lett. B **679**, 6 (2009) [arXiv:0905.0055 [hep-th]].

## Q-ball formation in gravity mediation

In collaboration with the members of ICRR and IPMU.

We investigated the formation of Q-balls in gravity mediation using 1D, 2D and 3D lattice simulations of the complex scalar field. From these simulations, we calculated the charge distributions of the Q-balls and clarified the relations among the energy, charge and size of them. In the formation epoch, the scalar field firstly forms the filamentary structure, and we found that, at the intersections of the filaments, the largest Q-balls are formed, which forms the peak in the final distribution. Then the filaments are torn to small pieces, and also in the void region, very small Q-balls are formed. Besides, we focused on the cases with elliptic orbits of the scalar fields in the initial time. In these cases, the resultant Q-balls are highly excited, and after a while, they transit to mildly excited states by discarding the excess energy which creates negative charge Q-balls.

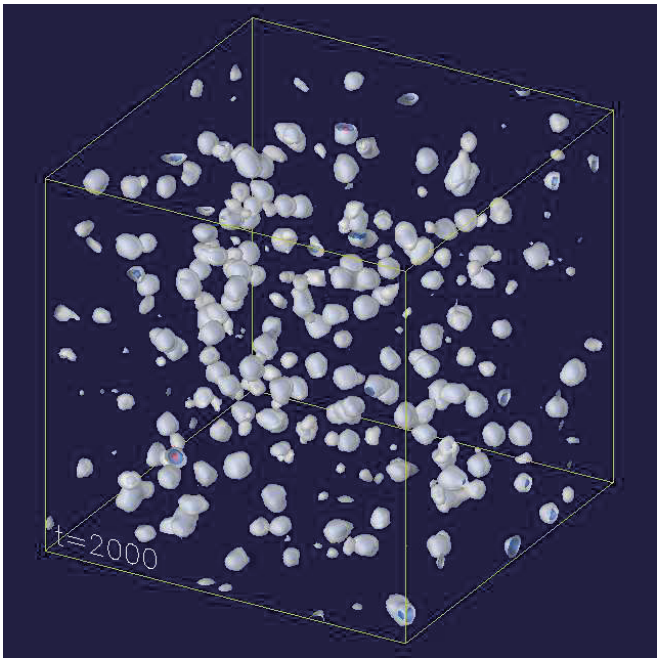


Fig. 1. Q-ball formation.

### Bibliography

[1] T. Hiramatsu, M. Kawasaki and F. Takahashi, arXiv:1003.1779, to be published in JCAP.

## Gravitational Waves from Collapsing Domain Walls

In collaboration with the members of ICRR.

We study the production of gravitational waves from cosmic domain walls created during phase transition in the early universe. We investigate the process of formation and evolution of domain walls by running three dimensional lattice simulations. If we introduce an approximate discrete symmetry, walls become metastable and finally disappear. We calculate the spectrum of gravitational waves produced by collapsing metastable domain walls. Extrapolating the numerical results, we find the signal of gravitational waves produced by domain walls whose energy scale is around $10^{10}$-$10^{12}$GeV will be observable in the next generation gravitational wave interferometers.

### Bibliography

[1] T. Hiramatsu, M. Kawasaki and K. Saikawa, (JCAP, in prep), arXiv:1002.1555.

## Gravitational waves emitted by kinks on infinite cosmic strings

In collaboration with the members of ICRR.

We investigate gravitational waves(GWs) emitted by kinks on infinite strings using detailed estimations of the kink distribution on infinite strings. We find that the stochastic GW

background from kinks can be detected by future pulsar timing experiments for an appropriate value of the the string tension, if the typical size of string loops is much smaller than the horizon at their formation. Besides, we consider the effect of the GW background on the B-mode polarization of the cosmic microwave background(CMB). We find that the B-mode polarization due to kinks is comparable to that induced by the motion of the string network and can be detected by future CMB experiments if the tension of cosmic strings is large enough.

### Bibliography

[1] M. Kawasaki, K. Miyamoto and K. Nakayama, Phys. Rev. D, 81,103523 (2010) arXiv:1002.0652 [astro-ph.CO]

[2] M. Kawasaki, K. Miyamoto and K. Nakayama, arXiv:1003.3701 [astro-ph.CO]

## Probing the primordial power spectra with inflationary priors

In collaboration with the members of ICRR and IPMU.

We investigated constraints on power spectra of the primordial curvature and tensor perturbations with priors based on single-field slow-roll inflation models. Using data from recent observations of CMB and several measurements of geometrical distances in the late Universe, we performed the Bayesian parameter estimation and model selection for models that have separate priors on the slow-roll parameters. We confirmed that the scale-invariant Harrison-Zel'dovich spectrum is disfavored with increased significance from previous studies. We also showed that while current observations appear to be optimally modeled with simple models of single-field slow-roll inflation, data is not enough constraining to distinguish these models with different priors on slow-roll parameters.

### Bibliography

[1] M. Kawasaki and T. Sekiguchi, JCAP **1002**, 013 (2010) [arXiv:0911.5191 [astro-ph.CO]].

## Non-Gaussianity from Isocurvature Perturbations : Analysis of Trispectrum

In collaboration with the members of ICRR and IPMU.

Non-Gaussianity may exist in the CDM isocurvature perturbation. We provide general expressions for the bispectrum and trispectrum of both adiabatic and isocurvature perturbations. We apply our result to the QCD axion case, and found a consistency relation between the coefficients of the bispectrum and trispectrum : $\tau_{\rm NL}^{\rm (iso)} \sim 10^3 [f_{\rm NL}^{\rm (iso)}]^{4/3}$, if the axion is dominantly produced by quantum fluctuation. Thus future observations of the trispectrum, as well as the bispectrum, will be important for understanding the origin of the CDM and baryon asymmetry.

### Bibliography

[1] E. Kawakami, M. Kawasaki, K. Nakayama and F. Takahashi, JCAP **0909**, 002 (2009) [arXiv:0905.1552 [astro-ph.CO]].

## The R-axion and non-Gaussianity

In collaboration with the members of ICRR and IPMU.

We study cosmological implications of an R-axion, a pseudo Nambu-Goldstone boson associated with spontaneous breaking of an $U(1)_R$ symmetry, focusing on its quantum fluctuations generated during inflation. We show that, in the anomaly mediation, the R-axion decays into a pair of gravitinos, which eventually decay into the visible particles producing the neutralino LSP. As a result, the quantum fluctuations of the R-axion are inherited by the cold dark matter isocurvature density perturbation with potentially large non-Gaussianity. The constraints on the inflation scale and the initial misalignment are derived.

### Bibliography

[1] K. Nakayama and F. Takahashi, Phys. Lett. B **679**, 436 (2009) [arXiv:0907.0834 [hep-ph]].

## Axion isocurvature fluctuations with extremely blue spectrum

In collaboration with the members of ICRR and Kanagawa University.

We construct an axion model for generating isocurvature fluctuations with blue spectrum, which is suggested by recent analysis of admixture of adiabatic and isocurvature perturbations with independent spectral indices, $n_{\rm ad} \neq n_{\rm iso}$. The distinctive feature of the model is that the spectrum is blue at large scales while scale-invariant at small scales, which is naturally realized by the dynamics of the field.

### Bibliography

[1] S. Kasuya and M. Kawasaki, Phys. Rev. D **80** (2009) 023516.

## Gravitational Wave Background and Non-Gaussianity as a Probe of the Curvaton Scenario

In collaboration with the members of ICRR and RESCEU.

We study observational implications of the stochastic gravitational wave background and a non-Gaussian feature of scalar perturbations on the curvaton mechanism of the generation of density/curvature fluctuations, and show that they can determine the properties of the curvaton in a complementary manner to each other. Therefore even if Planck could not detect any non-Gaussianity, future space-based laser interferometers such as DECIGO or BBO could practically exhaust its parameter space.

## Bibliography

[1] K. Nakayama and J. Yokoyama, JCAP **1001**, 010 (2010) [arXiv:0910.0715 [astro-ph.CO]].


## Constraining Light Gravitino Mass from Cosmic Microwave Background

In collaboration with the members of ICRR, Kyoto Univ. and Saga Univ.

We investigate the possibilities of constraining the light gravitino mass $m_{3/2}$ from future cosmic microwave background (CMB) surveys. A model with light gravitino with the mass $m_{3/2} < O(10)$ eV is of great interest since it is free from the cosmological gravitino problem and, in addition, can be compatible with many baryogenesis/leptogenesis scenarios such as the thermal leptogenesis. We show that the lensing of CMB anisotropies can be a good probe for $m_{3/2}$ and obtain an expected constraint on $m_{3/2}$ from precise measurements of lensing potential in the future CMB surveys, such as the PolarBeaR and CMBpol experiments. If the gravitino mass is $m_{3/2}$=1 eV, we will obtain the constraint for the gravitino mass as $m_{3/2} < 3.2$ eV (95% C.L.) for the case with Planck+PolarBeaR combined and $m_{3/2} = 1.04^{+0.22}_{-0.26}$ eV (68% C.L.) for CMBpol. The issue of Bayesian model selection is also discussed.


## Bibliography

[1] K. Ichikawa, M. Kawasaki, K. Nakayama, T. Sekiguchi and T. Takahashi, JCAP **0908** (2009) 013 [arXiv:0905.2237 [astro-ph.CO]].


## Neutrino mass from cosmology: Impact of high-accuracy measurement of the Hubble constant

In collaboration with the members of ICRR, Kyoto Univ., Saga Univ. and Harvard-Smithsonian CfA.

We focused on the power spectrum of cosmic microwave background (CMB) anisotropies, the Hubble constant $H_0$, and the length scale for baryon acoustic oscillations (BAO) to investigate the constraint on the neutrino mass, $m_\nu$. We showed that combined with CMB and BAO data, a recent $H_0$ measurement reduces a upper limit on $m_\nu$ by about 40 %, compared with previous $H_0$ estimates. We also analyzed the impact of smaller uncertainty on measurements of $H_0$ as may be anticipated in the near term, in combination with CMB data from the Planck mission, and BAO data from the SDSS/BOSS program. A future measurement of $H_0$ at 1 % accuracy level will offer a constraint $\delta m_\nu < 0.04$ eV (95% C.L.), which is 50 % better than those achieved without external constraint. Constraints for a universe with a curvature $\Omega_k \neq 0$ and/or a equation of state for dark energy $w \neq -1$ are also investigated.


## Bibliography

[1] T. Sekiguchi, K. Ichikawa, T. Takahashi and L. Greenhill, JCAP **1003**, 015 (2010) [arXiv:0911.0976 [astro-ph.CO]].


## Effect of Long-lived Strongly Interacting Relic Particles on Big Bang Nucleosynthesis

In collaboration with the members of National Astronomical Observatory of Japan, Univ. Tokyo, and Univ. Notre Dame.

We study effects of relic long-lived strongly interacting massive particles (X) on big bang nucleosynthesis. Rates of nuclear reactions and beta decay of X-nuclei are calculated, and nuclear network calculations are performed. We find that this scenario can lead to elevated primordial abundances of $^9$Be and/or $^{10}$B which should be measured in the future. Long-lived colored particles with lifetimes longer than 200 s are found to be rejected.


## Bibliography

[1] M. Kusakabe, T. Kajino, T. Yoshida and G. J. Mathews, Phys. Rev. D **80** (2009) 103501.

[2] M. Kusakabe, T. Kajino, T. Yoshida and G. J. Mathews, IAU Symposium **268** (2010) 33 -38.


## Production of the p-Process Nuclei in the Carbon Deflagration Model for Type Ia Supernovae

In collaboration with the members of Japan Atomic Energy Agency, and Univ. Tokyo.

We calculate nucleosynthesis of proton-rich isotopes in the carbon deflagration model for Type Ia supernovae (SNe Ia). The seed abundances are derived by calculating the s-process nucleosynthesis occurring in repeating helium shell flashes on the carbon-oxygen white dwarf during mass accretion. We find that SNe Ia could make a larger contribution than SNe II to the solar system content of p-nuclei.


## Bibliography

[1] M. Kusakabe, N. Iwamoto and K. Nomoto, arXiv:1001.0145 [astro-ph.SR].


## New results on catalyzed big bang nucleosynthesis with a long-lived negatively charged massive particle

In collaboration with the members of National Astronomical Observatory of Japan, Univ. Tokyo, and Univ. Notre Dame.

We present new calculations of big bang nucleosynthesis with an a negatively charged massive unstable particle utilizing an improved nuclear reaction network and new reaction rates derived from recent rigorous quantum many-body calculations. We find that this is still a viable model to explain the observed $^6$Li and $^7$Li abundances in metal-poor halo stars. Nuclei heavier than Be are not produced significantly in this model.

## Bibliography

[1] M. Kusakabe, T. Kajino, T. Yoshida and G. J. Mathews,
Phys. Rev. D **81** (2010) 083521.

# OBSERVATORIES and A RESEARCH CENTER

**Location of the Institute and the Observatories in Japan**

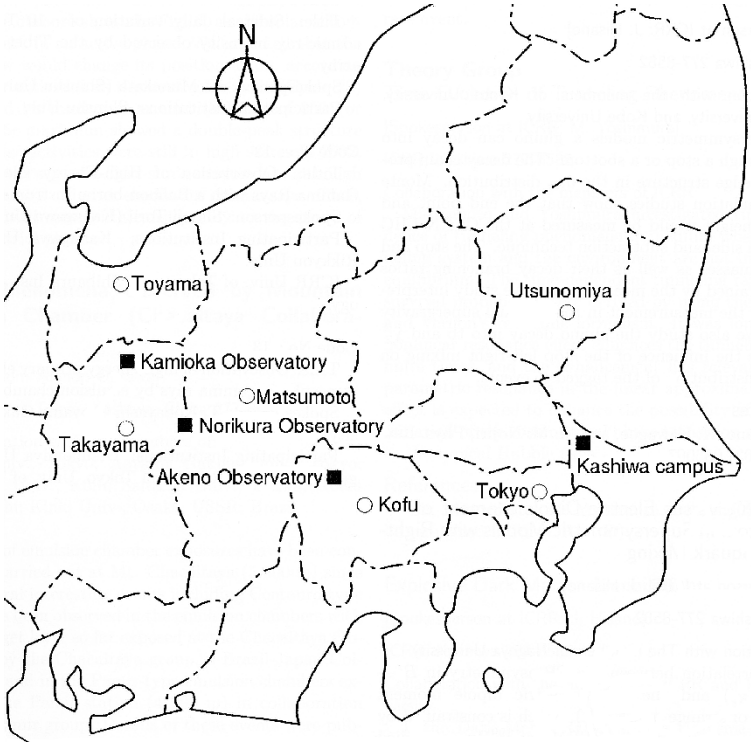


## Norikura Observatory

| | |
|---|---|
| Location: | Iwaitani, Nyukawa-cho, Takayama-shi, Gifu Prefecture 506-2254<br>N 36°06′, E 137°33′, 2770 m a.s.l. |
| Telephone (Fax): | +263-33-7456 |
| Telephone (satellite): | 090-7721-5674 |
| Telephone (car): | 090-7408-6224 |

## Akeno Observatory

| | |
|---|---|
| Location: | 5259 Asao, Akeno-machi, Hokuto-shi, Yamanashi Prefecture 407-0201<br>N 35°47′, E 138°30′, 900 m a.s.l. |
| Telephone / Fax: | +551-25-2301 / +551-25-2303 |

## Kamioka Observatory

| | |
|---|---|
| Location: | 456 Higashi-mozumi, Kamioka-cho, Hida-shi, Gifu Prefecture 506-1205<br>N 36°25′26″, E 137°19′11″, 357.5 m a.s.l. |
| Telephone / Fax: | +578-85-2116 / +578-85-2121 |

## Research Center for Cosmic Neutrinos

| | |
|---|---|
| Location: | 5-1-5 Kashiwanoha, Kashiwa, Chiba Prefecture 277-8582 |
| Telephone / Fax: | +4-7136-3138 / +4-7136-3115 |

# NORIKURA OBSERVATORY

## 1. Introduction

Norikura Observatory (36.10°N and 137.55°E) was founded in 1953 and attached to ICRR in 1976. It is located at 2770 m above sea level, and is the highest altitude manned laboratory in Japan. Experimental facilities of the laboratory are made available to all the qualified scientists in the field of cosmic ray research and associated subjects. The AC electric power is generated by the dynamo and supplied throughout the observatory. In 1996, two dynamos of 70 KVA each were replaced with the new ones. The observatory can be accessed easily by car and public bus in summer (July-September). The 50th anniversary of Norikura Observatory was celebrated in 2003.

The feasibility of the automatic operation of Norikura Observatory during winter period has been tested since winter 2004 in order to study the possibilities to reduce maintenance and labor costs without seriously damaging to the use of researches. A long-distance (∼40km) wireless LAN system (11M bps) was set up in 2003. Two new easy-to-handle and easy-to-maintain dynamos of 115 KVA each were installed in 2004 as well. The unmanned operation of Norikura Observatory was successful in the first winter, during which the battery backed-up solar panels and/or wind power generators kept supplying the electricity to the wireless LAN and ongoing cosmic-ray experiments.

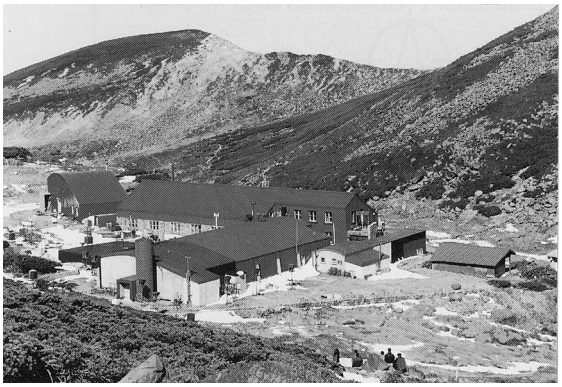

Fig. 1. Norikura Observatory.

Present major scientific interests of the laboratory is focused on the modulation of high energy cosmic rays in the interplanetary space associated with the solar activity and the generation of energetic particles by the solar flares, both of which require long-term monitoring. This research has been carried out by the group of universities, where ICRR provides them with laboratory facility. A part of the facility has been open for the environmental study at high altitude such as the aerosol removal mechanism in the atmosphere or for the botanical study of the high altitude environment.

## 2. Cosmic Ray Physics

For the modulation study[2], two small experiments have been operated continuously for a long time. One is a neutron monitor operated to study the correlation of solar activity and the cosmic ray flux. The other is a high counting muon telescope consisting of 36 $m^2$ scintillation counters to study the time variation of cosmic rays with energies of 10–100 TeV over 20 years. The neutron monitor data are open to researchers worldwide as a world observation network point (WDC). The 5 years from 2000 corresponded to the solar maximum (2000) to a declining phase in the solar cycle 23. The sun spot number in 2004 is approximately one fourth of the those at maximum. Nonetheless, there occurred active cosmic-ray phenomena associated with Coronal Mass Ejection (CME). As regards solar cosmic rays, although many ground level enhancement (GLE) phenomena took place every year, such GLEs were observed only by neutron monitors in Japan, as the maximum cosmic-ray energy was several GeV in the GLEs and the magnetic rigidity cutoff in Japan is approximately 10 GeV for charged particles initiating secondary muons. The sunspot numbers in the solar cycle 23 was smaller than those in the previous cycle 22, indicating less solar activities of cycle 23. Although the GLEs above 10 GeV were not observed in cycle 23, the total number of GLEs were greater in cycle 23 than in cycle 22. This suggests that the charged particle acceleration associated with CME was less frequent in the cycle 23 than in the cycle 23. On the other hand, Forbush decreases in galactic cosmic rays caused by CME in the Sun were observed frequently in cycle 23, though the solar activities have been in a declining phase since 2000. The worldwide observation of Forbush decreases may contribute significantly to space weather study.

In addition, space weather observation is actively made by a 25 $m^2$ muon hodoscope at Norikura Observatory[1], [2],[3],[4],[5], [6],[7],[8]. A loss cone anisotropy is observed by a ground-based muon hodoscope in operation at Norikura Observatory in Japan for 7 hours preceding the arrival of an interplanetary shock at Earth on October 28, 2003. Best fitting a model to the observed anisotropy suggests that the loss cone in this event has a rather broad pitch-angle distribution with a half-width about 50° from the interplanetary magnetic field (IMF). According to numerical simulations of high-energy particle transport across the shock, this implies that the shock is a ”quasi-parallel” shock in which the angle between the magnetic field and the shock normal is only 6°. It is also suggested that the leadtime of this precursor is almost independent of the rigidity and about 4 hour at both 30 GV for muon detectors and 10 GV for neutron monitors (see paper [7]).

The Sun is the nearest site to the Earth capable of accelerating particles up to high energies. When the Sun becomes

active, flares are frequently observed on its surface. The flare accelerates the proton and ion to high energy and they are detected on the Earth soon after the flare. Among the particles generated by the flare, high energy neutrons provide the most direct information about the acceleration mechanism as they come straight from the flare position to the Earth without deflected by the magnetic field.

In 1990, Nagoya group constructed a solar neutron telescope consisting of scintillators and lead plates, which measures the kinetic energy of incoming neutrons up to several hundred MeV. This telescope observed high energy neutrons associated with a large flare occurred on the 4th of June, 1991. The same event was simultaneously detected by the neutron monitor and the high counting muon telescope of Norikura Observatory. This is the most clear observation of solar neutrons at the ground level in almost ten years since the first observation at Jungfraujoch in 1982.

A new type of the large solar neutron telescope (64 $m^2$ sensitive area) was constructed by Nagoya group in 1996. It consists of scintillators, proportional counters and wood absorbers piled up alternately. This takes a pivotal role among a worldwide network of ground based solar neutron telescopes of the same type in Yangbajing in Tibet, Aragatz in Armenia, Gornergrat in Switzerland, Chacaltaya in Bolivia and Mauna Kea in Hawaii. The Sun is being watched for 24 hours using this network.

Fig. 2. New Solar-Neutron Telescope of Nagoya Group.

The Sun reached the maximum activity in 2000 and the active phase continued for the next few years. All the telescopes in Norikura Observatory, neutron telescope, neutron monitor, muon telescope and muon hodoscope, have been operated almost continuously through the solar cycle 23 in order to obtain comprehensive information on the solar flare phenomena. Important hints for understanding the mechanism of cosmic-ray acceleration near the solar surface will be obtained by these measurements, especially by energy spectra measured by the timing information of arriving neutrons and muons.

Furthermore, the relation between the electric fields induced by thunderclouds is studied recently[10]. The electric fields with thunderclouds change the intensity of secondary cosmic rays observed on the ground. This effect has been investigated using several detectors located at Norikura Observatory where excesses of 1 % and more of the average counting rate are observed when the observatory is covered with thunderclouds. A frequency analysis of the time series of days with such excesses for the period 26 October 1990 to 15 January shows the expected summer maximum in the rate of occurrence and, surprisingly, a 26-day variation. An electric field mill was installed to help determine the relationship between the intensity variations and the strength and direction of the field near the detector system: the excess is usually observed when a negative electric field (accelerating negative charges downward) greater than 10 kV/m is present in the atmosphere above the observatory. Based on Monte Carlo simulations, it is predicted that excess counting rates measured without charge discrimination will be expected as a consequence of the excess of positive muons among the secondary cosmic rays.

Subsequently, during thunderstorms on 2008 September 20, an intense radiation burst, comprising $\gamma$ rays and electrons, was detected [11] by at the Norikura observatory. Outside the observatory, a radiation detection system was set up on 2008 September 4, and operated it until 2008 October 2. The system has a radiation monitor and environmental sensors. The radiation monitor consists of a spherical NaI scintillator with a diameter of 7.62 cm, and a 5 mm thick plastic scintillator with an area of 45 $\times$ 40 $cm^2$. The plastic scintillator is enclosed in an aluminum box with the top and bottom being 1 mm and 3 mm thick, respectively. Each scintillator has a photomultiplier (HAMAMATSU R878) of its own, and each output signal is fed to a self-triggering electronics system, incorporating a 12 bit ADC. The burst, lasting 90 seconds, was associated with thunderclouds rather than lightning. The photon spectrum, extending to 10 MeV, can be interpreted as consisting of bremsstrahlung $\gamma$ rays arriving from a source which is 60 - 130 m in distance at 90% confidence level. The observed electrons are likely to be dominated by a primary population escaping from an acceleration region in the source.

In addition to the long-term cosmic-ray observations mentioned above, various kinds of short-dated experiments are carried out every year taking an advantage of the high altitude of the observatory. A few examples include a search for super heavy particles with plastic plates, a precise measurement of atmospheric gamma rays and muons, collection of cosmic dusts contained in the snow,measurement of air fluorescence light yield for ultra high-energy cosmic-ray observation and the performance study of the balloon borne cosmic ray experiments.

## 3. Environmental Study

One of the interesting topics is atmospheric environment especially relating with atmospheric aerosol particles and water soluble gases. Because of its height, AC power supply, accommodation facility, and accessibility of cargos, the cosmic ray observatory at Mt. Norikura provides a very unique opportunity for atmospheric observation, especially for free-tropospheric conditions. (The atmosphere lower than a few kilometer is highly affected by the ground. This height level is named as 'atmospheric boundary layer'. The height of the

boundary layer is about 4 km in daytime and about 2 km in nighttime around Norikura area. The atmosphere higher than this atmospheric boundary layer is called 'free troposphere'.) Originally, atmospheric observation at the cosmic ray observatory was initiated to study cosmogenic radionuclides with Prof. Suzuki at Shizuoka University. During early stage of the research at Mt. Norikura, a local effect of air contamination was recognized. To reduce air contamination from diesel exhausts and other activities around the observatory, an atmospheric observation hut (6 $m^2$) was installed at the west end (windward) of the observatory in September 1999. From year 2000, continuous monitoring (mostly mid-May to mid-October) of meteorology was started, number-size distribution of aerosols, dew point, aerosol chemical composition, ozone and radon concentrations, and column amount of aerosols from sky radiometer and ceilometer. Monitoring of ozone and radon concentrations was extended during 2 winters from 2001 to 2003. During summer season, also collected were rain, fog, water-condensed aerosol samples. These samples combined with other parameters were used in several thesis (master) works and provided useful information about future seeds of hygroscopic study of aerosols. During the past 5 years, the following results[12],[13],[14] were obtained at Mt. Norikura.

(1) Polluted air pumping effects over central Japanese Alps in summer

Under the clear sky conditions in summer, polluted air from mountain valley area is lifted up about 4km of altitude (1km above the mountain top) over Mt. Norikura. The height of observatory is within the atmospheric boundary layer in the daytime, and is out of (higher than) the atmospheric boundary layer in nighttime. The ratio of aerosol volume concentration for daytime (polluted valley wind) to nighttime (clean free-tropospheric) conditions was about 10. The air pumping effects over central Japanese Alps carry about 10 time higher concentration of aerosols to the free-troposphere over Japan in summer. Under the high-pressure system centered over the northwest Pacific in typical summer condition, backward air trajectories were originated from the northwest Pacific to Mt. Norikura and forward trajectories returned to the north Pacific with some deviations to east Russia and the Kurile Islands. The air pumping effects over mountain area provide a strong pollution source mechanism to the free-troposphere over the western Pacific region including East Asia.

(2) Seasonal variation of aerosol chemistry in free troposphere

An automated aerosol sampler was installed at the site in September 2000 to obtain seasonal aerosol samples. The sampler collected aerosols from mid-May to mid-October in 2001 and 2002. Results of its analysis showed seasonal changes in major and minor constituents of aerosols associating with changes of dominant air mass type over Japan.

(3) Vertical profiles of aerosols and clouds near the top of the atmospheric boundary layer

Ceilometer (lidar with small output energy) was installed in summer 2002, and was operated in 4 summer seasons. The aerosol and cloud profiles near the top of the atmospheric boundary layer have been observed. Some events of Asian dust, and of smoke from Siberian forest fire at lower free troposphere have been detected.

## 4. Botanical Study

It is predicted that ecosystems in high-latitudes and alpine regions are sensitive to global climatic warming. The significant increasing trends in air temperature are found in the Hida Mountains, where Mt. Norikura is located. Thus, effects of climatic change caused by global warming on alpine ecosystems must be urgently studied in the alpine region of central Japan. The Hida Mountains, strongly influenced by cold-air masses from Siberia in winter, receive some of the heaviest snowfall in the world. Due to heavy snowfall, dynamics of alpine ecosystems may be peculiar to the Hida Mountains. However, few studies have been made because of difficulty in approach to the alpine study site. The inter-university research program of ICRR, gave an opportunity to make an intensive study all year around in the alpine region on Mt. Norikura[15],[16].

(1) Tree line dynamics

The tree form of evergreen sub-alpine fir (Abies mariesii) is studied at the upper distribution limit (2500m above sea level)

on Mt. Norikura. Leader stems degenerate above the maximum snowpack line (3-4m high) , whereas branches below the snowpack line grow densely. In winter, leaves above snowpack line were severely damaged by environmental stresses, such as abrasion by wind-blown snow particles, desiccation, photoinhibition. Longevity of leaves was shortened to 4-5 years due to high mortality rate in winter. In contrast, leaves below snowpack line were protected from environmental stresses and their longevity was 11 years. As a result, biomass below the snowpack line takes more than 80with climate change should have unfavorable effects on tree line Abies mariesii.

(2) Alpine region

Pinus pumila, an alpine prostrated pine, is dominant in the alpine regions (2500∼3000m above sea level). At wind-protected sites, Pinus pumila grows vigorously with the tree height of 1-2m. They were beried in snowpack throughout the winter. At the wind-exposed ridge, growth is suppressed with the tree height of 0.2-0.5m. Throughout the winter, the surface of the pine community was exposed due to strong wind at the ridge. Leeward leaves were sound, because pine stems with high elasticity were prostrated and buried in snow. Thus, alpine pine can catch and accumulate snow to protect itself. This feature may be advantageous to alpine trees in comparison with sub-alpine trees (Abies mariesii). On the other hand, at the windward side (western), cuticular layer covering epidermal cells of leaf was abraded probably due to wind-blown

snow and ice particles. By spring, abraded leaves at the windward side were dead caused by desiccation and photoinhibition. Even Pinus pumila community could reduce its habitat in small snowfall condition caused by global warming.

Impact of global warming due to so-called greenhouse gases like CO2, CH4 and others on vegetation ecology is among the most serious environmental issues. To investigate how plants response to global warming, an experiment of greenhouse effect on vegetation has been continued at a high mountain, Mt. Norikura (3,025 m a.s.l.), central Japan, since 1997. Five open-top chambers which are small greenhouses with a size of maximum open-top diameter, the maximum basal diameter and the height of the chamber were 47 cm, 85 cm and 30 cm, respectively, were set over alpine plant communities consisting of small woody plants and herbaceous vegetation. At places inside and outside of the chambers, seasonal changes in vegetation growth and phenology were observed every month. Using automatic data-recorders, some climate elements such as air and ground temperatures, humidity and rainfall have been observed every hour. Some results through the experiment were quite remarkable. Due to the temperature enhancement of about 0.8 °C for air temperature and about 0.3 °C for ground temperature, plant growth rates and phenological changes showed notable differences between inside and outside of the chambers. The responses to warming, however, were different by different plant species. The results suggest[17],[18] that dominant species in plant community should be replaced by the species with a high physiological response to warming and with a growing form extending tree crown.

## Bibliography


[1] "Precursors of geomagnetic storms observed by the muon detector network", K. Munakata, J. W. Bieber, S. Yasue, C. Kato, M. Koyama, S. Akahane, K. Fujimoto, Z. Fujii, J. E. Humble, and M. L. Duldig, *J. Geophys. Res.*, Vol. 105, No.A12, pp. 27,457-27,468 (2000).

[2] "Solar cycle variations of modulation parameters of galactic cosmic- rays in the heliosphere", K. Munakata, H. Miyasaka, I. Sakurai, S. Yasue, C. Kato, S. Akahane, M. Koyama, D. L. Hall, Z. Fujii, K. Fujimoto, S. Sakakibara, J. E. Humble, and M. L. Duldig, *Adv. Space Res.*, Vol.29, No.10, pp.1527-1532 (2002).

[3] "A 1.7 year quasi-periodicity in cosmic ray intensity variation observed in the outer heliosphere", C. Kato, K. Munakata, S. Yasue, K. Inoue, and F. B. McDonald, *J. Geophys. Res.*, Vol.18, No.A10, p.1367, doi:10.1029/2003JA009897 (2003).

[4] "Exploration of the heliosphere by cosmic rays", K. Munakata, published as the chapter 2 of *Advances in Solar-Terrestrial Physics*, pp.101-116, edited by H. Oya, published by TERRAPUB, Tokyo (2004).

[5] "Cosmic-ray modulation in the heliosphere: global and near-earth measurements and modeling", K. Munakata, Rapporteur paper in 28th *International Cosmic Ray Conference*, Vol.8, edited by T. Kajita et al., pp.251-276, Univ. Acad. Press, Tokyo (2004).

[6] "Geometry of an interplanetary CME on October 29, 2003 deduced from cosmic rays", T. Kuwabara, K. Munakata, S. Yasue, C. Kato, S. Akahane, M. Koyama, J. W. Bieber, P. Evenson, R. Pyle, Z. Fujii, M. Tokumaru, M. Kojima, K. Marubashi, M. L. Duldig, J. E. Humble, M. Silva, N. Trivedi, W. Gonzalez and N. J. Schuch, *Geophys. Res. Lett.*, Vol.31, L19803, doi:10.1029/2004GL020803 (2004).

[7] "A "loss-cone" precursor of an approaching shock observed by a cosmic-ray muon hodoscope on October 28, 2003", K. Munakata, T. Kuwabara, S. Yasue, C. Kato, S. Akahane, M. Koyama, Y. Ohashi, A. Okada, T. Aoki, H. Kojima and J. W. Bieber, *Geophys. Res. Lett.*, Vol.32, L03S04, doi:10.1029/2004GL021469, 2005.

[8] "CME-geometry and cosmic-ray anisotropy observed by a prototype muon detector network", K. Munakata, T. Kuwabara, J. W. Bieber, P. Evenson, R. Pyle, S. Yasue, C. Kato, Z. Fujii, M. L. Duldig, J. E. Humble, M. R. Silva, N. B. Trivedi, W. D. Gonzalez and N. J. Schuch, *Adv. Space Res.*, doi:10.1016/j.asr.2003.05.064, 2005, in press.

[9] "Acceleration below Thunder Clouds at Mount Norikura", by the Tibet hybrid experiment", Y. Muraki *et al.*, Proceedings in the 28th International Cosmic Ray Conference, (31 July - 7 August 2003, Tsukuba, Japan), Vol.7, pp 4177-4180.

[10] "Effects of atmospheric electric fields on cosmic rays", Y. Muraki *et al.*, Phys. Rev. D, **69**, 123010–1-13 (2004).

[11] "Observation of an energetic radiation burst from mountain-top thunderclouds", H. Tsuchiya *et al.*, Phys. Rev. Lett., **102**, 255003 (2009).

[12] K. Osada, M. Kido, C. Nishita, K. Matsunaga, Y. Iwasaka, M. Nagatani, H. Nakada, Changes in ionic constituents of free tropospheric aerosol particles obtained at Mt. Norikura (2770 m a. s. l.), central Japan, during the Shurin period in 2000, Atmos. Environ., 36, 5469-5477, 2002.

[13] "Atmospheric diffusion process based on time change of $^{222}$Rn vertical profile", K. Yoshioka, Journal of Aerosol Research, Japan, 17, 267-275, 2002 (in Japanese).

[14] "Free-tropospheric aerosols based on airplane and mountain observations", K. Osada, Journal of Aerosol Research, Japan, 15, 335-342, 2000 (in Japanese).

[15] "Diurnal changes in needle gas exchange in alpine Pinus pumila during snow-melting and summer seasons", A. Ishida, T. Nakano, S. Sekikawa, E. Maruta, T. Masuzawa, Ecological Research 16, 107-116 (2001).

[16] "Effects of high light and low temperature during harsh winter on needle photodamage of Abies Mariesii growing at the forest limit on Mt. Norikura in Central Japan",

J. Yamazaki, A. Ohashi, Y. Hashimoto, E. Negishi, S. Kumagai, T. Kubo, T. Oikawa, E. Maruta, Plant Science 165, 257-264, (2003).

[17] "Chemistry of surface water at a volcanic summit area, Norikura, central Japan: Multivariate statistical approach", K. Anazawa and H. Ohmori, Chemosphere, 45, 807-816, (2001).

[18] "Experimental research on vegetation response to artificial warming on a mid-latitude high mountain, central Japan", H. Ohmori, J.H. Iguchi, T. Ohta, A. Terazono and K. Hikita, Geogr. Rev. Japan, 77, 301-320, (2004).

# AKENO OBSERVATORY

The Observatory is in Akeno town of Hokuto-city situated 20 km west of Kofu and 130 km west of metropolitan Tokyo. The location is at the longitude of 138.5°E and the latitude of 35.5°N. The altitude is ∼900 m above sea level (Fig.1).

The Observatory was established in 1977 as a research center for air shower studies in the very high energy region. It has been administered by the ICRR as a facility of joint-university-use.

The Akeno Air Shower Experiment started in 1979 with an array covering 1 $km^2$ area (1 $km^2$ array). The array was enlarged to 20 $km^2$ in 1985 and was gradually expanded to Akeno Giant Air Shower Array (AGASA) of approximately 100 $km^2$ area by 1990.

Fig. 1. Aerial View of Akeno Observatory and 1 $km^2$ array area

One of the distinctive features of Akeno experiments is that the measurement was made over five decades of energies well covering $10^{15}$ eV - $10^{20}$ eV by using both the surface detector (for electromagnetic component) and the shielded detector (for muon component). The wide energy coverage was accomplished by the arrays of scintillation detectors of various inter-detector spacings from 3 m to 1 km and with different triggering conditions.

The AGASA was an air shower array composed of 111 scintillation detectors and 27 muon detectors. Each component was placed by about 1 km separation and covered the ground area of 100 $km^2$ in the neighboring villages of the observatory. All detectors were interconnected by optical fibers for the precise timing determination and the data transmission (Fig.2). The AGASA was the largest air shower array in the world. Its operation was ceased in January of 2004 after the construction of Telescope Array (TA) had been funded in 2003.

The AGASA observed a total of 11 events with energies exceeding $10^{20}$eV in 13 years of operation, and heralded rich physics of ultra-high energy cosmic rays now being explored by the Pierre Auger Observatory in Argentina and the Telescope Array (TA) in Utah, USA.

The observatory currently supports two experiments by the university users; one for the observation of galactic cosmic ray modulation by the muon telescope and another for the rapid follow-up observation of gamma ray bursts by the multi-color robotic telescope. It is also used for supporting the operation of TA and various research and development works related to the measurement of very high energy cosmic rays.

Fig. 2. AGASA scintillation detector and data acquisition system.

# KAMIOKA OBSERVATORY

Kamioka observatory is located at 1000 m underground (2700 m water equivalent) in the Kamioka Mine, Gifu prefecture, about 200 km west of Tokyo. The observatory was established in 1995 in order to operate Super-Kamiokande. The underground laboratories are located under Mt.Ikeno-yama and accessible to the experimental site through a 1.7 km horizontal tunnel. The observatory also has surface research buildings and a dormitory located at the distance of 15 minutes drive from the entrance of the mine. The Super-Kamiokande experiment had discovered neutrino oscillations through the observations of atmospheric and solar neutrinos (see the section for Neutrino and Astroparticle Division). The atmospheric neutrino oscillation was confirmed by the K2K accelerator neutrino experiment, which was conducted between 1999 and 2004. A new long baseline neutrino oscillation experiment (the T2K experiment) using a high intensity beam, 50 times of the K2K neutrino beam, by the J-PARC proton accelerator has started in 2009.

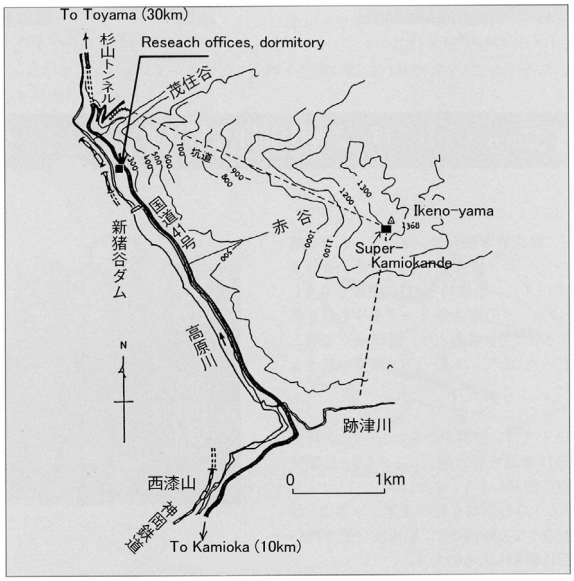


Fig. 1. Map of Kamioka observatory.

The low cosmic ray flux and low seismic noise environment in the underground site enables us to conduct various researches. There is a 100 m long laser interferometer, which is a proto-type of the planned 3 km gravitational wave antenna called LCGT, aiming to detect gravitational waves from extraterrestrial sources (see section of Astrophysics Gravity Division). Using the low radioactive background environment in the Kamioka Mine, A dark matter experiment, called XMASS is being prepared. The XMASS group has performed R&D study using a small proto-type detector and subsequently, the construction of the 800kg liquid xenon detector was started in 2007 and will be ready for data taking by the summer in 2010. The R&D study of a tracking type detector for dark matter search by the Kyoto University group (the NEWAGE experiment) has also been performed in an underground laboratory. The construction of the CANDLE experiment (Osaka Univ.), a double beta decay experiment in the Kamioka Underground Observatory, has started in 2009. The study to improve the neutrino detection sensitivity by adding gadolinium to Super-Kamiokande is on going. Especially in 2009, a new cavern dedicated for the R&D study of the gadolinium project was excavated. In order to support those experiments and also related R&D works, the Observatory is equipped with low background Germanium detector, ICP-MS and so on to measure extremely low radioactive backgrounds.

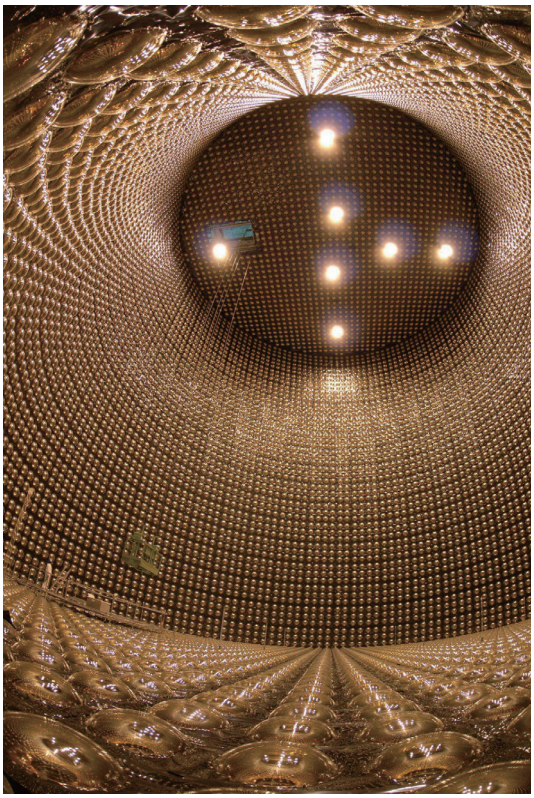

Fig. 2. Super-Kamiokande detector.

Fig. 3. 100 m baseline laser interferometers for gravitational wave and geophysics in Kamioka mine.

# RESEARCH CENTER FOR COSMIC NEUTRINOS

The Research Center for Cosmic Neutrinos (RCCN) was established in April, 1999. The main objective of this Center is to study neutrinos based on data from various observations and experiments. In order to promote studies of neutrino physics, it is important to provide the occasion to discuss theoretical ideas and experimental results on neutrino physics. Therefore, one of the most important practical jobs of this Center is the organization of neutrino-related meetings. On Feb. 9th, 2010, we hosted one domestic neutrino workshop on "the $\theta_{13}$ angle". About 40 physicists participated in this meeting.

Members of this Center have been involved in the Super-Kamiokande and T2K experiments, carrying out researches in neutrino physics. Atmospheric neutrino data from Super-Kamiokande give one of the most precise pieces of information on neutrino oscillations. With increased data, it is more important to have better predictions of the neutrino flux. Therefore, in addition to data analysis of the above experiments, we work on predicting the atmospheric neutrino flux.

It is important that the general public knows about the achievements in the present science. For this reason, we have a public lecture every year. From FY2009, two public lectures per year are co-sponsored by this Institute and the Institute for the Physics and Mathematics of the Universe. The spring lecture is co-organized by RCCN and the Public Relation Office of ICRR. The spring public lecture was held on April 18 (Sat.) at Kashiwa. About 200 people heard the lecture.


Fig. 1. Public lecture held in Kashiwa in April 18, 2009.

This Center, together with the computer committee of ICRR, is in charge of operating the central computer system in ICRR. It had been highly utilized for the analyses and simulations of the various cosmic-ray physics. This Center also supported the users of the computer system, including the physicists working outside ICRR.

Since 2004, this Center has been acting as a body for accepting the ICRR inter-university programs related to the low-background underground facility in the Kashiwa campus. The facility is currently equipped with 4 Ge detectors mainly for the measurements of cosmic radioactive isotopes. The scientific activities that are related to this facility is described elsewhere.

# APPENDICES

# A. ICRR Workshops and Ceremonies

## 58th Fujihara seminar: World-wide Network for Gravitational Wave Observation

Date: August 27-29th, 2009
Place: Shonan Village Center, Hayama, Kanagawa, Japan

**Outline:** The Institute for Cosmic Ray Research hosted the workshop/seminar, titled "World-wide Network for Gravitational Wave Observation", at Hayama, Kanagawa, Japan, from May 27 to 29, 2009. This seminar was sponsored by the Fujihara Foundation of Science, and the scientific program was under the oversight of the Gravitational Wave International Committee (GWIC). The main theme of the seminar was to discuss the development of a world-wide network of gravitational wave detectors to study gravitational wave signal from astrophysical sources, and especially the strategies to use gravitational waves with other signals to probe the universe.

**Participants:** 50 from Japan, 15 from USA, 5 from UK, 4 from Germany, 5 from Australia, 3 from Italy, and 2 from France.

# B. ICRR Seminars

1. Apr 15, 2009: S. T. Petcov (SISSA and INFN-Sezione di Trieste), "Neutrino Mixing, Oscillations, Leptonic CP-Violation and Leptogenesis"
2. Apr 24, 2009: Masato Yamanaka (ICRR, University of Tokyo), "A Solution to the Li-7 Problem by the Long Lived Stau"
3. May 8, 2009: Koji Ishiwata (Tohoku University), "High Energy Cosmic Rays from Supersymmetric Dark Matter"
4. May 15, 2009: Michihisa Takeuchi (ICRR, University of Tokyo), "Top partner reconstruction using jet events at the LHC"
5. May 22, 2009: Motohiko Kusakabe (ICRR, University of Tokyo), "Effect of Long-lived Strongly Interacting Massive Particles on Big Bang Nucleosynthesis"
6. Jun 5, 2009: Riccardo DeSalvo (LIGO Lab., Caltech), "Noisy Metal Blocking the Sensitivity of Gravitational Wave Detectors"
7. Jun 19, 2009: Testuo Shindo (Kogakuin University), "The Gravitino Problem in a leptogenesis Scinario and R-parity Violations"
8. Jul 3, 2009: Kunihito Ioka (KEK), "Cosmic-Ray Positrons from Astrophysical Sources: GRBs, Pulsars and SNRs"
9. Jul 24, 2009: Masatake Ohashi (ICRR, University of Tokyo), "Status of the Kamioka Cryogenic Interferometer CLIO"
10. Jul 31, 2009: Ryoji Enomoto (ICRR, University of Tokyo), "CANGAROO telescope for TeV gamma-ray observation (History, recent results, and future?)"
11. Aug 7, 2009: Masaki Fukushima (ICRR, University of Tokyo), "Status of Ultra-high Energy Cosmic Ray measurement, a report from the ICRC in Lodz."
12. Aug 27, 2009: Masami Ouchi (The Carnegie Institution of Washington), "Exploring the First Two Billion Years of the Universe with Subaru Telescope"
13. Aug 28, 2009: Akira Konaka (TRIUMF, ICRR, University of Tokyo), "Status of the T2K project"
14. Aug 28, 2009: Yoichi Asaoka (ICRR, University of Tokyo), "Ashra Observation"
15. Sep 18, 2009: Masahiro Teshima (Max-Planck-Institut fuer Physik, Munich), "Very High Energy Gamma Ray Astronomy with MAGIC telescopes"
16. Oct 9, 2009: Masahiro Takada (IPMU, University of Tokyo), "Neutrino Mass and Cosmology"

17. Oct 23, 2009: Yusuke Uchiyama (ICEPP, the University of Tokyo), ”MEG Experiment –From the First Data–”
18. Nov 18, 2009: Marco Casolino (INFN & University of Rome Tor Vergata), ”Indirect Dark Matter Search from Space and Ground: Status and Perspectives”
19. Nov 25, 2009: Hiroshi Suzuki (RIKEN), ”2D N=(2,2) SYM on the Lattice”
20. Nov 27, 2009: Toshifumi Yamasita (Nagoya University), ”SUSY Flavor Violations via RGEs in Non-renormalizable SU(5) Model”
21. Dec 4, 2009: Jun’ichi Yokoyama (RESCEU, University of Tokyo), ”Probing Early Universe via Gravitational Waves”
22. Jan 29, 2010: Toshio Terasawa (ICRR, University of Tokyo), ”On the R/D Study of Radar Observation of Cosmic Ray Air Showers”
23. Feb 22, 2010: Naohito Saito (KEK), ”Challenges for New Muon g-2/EDM experiment at J-PARC”
24. Mar 18, 2010: Tomo Takahashi (Saga University), ”Probing the physics of the early Universe with non-Gaussianity”
25. Mar 26, 2010: Hirohiko M. Shimizu (KEK), ”Neutron Fundamental Physics at J-PARC”

# C. List of Publications

## (a) Papers Published in Journals

1. ”Atmospheric neutrino oscillation analysis with sub-leading effects in Super-Kamiokande I, II and III”, Super-Kamiokande Collaboration (R. Wendell and C. Ishihara et al.), to be published in Phys. Rev. D. [arXiv:1002.3471 [hep-ex]].
2. ”High-speed charge-to-time converter ASIC for the Super-Kamiokande detector”, H. Nishino et al., Nucl. Instrum. Meth. A610, 710, 2009. [arXiv:0911.0986 [hep-ex]].
3. ”Search for Astrophysical Neutrino Point Sources at Super-Kamiokande”, Super-Kamiokande Collaboration (E. Thrane et al.), Astrophys. J. 704, 503, 2009. [arXiv:0907.1594 [hep-ex]].
4. ”Search for Neutrinos from GRB 080319B at Super-Kamiokande”, Super-Kamiokande Collaboration (E. Thrane et al.), Astophys. J. 697, 730, 2009.
5. ”Distillation of liquid xenon to remove krypton”, XMASS Collaboration, Astropart. Phys. 31, 290, 2009.
6. ”Development of a large area VUV sensitive gas PMT with GEM/$\mu$ PIC”, H. Sekiya, et al., Journal of Instrumentation. 4 P11006, 2009.
7. ”A new imaging device based on UV scintillators and a large area gas photomulitiplier”, H. Sekiya, et al., to be published in Nuclear Instrument and Methods in Physics Research A, 2010.
8. ”Collection and release of radon in argon gas, and the development of low level radon concentration measurement”, Motoyasu Ikeda, et al., RADIOISOTOPES, 59, 29, 2010.
9. ”Constraints on inelastic dark matter from XENON10”, J. Angle et al, Phys. Rev. D80, 115005, 2009.
10. ”New measurement of the relative scintillation efficiency of xenon nuclear recoils below 10 keV”, E. Aprile, et al., Phys. Rev. C79, 045807, 2009.
11. ”Design and Performance of the XENON10 Dark Matter Experiment”, E. Aprile et al. [arXiv:1001.2834v1 [hep-ex]].
12. ”Measurement of neutral current pion production on carbon in a few GeV neutrino beam”, SciBooNE Collaboration (Y. Kurimoto et. al), Phys. Rev. D81, 033004, 2010. [arXiv:0910.5768 [hep-ex]].
13. ”Measurement of inclusive neutral current neutral pi0 production on carbon in a few GeV neutrino beam”, SciBooNE Collaboration, Phys. Rev. D81, 033004, 2010.
14. ”Further study of neutrino oscillation with two detectors in Kamioka and Korea”, Dufour, F. and Kajita, T. and Kearns, E. and Okumura, K., Phys. Rev. D81, 093001, 2010. [arXiv:1001.5165 [hep-ph]].

15. ”Atmospheric neutrinos and discovery of neutrino oscillations”, Takaaki Kajita, Proc. of the Japan Academy Series B86, 303, 2010.

16. ”CANGAROO-III Observation of TeV Gamma Rays from the Vicinity of PSR B1706–44”, R. Enomoto et al., Astrophys. J, 703, 1725, 2009.

17. ”On site calibration for new fluorescence detectors of the telescope array experiment”, H.Tokuno et al., Nucl. Instr. and Methods A601, 364, 2009.

18. ”Limits on Nonstandard Forces in the Submicrometer Range”, M. Masuda and M. Sasaki, Phys. Rev. Lett. 102, 171101, 2009.

19. ”Observation of TeV Gamma Rays from the Fermi Bright Galactic Sources with the Tibet Air Shower Array”, M. Amenomori et al., ApJ, 709, L6, 2010.

20. ”On Temporal Variations of the Multi-TeV Cosmic Ray Anisotropy Using the Tibet III Air Shower Array”, M. Amenomori et al., ApJ, 711, 119, 2010.

21. ”Recent results on gamma-ray observation by the Tibet air shower array and related topics”, M. Amenomori et al., J. Phys. Soc. Jpn., 78, 88, 2009.

22. ”Chemical Composition of Cosmic Rays around the Knee Observed by the Tibet Air-Shower-Core Detector”, M. Amenomori et al., J. Phys. Soc. Jpn., 78, 206, 2009.

23. ”DECIGO pathfinder”, Masaki Ando, et al., Class. Quantum Grav., 26, 094019, 2009.

24. ”Status of Japanese gravitational wave detectors”, K Arai, et al., Class. Quantum Grav., 26, 204020, 2009.

25. ”Underground Cryogenic Laser Interferometer CLIO”, Shinji Miyoki and CLIO and LCGT Collaborators, J. Phys.: Conf. Ser., 203, 012075, 2010.

26. ”Thermal-noise-limited underground interferometer CLIO”, K. Agatsuma, et al., Class. Quantum Grav., 27, 084022, 2010.

27. ”Direct Measurement of Thermal Fluctuation of High-Q Pendulum”, K. Agatsuma, et al., Phys. Rev. Lett., 104, 040602, 2010.

28. ”Cross-correlation weak lensing of SDSS galaxy clusters I: measurements”, E. S. Sheldon, et al., Astrophys. J. 703, 2217, 2009.

29. ”The seventh data release of the Sloan Digital Sky Survey”, SDSS Collaboration(K. N. Abazajian, et al.), Astrophys. J. Suppl. 182, 543, 2009.

30. ”The greater impact of mergers on the growth of massive galaxies: implications for mass assembly and evolution since $z \sim 1$”, K. Bundy, et al., Astrophys. J. 697, 1369, 2009.

31. ”Measuring the galaxy-mass and galaxy-dust correlations through magnification and reddening”, B. Menard, et al., to be published in Mon. Not. Roy. astr. Soc. 2009. [ArXiv: 0902.4240 [astroph]].

32. ”Properties of disks and bulges of spiral and lenticular galaxies in the Sloan Digital Sky Survey”, N. Oohama, et al., Astrophys. J. 705. 245, 2009.

33. ”Luminosity functions of Type la supernovae and their host galaxies from the Sloan Digital Sky Survey”, N. Yasuda, et al., Astron, J. 139, 39, 2010.

34. ”Baryon acoustic oscillation in the Sloan Digital Sky Survey data release 7 galaxy sample”, W. J. Percival, et al., Mon. Not. Roy. astr. Soc. 401, 2148, 2010.

35. ”Primordial Black Holes as All Dark Matter”, P. H. Frampton, M. Kawasaki, F. Takahashi and T. T. Yanagida, JCAP, 1004, 023, 2010.

36. ”Right-handed sneutrino dark matter and big-bang nucleosynthesis”, K. Ishiwata, M. Kawasaki, K. Kohri and T. Moroi, Phys. Lett. B689, 163, 2010.

37. ”Density Fluctuations in Thermal Inflation and Non-Gaussianity”, M. Kawasaki, T. Takahashi and S. Yokoyama, JCAP, 0912, 012, 2009.

38. ”On some hybrid-types of Q balls in the gauge-mediated supersymmetry breaking”, S. Kasuya and M. Kawasaki, Phys. Rev. D80, 123529, 2009.

39. ”Cosmological Constraints on a Massive Neutrino,” M. Kawasaki and K. Sato, Prog. Theor. Phys., 122, 205, 2009.

40. ”Axion isocurvature fluctuations with extremely blue spectrum”, S. Kasuya and M. Kawasaki, Phys. Rev. D80, 023516, 2009.

41. ”Axion braneworld cosmology”, C. Bambi, M. Kawasaki and F. R. Urban, Phys. Rev. D80, 023533, 2009.

42. ”Inhomogeneous baryogenesis, cosmic antimatter, and dark matter”, A. D. Dolgov, M. Kawasaki and N. Kevlishvili, Nucl. Phys. B807, 229, 2009.

43. ”Numerical study of Q-ball formation in gravity mediation”, T. Hiramatsu, M. Kawasaki and F. Takahashi, [arXiv:1003.1779 [hep-ph]].

44. ”Conformal Inflation, Modulated Reheating, and WMAP5”, T. Kobayashi and S. Mukohyama, Phys. Rev. D79, 083501, 2009.

45. ”Cosmological Constraints on Rapid Roll Inflation”, T. Kobayashi, S. Mukohyama and B. A. Powell, JCAP, 0909, 023, 2009.

46. ”Curvatons in Warped Throats”, T. Kobayashi and S. Mukohyama, JCAP, 0907, 032, 2009.

47. ”Effects of Light Fields During Inflation”, T. Kobayashi and S. Mukohyama, Phys. Rev. D81, 103504, 2010.

48. ”Effect of Long-lived Strongly Interacting Relic Particles on Big Bang Nucleosynthesis”, M. Kusakabe, T. Kajino, T. Yoshida and G. J. Mathews, Phys. Rev. D80, 103501, 2009.

49. ”Production of the p-Process Nuclei in the Carbon Deflagration Model for Type Ia Supernovae”, M. Kusakabe, N. Iwamoto and K. Nomoto, [arXiv:1001.0145 [astro-ph.SR]].

50. ”New results on catalyzed BBN with a long-lived negatively-charged massive particle”, M. Kusakabe, T. Kajino, T. Yoshida and G. J. Mathews, Phys. Rev. D81, 083521, 2010.

51. ”Gravitational waves from kinks on infinite cosmic strings”, M. Kawasaki, K. Miyamoto and K. Nakayama, Phys. Rev. D81, 103523, 2010.

52. ”Diffuse gamma-ray background and cosmic-ray positrons from annihilating dark matter”, M. Kawasaki, K. Kohri and K. Nakayama, Phys. Rev. D80, 023517, 2009.

53. ”Phenomenological Aspects of Horava-Lifshitz Cosmology”, S. Mukohyama, K. Nakayama, F. Takahashi and S. Yokoyama, Phys. Lett. B679, 6, 2009.

54. ”Non-Gaussianity from Isocurvature Perturbations : Analysis of Trispectrum”, E. Kawakami, M. Kawasaki, K. Nakayama and F. Takahashi, JCAP, 0909, 002, 2009.

55. ”Upward muon signals at neutrino detectors as a probe of dark matter properties”, J. Hisano, K. Nakayama and M. J. S. Yang, Phys. Lett. B678, 101, 2009.

56. ”Constraining Light Gravitino Mass from Cosmic Microwave Background”, K. Ichikawa, M. Kawasaki, K. Nakayama, T. Sekiguchi and T. Takahashi, JCAP, 0908, 013, 2009.

57. ”The R-axion and non-Gaussianity”, K. Nakayama and F. Takahashi, Phys. Lett. B679, 436, 2009.

58. ”Effects of Dark Matter Annihilation on the Cosmic Microwave Background”, T. Kanzaki, M. Kawasaki and K. Nakayama, to be published in Prog. Theor. Phys. [arXiv:0907.3985 [astro-ph.CO]].

59. ”Gravitational Wave Background and Non-Gaussianity as a Probe of the Curvaton Scenario”, K. Nakayama and J. Yokoyama, JCAP, 1001, 010, 2010.

60. ”Implications of CDMS II result on Higgs sector in the MSSM”, J. Hisano, K. Nakayama and M. Yamanaka, Phys. Lett. B684, 246, 2010.

61. ”Gravitational waves from kinks on infinite cosmic strings”, M. Kawasaki, K. Miyamoto and K. Nakayama, to be published in Phys. Rev. D. [arXiv:1002.0652 [astro-ph.CO]].

62. ”Constraining Light Gravitino Mass from Cosmic Microwave Background”, K. Ichikawa, M. Kawasaki, K. Nakayama, T. Sekiguchi and T. Takahashi, JCAP, 0908, 013, 2009.

63. ”Neutrino mass from cosmology: Impact of high-accuracy measurement of the Hubble constant”, T. Sekiguchi, K. Ichikawa, T. Takahashi and L. Greenhill, JCAP, 1003, 015, 2010.

64. ”Probing the primordial power spectra with inflationary priors”, M. Kawasaki and T. Sekiguchi, JCAP, 1002, 013, 2010.

65. ”WIMP dark matter in gauge-mediated SUSY breaking models and its phenomenology”, J. Hisano, S. Sugiyama, T. Takesako and M. Yamanaka, [arXiv:1003.3648 [hep-ph]].

66. ”A new idea to search for charged lepton flavor violation using a muonic atom”, M. Koike, Y. Kuno, J. Sato and M. Yamanaka, arXiv:1003.1578 [hep-ph].

67. ”Stau relic density at the Big-Bang nucleosynthesis era consistent with the abundance of the light element in the coannihilation scenario”, T. Jittoh, K. Kohri, M. Koike, J. Sato, T. Shimomura and M. Yamanaka, [arXiv:1001.1217 [hep-ph]].

68. ”Implications of CDMS II result on Higgs sector in the MSSM”, J. Hisano, K. Nakayama and M. Yamanaka, Phys. Lett. B684, 246, 2010.

69. ”Higgs Production via Gluon Fusion in a Six Dimensional Universal Extra Dimension Model on $S^2/Z_2$”, N. Maru, T. Nomura, J. Sato and M. Yamanaka, Eur. Phys. J. C66, 283, 2010.

70. ”The Universal Extra Dimensional Model with $S^2/Z_2$ extra-space”, N. Maru, T. Nomura, J. Sato and M. Yamanaka, Nucl. Phys., B830, 414, 2010.

71. ”Waiting for $\mu \to e\gamma$ from the MEG experiment”, J. Hisano, M. Nagai, P. Paradisi and Y. Shimizu, JHEP, 0912, 030, 2009.

72. ”Dark matter and collider phenomenology of split-UED”, C. R. Chen, M. M. Nojiri, S. C. Park, J. Shu and M. Takeuchi, JHEP, 0909, 078, 2009.

73. ”First direct detection of ions originating from the Moon by MAP-PACE IMA onboard SELENE(KAGUYA)”, S. Yokota et al., Geophys. Res. Lett. 36:L11201.1, 2009.

74. ”Pairwise energy gain-loss feature of solar wind protons in the near-Moon wake”, M. N. Nishino et al., Geophys. Res. Lett. 36:L12108.1, 2009.

75. ”Solar-wind proton access deep into the near-Moon wake”, M. N. Nishino et al., Geophys. Res. Lett. 36:L16103.1, 2009.

76. ”Plasma instabilities as a result of charge exchange in the downstream region of supernova remnant shocks”, Y. Ohira et al., Astrophys. J. Lett. 703:L59, 2009.

77. ”Slow heating model of gamma-ray burst: Photon spectrum and delayed emission”, K. Asano and T. Terasawa, Astrophys. J. 705:1714, 2009.

78. ”First in situ observation of the Moon-originating ions in the Earth’s Magnetosphere by MAP-PACE on SELENE(KAGUYA)”, T. Tanaka et al., Geophys. Res. Lett. 36:L22106.1, 2009.

79. ”27-day variation in cloud amount and relationship to the solar cycle”, Y. Takahashi, et al., Atmos. Chem. Phys., 10, 1577, 2010.

80. ”Universality test of the charged Higgs boson couplings at the LHC and at B factories”, Alan S. Cornell, et al., to be published in Phys. Rev. D, 2009. [arXiv:0906.1652 [hep-ph]].

## (b) Conference Papers

1. ”Search for GUT monopoles at Super-Kamiokande”, K. Ueno, Proceedings of the 31th International Cosmic Ray Conference, 2009.

2. ”The solar neutrino measurements”, Y. Koshio, Proceedings of the International Symposium on Multiparticle Dynamics, 2009.

3. ”The path forward: Monte Carlo convergence discussion”, Y.Hayato, Jan. T. Sobczyk, Chirs Walter, G.P.Zeller, 6th International Workshop on Neutrino-Nucleus Interactions in the Few-GeV Region ( NuINT 09 ), AIP Conf. Proc., 1198, 312, 2009.
4. ”Kamiokande and Super-Kamiokande results on neutrino astrophysics”, M. Nakahata, Proceedings of the thirteenth international workshop on Neutrino Telescopes, 2009.
5. ”Commissioning of the New Electronics and Online System for the Super-Kamiokande Experiment”, S. Yamada, et al., IEEE-NPSS Real Time Conference 2009, IEEE Transactions on Nuclear Science, vol.57, issue 2, 428, 2009.
6. ”Search for neutrino charged current coherent pion production at SciBooNE”, K. Hiraide, 6th International Workshop on Neutrino-Nucleus Interactions in the Few-GeV Region (NuInt09), AIP Conf.Proc. 1189, 249 2009. [arXiv:0909.5127 [hep-ex]].
7. ”Search for neutrino charged current coherent pion production in SciBooNE”, K. Hiraide, 23th Rencontres De Physique De La Vallee D’Aoste, Nuovo Cim.032C, 75, 2009.
8. ”Recent results from SciBooNE”, K. Hiraide, 45th Karpacz Winter School in Theoretical Physics: Neutrino interactions: from theory to Monte Carlo simulations, Acta Physica Polonica B40, 2659, 2009.
9. ”Search for Nucleon decay in Super-Kamiokande”, M. Miura, Recontres de Moriond EW, XLIVth Recontres de Moriond, Electroweak interactions and Unified Theories, 2009.
10. ”Search for proton decay $p \rightarrow nuK^{+}$ in Super-Kamiokande”, M. Miura, Proceedings of the 31st ICRC, 2009.
11. ”A Search for supernova relic neutrinos at Super-Kamiokande”, Takashi Iida , Kirk Bays for the Super-Kamiokande Collaboration, Journal of Physics: Conference Series 203, 012088, 2010.
12. ”Status of Super-Kamiokande and early atmospheric neutrino data from SK-IV”, Yoshihisa OBAYASHI for the Super-Kamiokande collaboration, PROCEEDINGS OF THE 31st ICRC, 2009.
13. ”Neutrino oscillations: Discovery, current status, future directions”, Takaaki Kajita, Int. J. Mod. Phys. A24, 3437, 2009.
14. ”Megaton class water Cherenkov detector in East Asia”, Takaaki Kajita, Prepared for 13th International Workshop on Neutrino Telescopes:Un altro modo di guardare il cielo: Tribute to Galileo, 2009.
15. ”Status and prospect of atmospheric neutrinos and long baseline studies”, Takaaki Kajita, J. Phys. Conf. Ser. 203, 012012, 2010.
16. ”Final result of neutron-antineutron oscillation search in Super-Kamiokande I”, Jun Kameda for Super-Kamiokande collaboration, PROCEEDINGS OF THE 31st ICRC, 2009.
17. ”Observations of the Unidentified VHE Gamma-Ray Source HESS J1614–518 with CANGAROO-III”, T. Mizukami et al., Proceedings of the 31st International Cosmic Ray Conference (Lodz), 0973, 2009.
18. ”CANGAROO-III Search for Galactic Sources”, R. Enomoto et al., Proceedings of the 31st International Cosmic Ray Conference (Lodz), 0799, 2009.
19. ”Search for TeV Gamma-Rays around the Merger Cluster Abell 3376 with CANGAROO-III”, T. Matoba et al., Proceedings of the 31st International Cosmic Ray Conference (Lodz), 0735, 2009.
20. ”TeV Gamma-Ray Observations of Some Extragalactic Objects with CANGAROO-III”, K. Nishijima et al., Proceedings of the 31st International Cosmic Ray Conference (Lodz), 0565, 2009.
21. ”Measurement of Ultra-high Energy Cosmic Rays by Telescope Array (TA)”, H. Sagawa for the Telescope Array Collaboration, the 31st International Cosmic Ray Conference, Lodz, Poland, 2009.
22. ”Overview of the Telescope Array Experiment”, T. Abu-Zayyad, et al., the 31st International Cosmic Ray Conference, Lodz, Poland, 2009.
23. ”Performance of TA Surface Array”, T. Nonaka et al., the 31st International Cosmic Ray Conference, 2009.
24. ”Performance of the Fluorescence Detector of the Telescope Array experiment”, H. Tokuno et al., the 31st International Cosmic Ray Conference, 2009.
25. ”An Electron Linear Accelerator for end-to-end absolute energy calibration of atmospheric fluorescence telescopes of the Telescope Array experiment”, T. Shibata et al., the 31st International Cosmic Ray Conference, 2009.

26. ”Measurement of the spectrum of ultra-high energy cosmic rays by the Telescope Array surface array”, A. Taketa et al., the 31st International Cosmic Ray Conference, 2009.

27. ”Energy determination of air shower array based on the “full” Monte Carlo simulation for the Telescope Array”, E. Kido et al., the 31st International Cosmic Ray Conference, 2009.

28. ”Using CORSIKA to quantify Telescope Array surface detector response”, B. T. Stokes et al., the 31st International Cosmic Ray Conference, 2009.

29. ”Hybrid Measurement of the Telescope Array Experiment”, D. Ikeda et al., the 31st International Cosmic Ray Conference, 2009.

30. ”The Energy Spectrum of UHECR’s using the TA Fluorescence Detectors in Monocular Mode” D. R. Bergman et al., the 31st International Cosmic Ray Conference, 2009.

31. ”Measuring the Spectrum of Ultrahigh Energy Cosmic Rays using the Monte Carlo Technique” L. M. Scott et al., the 31st International Cosmic Ray Conference, 2009.

32. ”Toward a comparison of fluorescence energy scale and spectra between Telescope Array and the High Resolution Fly’s Eye”, C. C. H. Jui et al., the 31st International Cosmic Ray Conference, 2009.

33. ”Search for large-scale anisotropy of ultra-high energy cosmic rays with the Telescope Array first year data”, P.Tinyakov et al., the 31st International Cosmic Ray Conference, 2009.

34. ”Distribution of arrival directions obtained from the first year data of Telescope Array”, N.Sakurai et al., the 31st International Cosmic Ray Conference, 2009.

35. ”Point source search with the Telescope Array”, I.Tkachev et al., the 31st International Cosmic Ray Conference, 2009.

36. ”Mass Composition Study of Ultra-high Energy Cosmic Ray with the Telescope Array Fluorescence Detector Stereo Events”, Y.Tameda et al., the 31st International Cosmic Ray Conference, 2009.

37. ”Search for ultra-high energy photons in Telescope Array surface detector first-year data”, G.I.Rubtsov et al., the 31st International Cosmic Ray Conference, 2009.

38. ”Calibration of the Telescope Array Experiment Fluorescence Detectors”, D.Ikeda et al., the 31st International Cosmic Ray Conference, 2009.

39. ”Measurement of atmospheric transparencies with LIDAR for Telescope Array”, T.Tomida et al., the 31st International Cosmic Ray Conference, 2009.

40. ”Cloud Monitoring with an Infra-Red Camera for the Telescope Array Experiment”, M.Chikawa et al., the 31st International Cosmic Ray Conference, 2009.

41. ”Absolute Gain Calibration of PMT for the Fluorescence Detector of the Telescope Array Experiment”, S.Kawana et al., the 31st International Cosmic Ray Conference, 2009.

42. ”Temperature characteristics of PMTs and calibration light sources for the Telescope Array Fluorescence Detectors”, S.Ogio et al., the 31st International Cosmic Ray Conference, 2009.

43. ”The trigger and DAQ system of the surface detector array of the Telescope Array experiment”, A.Taketa et al., the 31st International Cosmic Ray Conference, 2009.

44. ”Wide area radio network for the Telescope Array experiment”, T.Nonaka et al., the 31st International Cosmic Ray Conference, 2009.

45. ”A northern sky survey for PeV gamma rays using the Tibet air shower array with water-Cherenkov-type underground muon detectors”, The Tibet AS$\gamma$ Collaboration (M. Amenomori et al.), Proceedings of the 31st International Cosmic Ray Conference, Lodz, Poland, 2009.

46. ”Tibet AS+MD Project”, The Tibet AS$\gamma$ Collaboration (M. Amenomori et al.), Proceedings of the 31st International Cosmic Ray Conference, 2009.

47. ”Demonstration of hadronic cosmic-ray rejection power by a water Cherenkov underground muon detector with the Tibet air shower array”, The Tibet AS$\gamma$ Collaboration (M. Amenomori et al.), Proceedings of the 31st International Cosmic Ray Conference, 2009.

48. ”Interpretation of the cosmic-ray energy spectrum and the knee inferred from the Tibet air-shower experiment”, The Tibet AS$\gamma$ Collaboration (M. Amenomori et al.), Proceedings of the 31st International Cosmic Ray Conference, 2009.

49. ”Large-scale sidereal anisotropy of multi-TeV galactic cosmic rays and the heliosphere”, The Tibet AS$\gamma$ Collaboration (M. Amenomori et al.), Proceedings of the 31st International Cosmic Ray Conference, 2009.

50. ”New estimation of the power-law index of the cosmic-ray energy spectrum as determined by the Compton-Getting anisotropy at solar time frame”, The Tibet AS$\gamma$ Collaboration (M. Amenomori et al.), Proceedings of the 31st International Cosmic Ray Conference, 2009.

51. ”Sun’s Shadow in changing phase from the Solar Cycle 23 to 24 Observed with the Tibet Air Sower Array”, The Tibet AS$\gamma$ Collaboration (M. Amenomori et al.), Proceedings of the 31st International Cosmic Ray Conference, 2009.

52. ”The sidereal anisotropy of multi-TeV cosmic rays in an expanding Local Interstellar Cloud”, The Tibet AS$\gamma$ Collaboration (M. Amenomori et al.), Proceedings of the 31st International Cosmic Ray Conference, 2009.

53. ”Curvatons in Warped Throats”, T. Kobayashi and S. Mukohyama, Invisible Universe International Conference, 2009.

54. ”Curvatons in Warped Throats”, T. Kobayashi and S. Mukohyama, The 19th Workshop on General Relativity and Gravitation in Japan, 2009.

55. ”Constraining single-field slow-roll inflation models with Bayesian model selection”, T. Sekiguchi and M. Kawasaki, The 19th Workshop on General Relativity and Gravitation in Japan, 2009.

56. ”Big Bang Nucleosynthesis with long-lived strongly interacting relic particles”, M. Kusakabe, T. Kajino, T. Yoshida and G. J. Mathews, IAU Symposium 268: Light elements in the Universe, 2010.

57. ”Signature of Long-lived Relic Particles on Primordial Light Element Abundances in Big Bang Nucleosynthesis”, M. Kusakabe, T. Kajino, T. Yoshida and G. J. Mathews, The 10th International Symposium on Origin of Matter and Evolution of the Galaxies (OMEG10), to be published in an AIP conference series.

58. ”Signatures of dark matter annihilation in the light of PAMELA/ATIC anomaly”, K. Nakayama, Proceedings of Seventh International Heidelberg Conference on Dark Matter in Astro and Particle Physics, 2009.

59. ”Production Rate of Second KK Gauge Bosons in UED Models at LHC”, S. Matsumoto, J. Sato, M. Yamanaka and M. Senami, 4th International Workshop on the Dark Side of the Universe (DSU 2008), AIP Conf. Proc., 1115, 297, 2009.

60. ”Relic abundance of dark matter in universal extra dimension models with right-handed neutrinos”, S. Matsumoto, J. Sato, M. Senami and M. Yamanaka, 4th International Workshop on the Dark Side of the Universe (DSU 2008), AIP Conf. Proc., 1115, 314, 2009.

61. ”Possible solution to the Li-7 problem by the long lived stau”, T. Jittoh, K. Kohri, M. Koike, J. Sato, T. Shimomura and M. Yamanaka, 4th International Workshop on the Dark Side of the Universe (DSU 2008), AIP Conf. Proc., 1115, 285, 2009.

62. ”Cosmological promising parameters of stau in the minimal supersymmetric standard model”, T. Jittoh, K. Kohri, M. Koike, J. Sato, T. Shimomura and M. Yamanaka, Particle Physics, Astrophysics And Quantum Field Theory: 75 Years Since Solvay (PAQFT 08), Int. J. Mod. Phys., A24, 3501, 2009.

63. ”Production rate of second KK gauge bosons in UED models at LHC”, S. Matsumoto, J. Sato, M. Yamanaka and M. Senami, Particle Physics, Astrophysics And Quantum Field Theory: 75 Years Since Solvay (PAQFT 08), Int. J. Mod. Phys. A24, 3515, 2009.

64. ”Search for radio echoes from EAS with the MU radar, Shigaraki, Japan”, T. Terasawa et al., Proceedings of 31st International Cosmic Ray Conference, session H.E.1.6, paper #0199, 2009.

65. ”Influence of the Schwabe/Hale solar cycles on climate change during the Maunder Minimum”, H. Miyahara, Y. Yokoyama, Y. T. Yamaguchi, Proceedings of the IAU XXVII General Assembly, 2009.

66. ”Transitions of the eleven-year solar cycle and its influence on climate change”, Hiroko Miyahara, Proceedings of the Second Symposium on”Historical Records and Modern Science, 126, 2009.

## (c) ICRR Reports

1. ICRR-Report-539-2009-1
   "The Universal Extra Dimensional Model with $S^2/Z_2$ extra-space"
   Nobuhito Maru, Takaaki Nomura, Joe Sato and Masato Yamanaka.

2. ICRR-Report-540-2009-2
   "Constraining Light Gravitino Mass from Cosmic Microwave Background"
   Kazuhide Ichikawa, Masahiro Kawasaki, Kazunori Nakayama, Toyokazu Sekiguchi and Tomo Takahashi.

3. ICRR-Report-541-2009-3
   "search for TeV Gamma-ray Emission from the Supernova Remnant W44 with the CANGAROO-III telescopes"
   Yohei Yukawa.

4. ICRR-Report-542-2009-4
   "Diffuse gamma-ray background and cosmic-ray positrons from annihilating dark matter"
   Masahiro Kawasaki, Kazunori Kohri and Kazunori Nakayama.

5. ICRR-Report-543-2009-5
   "Cosmological constraints on rapid roll inflation"
   Shinji Mukohyama and Brian A. Powell.

6. ICRR-Report-544-2009-6
   "Non-Gaussianity from Isocurvature Perturbations : Analysis of Trispectrum"
   Etsuko Kawakami, Masahiro Kawasaki, Kazunori Nakayama and Fuminobu Takahashi.

7. ICRR-Report-545-2009-7
   "Upward muon signals at neutrino detectors as a probe of dark matter properties"
   Junji Hisano, Kazunori Nakayama and Masaki J.S. Yang.

8. ICRR-Report-546-2009-8
   "Curvatons in Warped Throats"
   Takeshi Kobayashi and Shinji Mukohyama.

9. ICRR-Report-547-2009-9
   "Higgs Production via Gluon Fusion in a Six Dimensional Universal Extra Dimension Model on $S^2/Z_2$"
   Nobuhito Maru, Takaaki Nomura, Joe Sato and Masato Yamanaka.

10. ICRR-Report-548-2009-10
    "Phenomenological Aspects of Hořava-Lifshitz Cosmology"
    Shinji Mukohyama, Kazunori Nakayama, Fuminobu Takahashi and Shuichiro Yokoyama.

11. ICRR-Report-549-2009-11
    "The R-axion and non-Gaussianity"
    Kazunori Nakayama and Fuminobu Takahashi.

12. ICRR-Report-550-2009-12
    "Effects of Dark Matter Annihilation on the Cosmic Microwave Background"
    Toru Kanzaki, Masahiro Kawasaki and Kazunori Nakayama.

13. ICRR-Report-551-2009-13
    "Gravitational Wave Background and Non-Gaussianity as a Probe of the Curvaton Scenario"
    Kazunori Nakayama and Jun'ichi Yokoyama.

14. ICRR-Report-552-2009-14
    "Neutrino mass from cosmology: Impact of high-accuracy measurement of the Hubble constant"
    Toyokazu Sekiguchi, Kazuhide Ichikawa, Tomo Takahashi and Lincoln Greenhill.

15. ICRR-Report-553-2009-15
    "The Affleck-Dine Mechanism in Conformally Sequestered Supersymmetry Breaking"
    Kazunori Nakayama and Fuminobu Takahashi.

16. ICRR-Report-554-2009-16
    "Probing the primordial power spectra with inflationary priors"
    Masahiro Kawasaki and Toyokazu Sekiguchi.

17. ICRR-Report-555-2009-17
    ”Right-handed sneutrino dark matter and big-bang nucleosynthesis”
    Koji Ishiwata, Masahiro Kawasaki, Kazunori Kohri and Takeo Moroi.

18. ICRR-Report-556-2009-18
    ”Implications of CDMS II result on Higgs sector in the MSSM”
    Junji Hisano, Kazunori Nakayama and Masato Yamanaka.

19. ICRR-Report-557-2009-19
    ”Stau relic density at the Big-Bang nucleosynthesis era consistent with the abundance of the light element nuclei in the coannihilation scenario”
    Toshifumi Jittoh, Kazunori Kohri, Masafumi Koike, Joe Sato, Takashi Shimomura and Masato Yamanaka.

20. ICRR-Report-558-2009-20
    ”Gravitational waves from kinks on infinite cosmic strings”
    Masahiro Kawasaki, Koichi Miyamoto and Kazunori Nakayama.

21. ICRR-Report-559-2009-21
    ”Gravitational Waves from Collapsing Domain Walls”
    Takashi Hiramatsu, Masahiro Kawasaki and Ken’ichi Saikawa.

22. ICRR-Report-560-2009-22
    ”Full three flavor oscillation analysis of atmospheric neutrino data observed in Super-Kamiokande”
    Chizue Ishihara.

23. ICRR-Report-561-2009-23
    ”Effects of Light Fields During Inflation”
    Takeshi Kobayashi and Shinji Mukohyama.

24. ICRR-Report-562-2009-24
    ”A new idea to search for charged lepton flavor violation using a muonic atom”
    Masafumi Koike, Yoshitaka Kuno, Joe Sato and Masato Yamanaka.

25. ICRR-Report-563-2009-25
    ”Precise Measurement of Solar Neutrinos with Super-Kamiokande III”
    Motoyasu Ikeda.

26. ICRR-Report-564-2009-26
    ”Search for Supernova Relic Neutrino at Super-Kamiokande”
    Takashi Iida.

27. ICRR-Report-565-2009-27
    ”Numerical study of Q-ball formation in gravity mediation”
    Takashi Hiramatsu, Masahiro Kawasaki and Fuminobu Takahashi.

28. ICRR-Report-566-2009-28
    ”WIMP dark matter in gauge-mediated SUSY breaking models and its phenomenology”
    Junji Hisano, Kazunori Nakayama, Shohei Sugiyama, Tomohiro Takesako and Masato Yamanaka.

# D. Doctoral Theses

1. ”Precise Measurement of Solar Neutrinos with Super-Kamiokande III”,
   M. Ikeda,
   Ph.D Thesis, Mar. 2010.
2. ”Search for Supernova Relic Neutrino at Super-Kamiokande”,
   T. Iida,
   Ph.D Thesis, Mar. 2010.
3. ”Full three flavor oscillation analysis of atmospheric neutrino data observed in Super-Kamiokande”,
   C. Ishihara,
   Ph.D. Thesis, Mar. 2010.

# E. Public Relations

## (a) ICRR News

ICRR News is a newspaper published quarterly in Japanese to inform the Institute’s activities. This year’s editors were H.Sagawa. It includes :

1. reports on investigations by the staff of the Institute or made at the facilities of the Institute,
2. reports of international conferences on topics relevant to the Institute’s research activities,
3. topics discussed at the Institute Committees,
4. list of publications published by the Institute [ICRR-Report, ICRR-Houkoku (in Japanese)],
5. list of seminars held at the Institute,
6. announcements,
7. and other items of relevance.

The main topics in the issues in 2009 fiscal year were:

**No.69** (Oct 1, 2009)

- 40 years history of air shower experiments, Naoaki Hayashida.
- Report on 27th grand conference of the International Astronomical Union, Hiroko Miyahara.
- CTA project, Ryoji Enomoto.
- Phenomena of high energy cosmic ray below $10^{1}$8eV, Masato Takita.
- Study of absolute Energy calibration for air shower energy by an small electron accelerator, Tatsunobu Shibata.
- Staff reassignment.
- ICRR-Seminar.
- ICRR-Report.

**No.70** (Nov 1, 2009)

- Report on XMASS experiment, Masaki Yamashita.
- Current status of the CLIO, Shinji Miyoki.

- Staff reassignment.
- ICRR-Seminar.
- ICRR-Report.

**No.71** (Jan 31, 2010)

- Report on open campus 2009, Hideo Itoh.
- Effect for the BBN by interacting exotic particles, Motohiko Kusakabe.
- Report on Study in the Ashra Mauna Loa observatory, Yoichi Asaoka.
- Staff reassignment.
- ICRR-Seminar.
- ICRR-Report.

**No.72** (Mar 15, 2010)

- Report on the Meeting for Presenting the Results of Inter-University Research in JFY2009, Hiroyuki Sagawa.
- Study of effect on cosmic ray for climate change, Hiroko Miyahara.
- Staff reassignment.
- ICRR-Seminar.
- ICRR-Report.

## (b) Public Lectures

- ”New cosmic ray searching age, Dark Matter and Gravitational Wave detections”, Mar 13, Hiroo Gakuen, Hideo Itoh (ICRR, University of Tokyo).
- ”Science cafe Galilaus Galilaei”, Feb 21, 2010, Nagoya-city, Aichi, Masayuki Nakahata (ICRR, University of Tokyo).
- ”GSA Science Cafe”, Feb 14, 2010, Kamioka-cho, Hida-city, Gifu, Yoichiro Suzuki (ICRR, University of Tokyo).
- ”Invisible matters and its detection”, Jan 8, 2010, Yubari High school, Hideo Itoh (ICRR, University of Tokyo).
- ”About Super-Kamiokande”, Dec 22, 2009, Kisaradu, Chiba, Yumiko Takenaga (ICRR, University of Tokyo).
- ”About higher dimensional world”, Dec 5, 2009, Gunma National College of Technology, Gunma, Hideo Itoh (ICRR, University of Tokyo).
- ”JPS Public Lecture”, Nov 7, 2009, Komaba, Tokyo, Masayuki Nakahata (ICRR, University of Tokyo).
- ”Neutrinos and Dark Matters”, Nov 6, 2009, Toyama-city, Toyama, Atsushi Takeda (ICRR, University of Tokyo).
- ”Searching Dark Matter -XMASS experiment in Kamioka mine-”, Oct 31, 2009, ICRR, Chiba, Masaki Yamashita (ICRR, University of Tokyo).
- ”Examination of solar and cosmic ray variations during the past two millenia by analyzing cedar trees from Yaku Island”, Oct 30, 2009, ICRR, Chiba, Hiroko Miyahara (ICRR, University of Tokyo).
- ”SSH Takasaki High School”, Oct 16, 2009, Kamioka-cho, Hida-city, Gifu, Atsushi Takeda (ICRR, University of Tokyo).
- ”Joint Public Lectures on ICRR and IPMU, ”Searching the Universe”, Oct 10 2009, Hitotsubashi-hall, Tokyo,
  ”Over the boundary of the Universe”, Hitoshi Murayama (IPMU, University of Tokyo).
  ”Searching the Universe from the Underground of Kamioka mine”, Masayuki Nakahata (ICRR, University of Tokyo).
- ”Tachibana Gakuen High School”, Oct 2, 2009, Kamioka-cho, Hida-city, Gifu, Ko Abe (ICRR, University of Tokyo).

- ”What is a Physicist?”, Sep 2, 2009, Ikebukuro, Tokyo, Yumiko Takenaga (ICRR, University of Tokyo).
- ”JST Project for girl students to choose the science course”, Aug 27, 2009, Kamioka-cho, Hida-city, Gifu, Masaki Yamashita and Naho Tanimoto (ICRR, University of Tokyo).
- ”SSH Senior High School attached to Kyoto University of Education”, Aug 26, 2009, Kamioka-cho, Hida-city, Gifu, Atsushi Takeda (ICRR, University of Tokyo).
- ”SSH Asahigaoka High School”, Aug 12, 2009, Kamioka-cho, Hida-city, Gifu, Ko Abe (ICRR, University of Tokyo).
- ”JST Science Camp”, Aug 11, 2009, Kamioka-cho, Hida-city, Gifu, Makoto Miura (ICRR, University of Tokyo).
- ”Feel the Super-Kamiokande. Let’s see invisible particles.”, Aug 9, 2009, Takashimaya, Shinjuku, Tokyo, Yoichiro Suzuki (ICRR, University of Tokyo).
- ”Yumeno Tamago Jyuku; Hida Academy Summer Seminar”, Aug 7, 2009, Kamioka-cho, Hida-city, Gifu, Jun Kameda (ICRR, University of Tokyo).
- ”JST Project of Regional Activities for Understanding of Science & Technology”, Aug 6 and 20, 2009, Kamioka-cho, Hida-city, Gifu, Yoshihisa Obayashi, Masato Shiozawa and Shigetaka Moriyama (ICRR, University of Tokyo).
- ”Hirameki Tokimeki Science”, Aug 1, 2009, Kamioka-cho, Hida-city, Gifu, Shigetaka Moriyama (ICRR, University of Tokyo).
- ”Elementary particle physics, from birth to flowering”, Jul 30, 2009, ICRR, Hideo Itoh (ICRR, University of Tokyo).
- ”SSH Yoshiki High Scool”, Jul 1, 2009, Kamioka-cho, Hida-city, Gifu, Yoshihisa Obayashi (ICRR, University of Tokyo).
- ”SSH Shizuoka-kita High School”, Apr 24, 2009, Kamioka-cho, Hida-city, Gifu, Hiroyuki Sekiya and Yumiko Takenaga (ICRR, University of Tokyo).
- ”About Cosmic Ray and ICRR”, Apr 24, 2009, Kashiwa library, Hideo Itoh (ICRR, University of Tokyo).
- ”Joint Public Lectures on ICRR and IPMU, ”Horking the Universe”, Apr 18 2009, Amuse Kashiwa, Tokyo, ”Production of the Stars and Galaxies in Dark Universe”, Naoki Yoshida (IPMU, University of Tokyo). ”Searching mystery of the Universe by Gravity Wave”, Kazuaki Kuroda (ICRR, University of Tokyo).

## (c) Visitors

KASHIWA Campus (Total: 8 groups, 121 peoples)

- Ministry of Education, Culture, Sports, Science and Technology
- Chiba Advanced Technology Experience Program
- Induction course of the University of Tokyo
- Others: 5 groups

KAMIOKA Observatory (Total: 128 groups, 2788 peoples)

- Yumeno Tamago Jyuku (Hida Academy for High School Students)
- High school students from Asian Science Camp
- MEXT Super Science High School (SSH) project: total 5 schools
- Schools and Universities: total 29 groups
- Researchers: total 16 groups
- Others: 76 groups

# F. Inter-University Researches

## Numbers of Researchers

| | Number of Applications | Number of Adoptions | Number of Researchers |
|---|---|---|---|
| Facility Usage | | | |
| Kamioka Observatory | 31 | 31 | 611 |
| Norikura Observatory | 9 | 9 | 72 |
| Akeno Observatory | 5 | 5 | 91 |
| Emulsion and Air Shower Facilities in Kashiwa | 3 | 3 | 19 |
| Low-level Radio-isotope Measurement Facilities in Kashiwa | 6 | 6 | 27 |
| Gravitational Wave Facilities in Kashiwa | 2 | 2 | 70 |
| Over Sea Facilities | 10 | 10 | 127 |
| Other | 21 | 21 | 221 |
| Collaborative Researches | | | |
| Cosmic Neutrino Researches | 28 | 28 | 556 |
| High Energy Cosmic Ray Researches | 49 | 49 | 604 |
| Theoretical Researches or Rudimental Researches | 11 | 11 | 191 |
| Research Center for Cosmic neutrinos | 5 | 5 | 31 |
| Others | | | |
| Conferences | 4 | 4 | 131 |
| Special Activity on Abroad | 0 | 0 | 0 |

## Research Titles

1. Precise measurement of Day/Night effect for B8 solar neutrinos
2. Study of nucleon decay $p \to \nu K$
3. Study of simulation for atmospheric neutrino
4. Sidereal daily variation of $\sim$10TeV galactic cosmic ray intensity observed by the Super-Kamiokande
5. Study of Supernova Relic Neutrinos
6. Study of solar neutrino energy spectrum
7. Tokai to Kamioka Long Baseline Experiment T2K
8. Study of ambient gamma-ray and neutron flux at Kamioka Observatory
9. Study in upward-going muons and high energy neutrinos
10. Study for the electron neutrino appearance search in the T2K experiment
11. Development of the new online DAQ system for Super-Kamiokande
12. Study of flavor identification of atmospheric neutrinos
13. Study of atmospheric neutrinos and neutrino oscillations
14. Neutrino interaction study using accelerator data
15. Search for proton decay via $e^+\pi^0$ mode
16. R&D of a Mton water Cherenkov Hyper-Kamiokande

17. Study of Solar Neutrino Flux
18. Energy calibration for Super-Kamiokande
19. Study for Supernova monitor
20. 3-flavor Oscillation study in atmospheric neutrinos
21. Neutrino workshop
22. Study for lowering backgrounds of radioisotopes in large volume detectors
23. Direction-sensitive dark matter search experiment
24. Study for double beta decay of 48Ca
25. Development of InP detector for measurement of solar pp/7Be$\nu$
26. Study for upgrade of XMASS detector
27. Study on absorption and scattering of vacuum ultraviolet light in liquid xenon
28. A study on emission spectrum of liquid xenon
29. Development of low concentration radon detection system
30. Integration of crustal activity observation around the Atotsugawa fault
31. Test of the ultra low background PMT for LXe in low temperature
32. A search for Dark Matter using Liquid Xenon Detector
33. Observation of Galactic Cosmic ray by the Large Area Muon Telescope
34. Multi-Color Imager for Transients, Survay and Monstrous Explosions
35. Observation of solar neutrons in solar cycle 24
36. Observation of the highest energy Solar Cosmic Rays
37. Observation of total ozone and UV solar radiation with Brewer spectrophotometer on the Norikura mountains
38. Space weather observation using muon hodoscope at Mt.Norikura
39. Continuous observation of microbarographs at high mountains
40. Observation of nightglow and its reflected and scattered light on the mountain
41. Study of particle acceleration in electric field using x and gamma rays from lightning and thunderclouds
42. Ecophysiological studies of alpine plants
43. A Study of the Radiation Damage to Polyimide film
44. Study of the composition of cosmic-rays at the knee
45. Study of Galactic Diffuse Gamma Rays
46. Observation of high-energy cosmic-ray electrons with emulsion chambers
47. Measurement of muon with emulsion at T2K muon pit
48. A R&D for a new atmospheric monitoring system
49. Experimental Study of High-energy Cosmic Rays in the Tibet AS $\gamma$ experiment
50. Development of advanced photon counter for the future IACT
51. Observation with All-sky Survey High Resolution Air-shower detector Ashra
52. Sidereal daily variation of 10TeV galactic cosmic-ray intensity observed by the Tibet air shower array

53. Monte Carlo simulation for the Tibet air shower array
54. Cosmic ray interactions in the knee and the highest energy regions
55. Study on High Energy Cosmic-Ray source by Observation Using Long Duration Balloon
56. A study on variation of interplanetary magnetic field with the cosmic-ray shadow by the sun
57. Calibrations of the TA fluorescence telescopes with a portable Nd:YAG laser
58. Bolivian Air Shower Joint Experiment
59. Optical observations of transient high-energy sources in the southern sky
60. Improvement of characteristics of the image sensor used in Ashra
61. Development of CANGAROO-III on-site data analysis system
62. Data Analysis of the UHECR data for the Auger Project II
63. CANGAROO-III Observation of gamma-rays in the southern sky
64. Study of the emission mechanism of unidentified TeV gamma-ray source
65. Development of the optical fiber image transfer system for Ashra
66. Observation of very-high-energy gamma-rays in Australia
67. Composition Study with the Telescope Array Data
68. Workshop on High Energy Gamma-Ray Astronomy
69. Search for High Energy Gamma-ray Emission from Star Forming Regions and Theoretical Research
70. Study of absolute energy calibration air shower by compact Electron LINAC
71. Study of Extremely-high Energy Cosmic Rays by Telescope Array
72. Study of radio detection of highest energy cosmic rays
73. Observation of TeV gamma-ray spectra from galactic objects
74. 4th Symposium on the Science by the CHIMON Observatory
75. R&D and Design of large-scale cryogenic gravitational wave telescope (XI)
76. Development of Local Suspension Point Interferometer for CLIO (I)
77. Gravitational Wave Detector in Kamioka (VIII)
78. Research of the Earths free oscillations based on simultaneous observations with a laser strainmeter and a superconducting gravimeter
79. Development of Sapphire Mirror Suspension for LCGT (V)
80. Modeling of type Ia supernovae spectra based on SDSS data
81. Evolution of the universe and particle physics
82. Comprehensive Researches on Cosmic Dusts
83. Study on solar activity, cosmic rays and climate using cosmogenic nuclide and stable isotopes in tree-rings
84. Reconstruction of cosmic ray intensity and spectrum in the past based on the content of cosmogenic nuclides in ice cores
85. Chemical study for Antarctic micrometeorites
86. Determination of $^{26}$Al in Antarctic meteorite samples
87. Detection of time variations for cosmogenic Be-7, Na-22

88. Detection of low level radioisotopes in tree rings
89. Continuous Measurement of Underground Laboratory Environment
90. Deposition Rate variation of natural activities $^{7}$Be and $^{210}$Pb
91. Precise calculation of the atmospheric neutrino flux
92. Simulation Study for the IceCube Neutrino Observatory
93. Future plan symposium for cosmic ray research

# G. List of Committee Members

**(a) Board of Councillors**

| | |
|---|---|
| KAJITA, Takaaki | ICRR, University of Tokyo |
| FUKUSHIMA, Masaki | ICRR, University of Tokyo |
| SUZUKI, Yoichiro | ICRR, University of Tokyo |
| KAWASAKI, Masahiro | ICRR, University of Tokyo |
| YAMAGATA, Toshio | University of Tokyo |
| MATSUMOTO, Yoichiro | University of Tokyo |
| NISHIKAWA, Koichiro | KEK |
| EGUCHI, Toru | YITP, Kyoto university |
| MIYAMA, Shoken | National Astronomical Observatory |
| SATO, Fumitaka | Konan University |
| YAMAZAKI, Toshimitsu | University of Tokyo |
| MURAKI, Yasushi | Konan University |
| MIZUTANI, Kouhei | Saitama University |
| INOUE, Hajime | Institute of Space and Astronautical Science |
| KOMAMIYA, Yukio | ICEPP, University of Tokyo |

**(b) Advisory Committee**

| | |
|---|---|
| KAJITA, Takaaki | ICRR, University of Tokyo |
| TORII, Shoji | Waseda University |
| KAJINO, Fumiyoshi | Konan University |
| ITOW, Yoshitaka | STEL, Nagoya University |
| TERASAWA, Toshio | Tokyo Institute of Technology |
| SAITO, Naohito | KEK |
| NISHIKAWA Koichiro | KEK |
| KODAMA, Hideo | KEK |
| AIHARA, Hiroaki | University of Tokyo |
| MORI, Masaki | Ritsumeikan University |
| FUKUSHIMA, Masaki | ICRR, University of Tokyo |
| FUKUGITA, Masataka | ICRR, University of Tokyo |
| NAKAHATA, Masayuki | ICRR, University of Tokyo |
| SUZUKI, Yoichiro | ICRR, University of Tokyo |
| KURODA, Kazuaki | ICRR, University of Tokyo |

**(c) User's Committee**

| | |
|---|---|
| YAMAMOTO, Tokonatsu | Konan University |
| TAMURA, Tadahisa | Kanagawa University |
| TORII, Shoji | Waseda University |
| OGIO, Shoichi | Osaka City University |
| MATSUBARA, Yutaka | Nagoya University |
| YOSHIDA, Shigeru | Chiba University |
| TERASAWA, Toshio | Tokyo Institute of Technology |
| MUNAKATA, Kazuki | Shinshu University |
| OHASHI, Masataka | ICRR, University of Tokyo |
| HAYATO, Yoshinari | ICRR, University of Tokyo |
| SAGAWA, Hiroyuki | ICRR, University of Tokyo |
| KANEYUKI, Kenji | ICRR, University of Tokyo |
| TAKITA, Masato | ICRR, University of Tokyo |
| HISANO, Junji | ICRR, University of Tokyo |

# H. List of Personnel

**Director** KAJITA Takaaki

**Vice-Director** FUKUSHIMA Masaki

**Kamioka Observatory (Neutrino and Astroparticle Division)**

| | | | |
|---|---|---|---|
| Scientific Staff | SUZUKI Yoichiro, | NAKAHATA Masayuki, | MORIYAMA Shigetaka, |
| | TAKEUCHI Yasuo, | SHIOZAWA Masato, | HAYATO Yoshinari, |
| | YAMASHITA Masaki, | MIURA Makoto, | OBAYASHI Yoshihisa, |
| | KOSHIO Yusuke, | KAMEDA Jun, | TAKEDA Atsushi, |
| | ABE Ko, | SEKIYA Hiroyuki, | YAMADA Satoru, |
| | NAKAYAMA Shoei, | OGAWA Hiroshi, | KOBAYASHI Kazuyoshi |
| Chief Secretary | KAIZU Satoshi, | TAKAKURA Kouji | |
| Technical Staff | MIZUHATA Minoru, | KANBE Tomio, | KUMAMARU Seiichi |
| Research Fellow | TAKENAGA Yumiko | | |
| Secretary | OKURA Youko, | MAEDA Yukari | |

**Research Center for Cosmic Neutrinos (Neutrino and Astroparticle Division)**

| | | | |
|---|---|---|---|
| Scientific Staff | KAJITA Takaaki, | KANEYUKI Kenji, | OKUMURA Kimihiro |
| Technical Staff | SHINOHARA Masanobu | | |
| Research Fellow | SHIMIZU Yuki, | TANIMOTO Naho, | KAJI Hiroshi |
| Secretary | WATANABE Keiko, | KITSUGI Atsuko | |

**High Energy Cosmic Ray Division**

| | | | |
|---|---|---|---|
| Scientific Staff | FUKUSHIMA Masaki, | ENOMOTO Ryoji, | YOSHIKOSHI Takanori, |
| | TAKITA Masato, | SASAKI Makoto, | TAKEDA Masahiro, |
| | SAKURAI Nobuyuki, | ASAOKA Yoichi, | OHISHI Michiko, |
| | OHNISHI Munehiro | | |
| Technical Staff | AOKI Toshifumi, | KOBAYASHI Takahide, | YOKOYAMA Ryoko, |
| | HOSHI Noboru, | KOIZUMI Chikako, | MORIMOTO Yusuke, |
| | YOKOTA kazuya, | MATSUMOTO Nobuhiro, | NAKADA Yuichiro |
| Research Fellow | TOKUNO Hisao, | SHIBATA Tatsunobu, | NONAKA Toshiyuki, |
| | KONDO Yoshimi, | YABUKI Masanori, | MASUDA Masataka |
| Secretary | SAWANO Sumiko, | KOKUBUN Yayoi, | KARASAKI Kie, |
| | TATSUMI Fusako, | OKAMURA Takako, | FUKUI Misa |

**AKENO Observatory (High Energy Cosmic Ray Division)**

| | | | |
|---|---|---|---|
| Scientific Staff | SAGAWA Hiroyuki | | |
| Technical Staff | OHOKA Hideyuki, | KAWAGUCHI Masami, | SHIMIZU Kanetoshi |

**Norikura (High Energy Cosmic Ray Division)**

| | | | |
|---|---|---|---|
| Technical Staff | YAMAMOTO Kuniyuki, | AGEMATSU Yoshiaki, | USHIMARU Tsukasa, |
| | ISHITSUKA Hideki, | SHIMODAIRA Hideaki | |

**Astrophysics and Gravity Division**

| | | | |
|---|---|---|---|
| Scientific Staff | FUKUGITA Masataka, | KURODA Kazuaki, | KAWASAKI Masahiro, |
| | OHASHI Masatake, | YASUDA Naoki, | HISANO Junji, |
| | MIYOKI Shinji, | UCHIYAMA Takashi, | MIYAKAWA Osamu, |
| | MIYAHARA Hiroko | | |
| Research Fellow | HIRAMATSU Takashi, | TAKEUCHI Michihisa | |
| Secretary | KIKUCHI Rie, | SAKAI Akiko, | YAMAKAWA Toshie |

**Graduate Students**

| | | | |
|---|---|---|---|
| Doctor | IKEDA Daisuke, | KIDO Eiji, | TAKETA Akimichi, |
| | SAKO Takashi, | | |
| | AITA Yuichi, | NODA Koji, | |
| | UESHIMA Kota, | IIDA Takashi, | UENO Ko, |
| | ISHIHARA Chizue, | IKEDA Motoyasu, | McLACHLAN Thomas Fukuei, |
| | LEE Ka-pik, | | |
| | AGATSUMA Kazuhiro, | SAITOH Takanori, | |
| | KAWAKAMI Etsuko, | KOBAYASHI Takeshi, | SEKIGUCHI Toyokazu, |
| | NAKAYAMA Kazunori, | SUGIYAMA Shohei, | |
| | KONISHI Kohki | | |
| Master | TAKAHASHI Yoshiaki, | | |
| | NAKAYAMA Koichi, | SODA Takashi, | TOYAMA Takeshi, |
| | INOUE Daisuke, | | |
| | HIRAI Shun, | ITOH Takashi, | |
| | IYOGI Kazuki, | SHINOZAKI Akihiro, | KOHZUMA Yuki, |
| | YOKOZAWA Takaaki, | NSHIIE Hironori, | |
| | SAIKAWA Kenichi, | MIYAMOTO Koichi, | KITAJIMA Naoya, |
| | TAKESAKO Tomohiro, | NAGATA Natsumi, | YAMAMOTO Yusuke, |
| | RYO Masaki | | |

**Administration Division**

| | | | |
|---|---|---|---|
| Scientific Staff | ITOH Hideo | | |
| Administrative Staff | ISHII Yoshikazu, | SETO Mikako, | SASADA Takaaki, |
| | IRIE Makoto, | OGURA Satoshi, | ARIDOME Ryutaro, |
| | AKIYAMA Makiko, | NISHIMORI Tomoe, | YAMAGUCHI Akiko, |
| | SAITO Akiko, | MARUMORI Yasuko, | KANEKO Saho, |
| | MATSUMOTO Tomoko | | |